AD-A183 055 INTERRUPTION OF NEURAL FUNCTION(U) COLORADO UNIV AT BOULDER DEPT OF ELECTRICAL AND COMPUTER ENGINEERING H WACHTEL MAY 87 153-6823 N00014-81-K-0307 1/2

UNCLASSIFIED F/G 6/7 NL

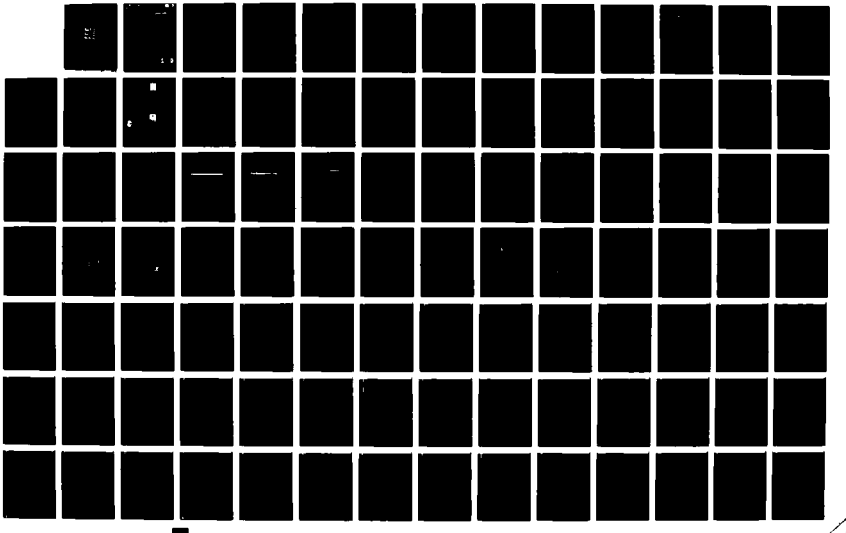

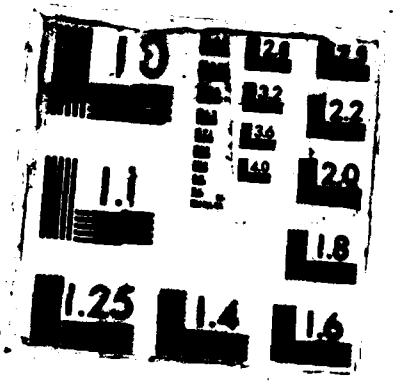
1.0
2.8
3.2
3.6
4.0
2.2
2.0
1.8
1.1
1.25
1.4
1.6

DTIC FILE COPY

SECURITY CLASSIFICATION OF THIS PAGE

UMENTATION PAGE

1a. REPORT: **AD-A183 055**	1b. RESTRICTIVE MARKINGS
2a. SECURITY	3. DISTRIBUTION/AVAILABILITY OF REPORT DISTRIBUTION STATEMENT A Approved for public release; Distribution Unlimited
2b. DECLASSIFICATION/DOWNGRADING SCHEDULE	
4. PERFORMING ORGANIZATION REPORT NUMBER(S) 153-6823	5. MONITORING ORGANIZATION REPORT NUMBER(S) N00014-81-K-0387
6a. NAME OF PERFORMING ORGANIZATION / 6b. OFFICE SYMBOL (If applicable)	7a. NAME OF MONITORING ORGANIZATION Department of the Navy
6c. ADDRESS (City, State and ZIP Code)	7b. ADDRESS (City, State and ZIP Code) Office of Naval Research 800 North Quincy Street Arlington, VA 22217
8a. NAME OF FUNDING/SPONSORING ORGANIZATION University of Colorado / 8b. OFFICE SYMBOL (If applicable)	9. PROCUREMENT INSTRUMENT IDENTIFICATION NUMBER
8c. ADDRESS (City, State and ZIP Code) Campus Box B-19 Boulder, CO 80309	10. SOURCE OF FUNDING NOS. PROGRAM ELEMENT NO. / PROJECT NO. / TASK NO. / WORK UNIT NO.
11. TITLE (Include Security Classification) Interruption of Neural Function	
12. PERSONAL AUTHOR(S) Howard Wachtel	
13a. TYPE OF REPORT FINAL	13b. TIME COVERED FROM 4/81 TO 5/85
14. DATE OF REPORT (Yr., Mo., Day) 87/05	15. PAGE COUNT 4
16. SUPPLEMENTARY NOTATION	

17. COSATI CODES			18. SUBJECT TERMS (Continue on reverse if necessary and identify by block number)
FIELD	GROUP	SUB. GR.	

19. ABSTRACT (Continue on reverse if necessary and identify by block number)

Wide microwave pulses (1 to 10 milliseconds long) and pulse trains were applied to a variety of neural preparations including molluscan ganglia, isolated rat brain slices and intact mouse brain. While different forms of effect were observed in each case a dependence on the associated temperature rate of rise appears to be the underlying factor in all cases. Although temperature rise rates were significant, total temperature elevations were minimal and of a "nondestractive" nature. The "neural modulatory" effects we have seen may thus prove to be useful as a noninvasive means of inputting information into the brain.

20. DISTRIBUTION/AVAILABILITY OF ABSTRACT	21. ABSTRACT SECURITY CLASSIFICATION
UNCLASSIFIED/UNLIMITED ☐ SAME AS RPT. ☐ DTIC USERS ☐	

22a. NAME OF RESPONSIBLE INDIVIDUAL	22b. TELEPHONE NUMBER (Include Area Code)	22c. OFFICE SYMBOL
Dr. Howard Wachtel	(303) 492-7713	

DD FORM 1473, 83 APR EDITION OF 1 JAN 73 IS OBSOLETE.

SECURITY CLASSIFICATION OF THIS PAGE

Final Report to the

OFFICE OF NAVAL RESEARCH

on a study of

INTERRUPTION OF NEURAL FUNCTION WITH ELECTROMAGNETIC FIELDS

performed under contract

N0014-81-K0387

Howard Wachtel
Department of Electrical and Computer Engineering
University of Colorado
Boulder, CO 80309-0425

Introduction

This Report reviews progress made in the final year of our ONR contract. Progress over the first two years was detailed in a report submitted along with our proposal for a third year of funding. That report is appended to this one, and, in summary, covers the following results of applying single "Wide Microwave Pulses" (WMP) to a variety of neural preparations including isolated molluscan (Aplysia) neurons, rodent hippocampal slides maintained in vitro, and the intact mouse brain.

1. Changes in membrane potential (Aplysia) or population spike (Hippocampal slice) or EEG (intact mouse) have fairly slow time courses.
2. All three effects follow a similar pattern of early, fairly long, excitation followed by an even longer period of inhibition.
3. In Aplysia neurons, there is a distinct reversal potential for the WMP induced change in V_M.
4. The effect (in Aplysia) seems to be dependent on small, but fairly rapid changes in temperature.
5. All of the above suggest a pharmacological type of response rather than a direct electrical one.

These findings suggested to us that trains of Wide Microwave Pulses might have selective effects on spontaneous neuronal activity patterns whose frequency lies close to the pulse repetition rate. Some specific questions that arose in conjunction with this hypothesis were:

1. Would a fairly brief WMP train (say 6 sec), that gave rise to 1°C (or less) temperature rise, significantly alter EEG activity?
2. If so, would the EEG changes seen be more or less the same as those previously seen for single WMP of equivalent energy content (i.e., giving rise to 1° C rise)?

3. Would such EEG changes be sensitive to the pulse repetition rate used (for constant Δ T and T?

4. Would EEG patterns indicating "resonance" between the pulse repetition rate and the EEG frequency component shifted be seen?

5. Could WMP pulse trains be used to selectively affect different neural activity patterns (or convey specific "signals" to the brain)?

In order to answer these questions the exposure and monitoring approach previously used for studying the effects of single WMP was redeployed for pulse studying the effects of WMP trains studies. These studies comprised the main body of an M.S. thesis authored by Mr. Abdelkrim Aitarkoub, which is appended to this report (Appendix B). Methodological details and specific results are well documented in this thesis and they have also been presented at the annual Bioelectromagnetics Society Conference as well as submitted for publication. In summary, these were the electroencephalographic results of exposing intact mice to WMP trains.

1. Controls showed no significant changes immediately following train (minutes 2 to 3) for EEG spectral frequencies in 4 to 12 Hz range.

2. WMP trains produced a variety of large, statistically significant changes in these EEG frequency bands for the same time interval.

3. The EEG changes produced by a 6 sec pulse train leading to a 1°C temperature rise were quite different (for all pulse repetition rates) than that elicited by a single wide pulse which gives the same temperature rise (and the same peak T).

4. The change in the EEG was highly dependent on the pulse repetition rate (PRR). In general, the EEG shift was smallest in the frequency bin corresponding to the PRR ("anti-resonance").

Conclusions

The selective effects of WMP trains on EEG signals suggests to us that such trains might be used to input information directly to the brain. Thus our original notion of wide microwave pulses as "interrupters" of neural function has shifted towards viewing them as "modulators" of neural function. To the extent that such modulations can emulate changes in neuronal activity normally brought about by sensory inputs and synaptic interactions, they might be useful in a "neuroprosthetic" context. For example it may be possible, using appropriate WMP trains, to stimulate the visual cortex in blind patients or the motor cortex in paralyzed stroke victims and thereby restore some modicum of normal function. Clearly much more investigation is necessary before any such application can be considered feasible but the possibility is intriguing nevertheless.

In looking back over the full span of our ONR sponsored negotiation it does appear that a consistent pattern of results emerged from the rather wide span of neural phenomena studied under the influence of wide microwave pulses (single pulses as well as pulse trains). All of the effects we have seen can be reconciled with the mechanistic scheme shown on the next page.

RESPONSE OF NEURONS TO WIDE MICROWAVE PULSES

Exposure to WMP

↓

Microwave energy absorption

↓

Small, but rapid $\dot{T}$ temperature rise ($\dot{T}$)

↓

Pseudopharmacological Interaction at pre or post synaptic mechanism sites

↓

Change in membrane potential

↓

Change in firing pattern, postsynaptic responses, EEG, etc.

Information on journal articles, books, etc. by H. Wachtel and/or F. Barnes, published in Fiscal Year 1985 (1 Oct 84 to 30 Sep 85). Please provide author's names, dates, title, journal, and page references as illustration:

1. "Neural effects of extremely low frequency fields as a function of induced tissue current density," *Biological and Human Health Effects of Extremely Low Frequency Magnetic Fields,* American Institute of Biological Sciences, Arlington, VA, May 1985.

2. "Synchronization of neural firing patterns by relatively weak ELF fields," *Biological Effects and Dosimetry of Static and ELF Electromagnetic Fields,* Plenum Publishing Co., pp. 313-328, 1985.

3. "Cell membrane temperature rate sensitivity as predicted from the Nernst equation," *J. BEMS,* 5, 113, 1984.

4. "Effect of DC electric fields on biological systems," "Physical mechanisms and ELF rectification, frequency-sensitive phenomena, safety, and some effects on biological systems," invited review, Charles Polk, Ed., *CRC Handbook of Biological Effects of Electromagnetic Fields,* Charles Polk, Elfrot Postow, Ed., pp. 99-138, 1986.

5. "Forces on Biological Particles in Electric Fields," invited article *J. Bioelectricity,* Vol. 4 (2), pp. 285-299, 1985.

6. "An exposure system for variable electromagnetic field orientation electrophysiological studies," (with J.D. Forster, H. Wachtel, R. Bowman and J. Frazer); *IEEE Microw. Theo. & Tech.,* 1983, Vol. 33, No. 8, pp. 674-680, August, 1985.

Abstracts by H. Wachtel or F. Barnes presented at meetings in Fiscal Year 1985, same format as above.

1. "Effects of Electromagnetic Fields on the Nervous System," *Proceedings of the Chemical Brain Conference* (March 1985).

2. "Possible Neuro-Therapeutic Uses of Electromagnetic Fields," *Proceedings of the 1985 Association for the Advancement of Medical Instrumentation,* (May 1985).

3. "Frequency Specific Effects of Microwave Pulse Trains on the EEG," *7th Annual Bioelectromagnetics Society Meeting Abstracts* (with A. Airtarkoub and F. Barnes) (June 1985).

4. "Measurements of the Distribution of 60 Hz Fields in Residences," *7th Annual Bioelectromagnetics Society Meeting Abstracts* (with D. Savitz and F. Barnes) (June 1985).

5. "Microwave Effects on Neural Membranes," *8th International Symposium on Bioelectrochemistry and Bioenergetics.*

6. "Interaction of Single Pulses of Microwave Energy and Neuronal Tissue," *Proceedings of the 7th Annual IEEE/EMBS Conference (September 1985).*

Awards and honors received in Fiscal Year 1985 by any investigators supported by the ONR contract, including Fellowships.

H. Wachtel: elected to BEMS Board of Directors; chosen as Chairman of 1986 Gordon Conference on Bioelectrochemistry.

Number of graduate students supported in whole or in part by the ONR contract during Fiscal Year 1985.

3 graduate students - leading to M.S. theses:

Ross Jacobson
A. Aitarkoub
B. Lister

Reports to ONR:

Report of the 8th International Symposium on Bioelectrochemistry and Bioenergetics, Bologna, Italy (December 1985), H. Wachtel and M. Blank. Published in "ONR European Science Notes."

An Exposure System for Variable Electromagnetic-Field Orientation Electrophysiological Studies

JOSEPH D. FORSTER, MEMBER, IEEE, FRANK S. BARNES, FELLOW, IEEE, HOWARD WACHTEL, RONALD R. BOWMAN, JAMES W. FRAZER, AND RICH CHALKER

Abstract—A TEM system for exposing isolated nerve cells at 2 GHz is described. The system allows for monitoring of transmembrane potentials by means of microelectrodes and variation of the angle between the electric-field vector and the cell. An *S*-parameter characterization of the system is included along with temperature profile measurements for the energy distribution within the exposure chamber. Additional data on the transient electrical characteristics of microelectrodes upon exposure to microwave pulses in this system are included along with a few examples of the response of *Aplysia* pacemaker neurons to microwave fields.

Key Words: Microwave; Nerve Cells; Cell Measurement Systems.

I. Introduction

A VALUABLE APPROACH in the study of the effects of microwaves on biological materials is to isolate a tissue so the effects on various biological feedback systems are minimized and the basic changes in the properties of individual cells can be studied and related directly to dosimetry. A coaxial system feeding a TEM line was chosen for the purpose of obtaining a broad-band system with a well-defined electromagnetic-field characterization [1]–[3]. The advantage of this system, which is shown in Figs. 1 and 2, is that the sides of the stripline of the TEM cell can contain slots large enough to allow for the mounting of isolated tissue samples on a plastic post which may be independently cooled. In addition, microelectrode probes are inserted into the cell at right angles to the electric field. This orientation minimizes the interaction between the RF field and the microelectrode probe. At the same time, it allows for independent control of the position of the cell and microelectrode with respect to the RF field. The TEM cell may be rotated on its base around the tissue sample, which is mounted on a fixed post. These slots also allow for the insertion of a high-impedance temperature probe (Vitek) at right angles to the electric field, for measurements of the rate of energy disposition into the cell sample.

The system has been characterized by measurement of the *S*-parameters and the rate of temperature rise as a function of position in the sample holder, and for rotation of the incident E field with respect to the sample holder. The field distributions and thermal characterizations show a consistent response which permits reasonable predictions to be made about the average field strengths and current densities in the cell preparations of interest for biological system studies. This system has been used primarily in studies of isolated *Aplysia* neurons, but it is applicable to a variety of situations in which small tissue samples need to be studied electrophysiologically.

Manuscript received September 7, 1984; revised March 18, 1985. This work was supported in part by ONR, under Contract N00014-81-K-0387.

J. D. Forster is with the Fonar Corporation, 110 Marcus Drive, Melville, NY 11747.

F. S. Barnes and H. Wachtel are with the Department of Electrical and Computer Engineering, University of Colorado, Campus Box 425, Boulder, CO 80309.

R. R. Bowman is with Vitek, Sentinal Rock Lane, Boulder, CO 80301.

J. W. Frazer is with UTSCC-M.D. Anderson Hospital, Section of Experimental Surgery, Box 17, 6723 Bertner Avenue, Houston, TX 77030.

R. Chalker is with the University of Colorado Health Science Center, 4200 E. Ninth Avenue, Denver, CO 80262.

II. Detailed Description of the Exposure System

The basic system is designed for matching the TEM section to a 50-Ω coaxial line in the frequency range from ~ 500 MHz to 2.45 GHz. The dimensions for the TEM cell and the holder for the cells are given in Fig. 2. These dimensions were picked primarily to allow sufficient room in the holder to anchor a neural ganglion (from the marine mollusk *Aplysia*) in a reasonable way, and secondarily, for the height of the TEM cell to be large enough to provide a relatively uniform expanse for the fields in its vicinity. The length of the TEM cell was chosen so that upon the application of a short at the output end, the peak of the standing wave is approximately centered on the cell holder at 2.45 GHz, as per the design of Wachtel *et al.* [1]. At lower frequencies, this maximum shifts towards the generator and the position of the short must be adjusted. The foregoing dimensions yield an impedance very close to 50 Ω while minimizing mismatches at transitions between it and the coaxial line. A still better match could be obtained by tapering the transition from the coaxial cable to the slotted section; however, for our application, this did not prove to be necessary.

The post that holds the tissue consists of two concentric plastic tubes with an H-shaped cap as shown in Fig. 1. This configuration serves two functions. The first is to allow cooling with distilled water which circulates close to the cell preparation, giving a relatively low thermal time con-

0018-9480/85/0800-0674$01.00 ©1985 IEEE

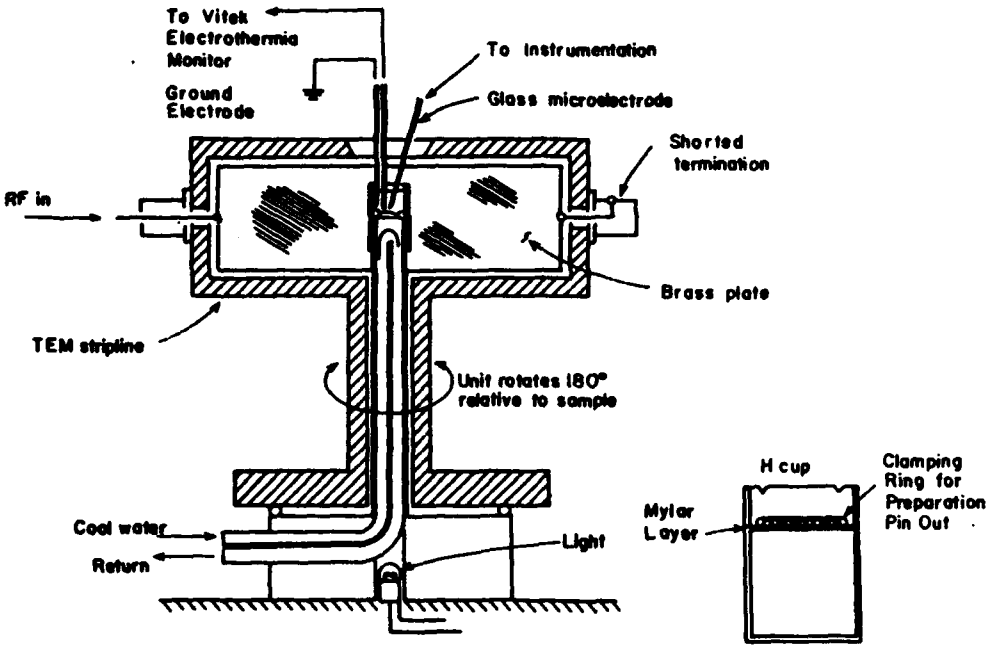

Fig. 1. Cutaway diagram of TEM cell.

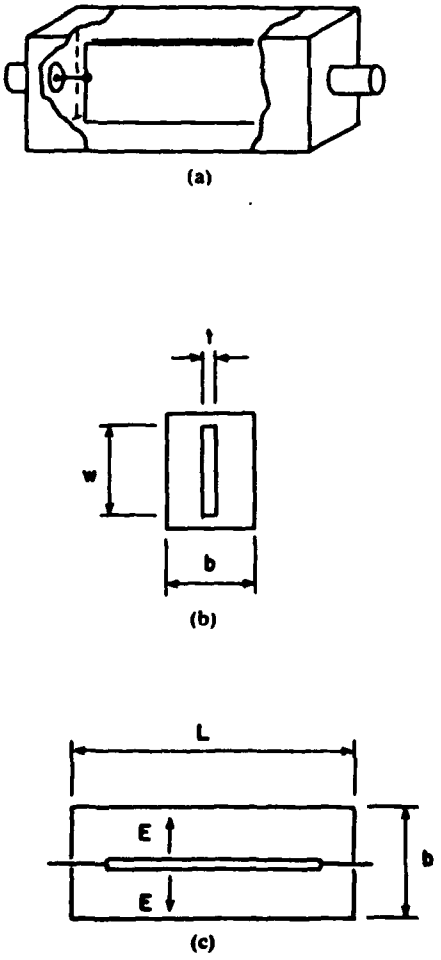

Fig. 2. (a) Cutaway diagram of stripline. (b) Cross-sectional view of stripline with dimension labels. (c) Top view of stripline with dimension labels. $W = 4.0$ cm, $t = 0.318$ mm, $b = 3.25$ cm, $L = 9.18$ cm.

stant of approximately 30 s (compared with an uncooled time constant of almost 20 min). In order to get this short time constant, the top of the post is machined to approximately 1 mm thick and the cup which is seated on it has a base which is formed from a thin Mylar sheet (0.16 mil). The post also includes a lamp for transilluminating the ganglion so that it can be viewed from the top side. This enables the experimenter to locate microelectrodes in a given cell and to orient the ganglion precisely along a reproducible set of axes.

III. Microwave Coupling

For isolated cell exposures, the microwave system as shown in Fig. 3 contains a generator which will provide up to 100 W of incident power into the stripline. The attenuator in the system yields nominal power reductions of up to 60 dB (which is useful for finding threshold values associated with changes in the cell characteristics). An isolator prevents feedback from the load to the generator, and both the incident and reflected powers are monitored through a bidirectional coupler. Exposure times are controlled by a coaxial switch that allows power to be directed into a dummy load except during experimental exposures. In normal operation, the stripline is terminated in a short so that the incident and reflected waves incident on a tissue are similar in size. The standing wave yields a more uniform energy deposition in the cell system than would result from a single traveling wave terminated in a matched load.

In order to further characterize this system, the TEM line was disconnected from its standard driving system and connected to an HP network analyzer Model No. 8410B, which allowed for direct measurements of the *S*-parameters. The basic characterization resulting from this evalua-

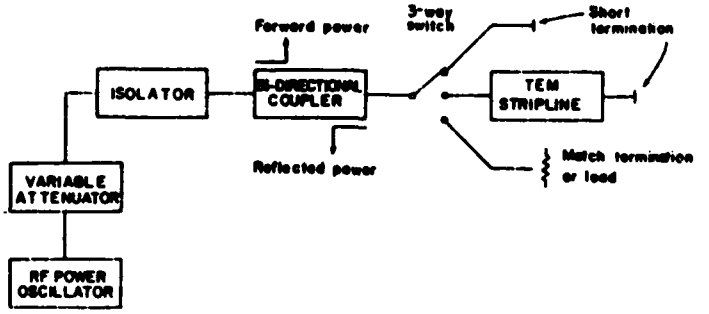

Fig. 3. Block diagram of microwave delivery system.

TABLE I
CHARACTERIZATION OF STRIPLINE AT 2 GHz

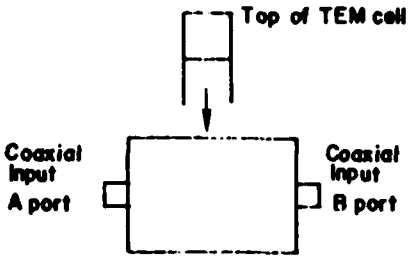

$\|S_{11}\|^2$ =	$\|S_{22}\|^2$ =	$\|S_{21}\|^2$ =	$\|S_{12}\|^2$ =	A port Measurements
.05	.04	.79	.79	Empty Cavity
.05	.05	.45	.45	Cavity and Post
.08	.08	.35	.40	Cavity, Post and Chamber with Saltwater

TABLE II
PORT A CONNECTED TO TEM CELL TERMINATED IN A SHORT;
PORT B CONNECTED TO ELECTRODE AT 2 GHz

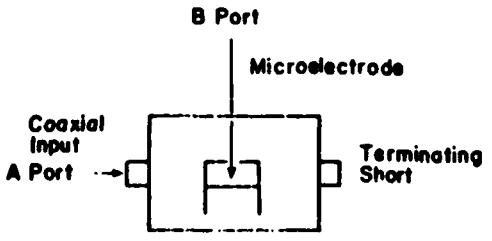

Results	
$\|S_{11}\|^2$	.71
$\|S_{12}\|^2$	3.2×10^{-5}
$\|S_{21}\|^2$	3.2×10^{-5}
$\|S_{22}\|^2$	.58

tion at 2 GHz is shown in Table I. The accuracy of the measurement system was ± 0.05 dB in magnitude and $\pm 2°$ in phase. These data show the characteristics of the stripline by itself, the effect of the water-filled post both with and without a sample, in perturbing the system, and the effect of the microelectrode.

Additional data in Table II depict the transmission characteristics at 2 GHz where the S-parameters are measured through the microelectrode. These data are significant because the TEM cell is relatively well-matched and the perturbations due to the water-filled post and cell sample are moderate. Furthermore, the data on transmission through the microelectrode show that the coupling coefficient for power through the microelectrode is typically less than one part in 10^5.

IV. Temperature Rise Rate and Profile Measurements

In order to corroborate our calculated dosimetry and to make measurements of the uniformity of the energy deposited in the tissue chamber, temperature-rise measurements were made with a high-impedance Vitek probe. The probe was also inserted at right angles to the electric field to minimize its effects on the field. The Vitek probe allows for measurements of the rate of rise of the temperature due to the absorption microwave power with an accuracy of $\pm 0.1°C$ and a spatial resolution of ~ 0.5 mm. The diameter of the Vitek probe is about 1 mm and its position is controlled with a micromanipulator. Any fluctuations due to inhomogeneity within the tissue were not resolvable. The

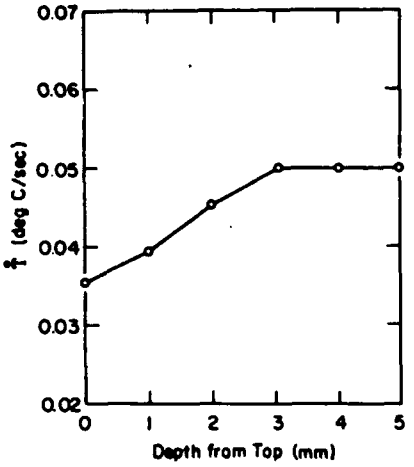

Fig. 4. Variations in the rate of temperature rise as a function of depth from top of the liquid in chamber, 0.5-cc saltwater, probe in center of chamber.

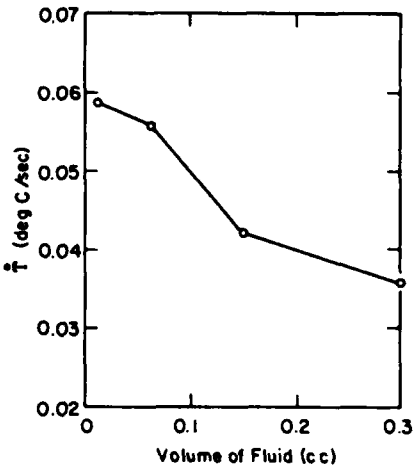

Fig. 6. Variations in rate of temperature rise as a function of volume of fluid in sample chamber, 0.5-cc saltwater at constant center location.

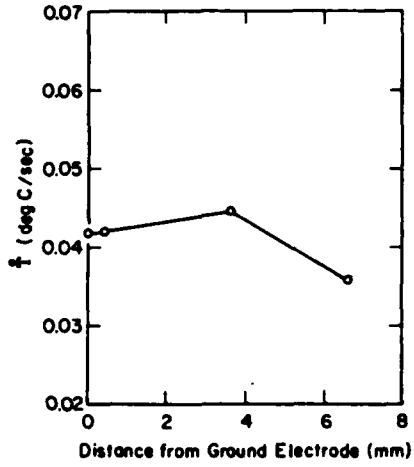

Fig. 5. Variations in rate of temperature rise as probe is varied from ground electrode at constant depth, 0.5-cc saltwater.

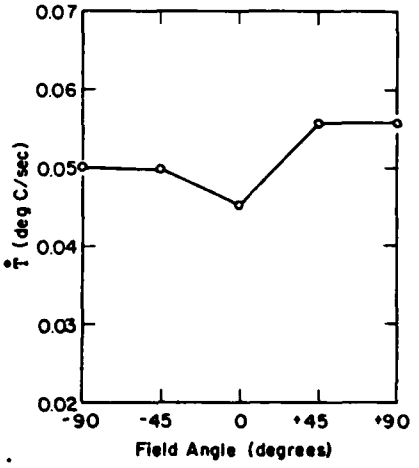

Fig. 7. Variations in rate of temperature rise as a function of field angle, 0.5-cc saltwater, probe at constant depth, center of chamber.

specific absorption rate (SAR) in a given portion of the tissue sample volume is closely proportional to the rate of the temperature rise since heat dissipation is relatively slow in the uncooled case. Plots of these temperature rates of rise as functions of position in the cell sample are shown in Figs. 4–6. At the center of the sample, temperature rates of rise from top to bottom of the sample varied by 0.015°C/s. This represents approximately a 30-percent variation from top to bottom. However, in the region where the cells are located ~3 mm below the surface, variations in temperature rate of rise were not measurable. Variations in the rate of rise of temperature as the probe is moved away from the center of the sample are about 10 percent over the first 4 mm. At the edges of the cup, the temperature rate of rise decreases by about 30 percent.

Putting an additional probe in the field makes essentially no difference in the temperature rate of rise (less than 10 percent). Increasing the volume of the fluid in the sample holder decreases the rate of temperature rise in an approximately linear way. More significantly, as the angle of field is rotated with respect to the sample (see Fig. 7), less than 10-percent variation in the rate of temperature rise occurs over a 180° rotation. The variation with angle for the water samples is probably the result of a slight tilt of the center post supporting the sample with respect to the stripline.

V. Characterization of the Microelectrodes

The microelectrodes are pulled to tip diameters of less than 1 μm using a standard electrode puller. Connection to this microelectrode is made with a silver chloride wire located outside the microwave field. To further reduce the disturbance of the microwave field by the electrode probing system, the ground electrode is made through a salt bridge using a larger diameter, low-impedance pipette (typically 100 kΩ), which is also located at the edge of the cup nearest the outside metal wall of the TEM cell and as close as possible to one of the RF ground plates. The ground electrode contains ~10-percent agar plus artificial sea water, which is the same solution as that used to bathe

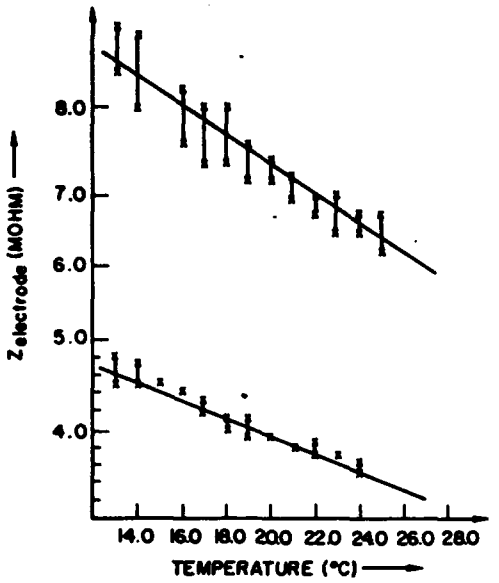

Fig. 8. Electrode impedance versus temperature.

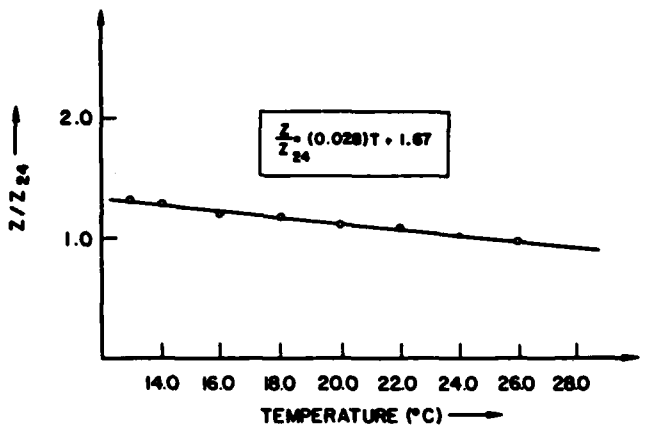

Fig. 9. Electrode impedance (normalized to impedance at 24°C) versus temperature.

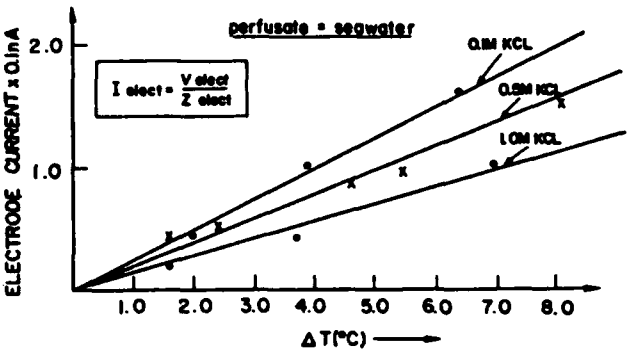

Fig. 10. The equivalent electrode current versus ΔT for three different electrode concentrations, where ΔI is calculated from the measured ΔV divided by the initial electrode resistance.

the preparation. Again, a silver chloride wire located outside the RF field is used to connect to the circuit ground bus.

In making intercellular microelectrode measurements under varying thermal environments, it is necessary to be aware of how the electrical characteristics of the microelectrodes change during the course of the measurements. A number of experiments are performed in order to determine:

1) the microelectrode impedance behavior as a function of temperature,
2) the magnitude and significance of equivalent electrode current contributed by the microelectrode under temperature excursions,
3) the effect of varying KCl concentrations in the microelectrodes on 2),
4) the microelectrode behavior as a function of the rate at which the temperature is changed ($\dot{T}$).

For these experiments, the microelectrodes are made of 2-mm capillary tubing using a standard electrode puller. After pulling and cooling, the electrodes are placed with blunt ends in ~3 cm of 0.5-M KCl electrolyte solution until the tips are filled by capillary action. They are then back-filled the rest of the way with the same 0.5-M KCl solution using a specially adapted syringe. The concentration of the electrolyte and the setting on the puller are such that the electrode impedance is in the range of 2 to 20 MΩ. After filling, the electrodes are checked for tip breakage and/or excessive bubbles under a microscope. Any showing defects are rejected.

A microelectrode is then placed in the micromanipulator and the system is set up for intracellular measurements but without a ganglion in the preparation chamber. The perfusion system (perfusate–sea water) is activated and a room-temperature baseline established. A known amount (≈1 nA) of amplifier-injected current is passed through the electrode and the response recorded on the chart recorder. The baseline perfusion temperature is then lowered and the measurement repeated for a range of temperatures between 13° and 26°C on two separate electrodes. The calculated impedance is shown as a function of temperature in Fig. 8. The curves in Fig. 8 are normalized to their impedance at 24°C and plotted in Fig. 9. This curve may be used to determine impedance changes as a function of temperature for any electrode with 0.5-M KCl and between 2 and 20 MΩ.

In other experiments with the same initial protocol, a microelectrode is subjected to perfusion-produced temperature "pulses" and its response is recorded on the chart recorder. The electrode potential shifts as a function of temperature excursion are then converted to equivalent electrode current by dividing the measured electrode voltage shift by the initial electrode resistance. The results are plotted as a function of the size of the temperature excursion (ΔT) in Fig. 10. They indicate an equivalent electrode injected current of less than 0.01 nA per 1° change in electrode temperature. This current is small enough that, under most circumstances, it has very little effect on the

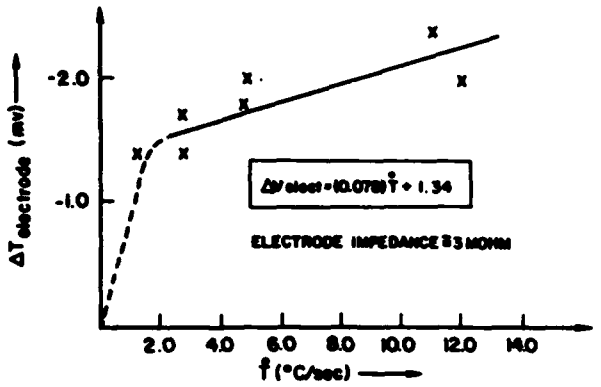

Fig. 11. Electrode potential shift versus $\dot{T}$ at 19°C.

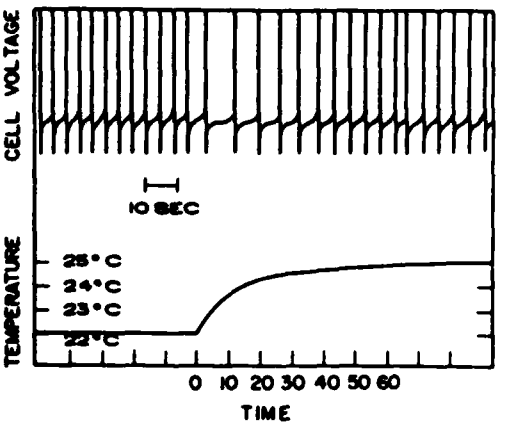

Fig. 12. The firing rate change as the result of the application of 15 W at 2.45 GHz. The absorbed power $P_a = 0.3$ W/cm^2, $T_{max} = 0.14$°C/s, and $\Delta T = 3$°C.

firing rate of the pacemaker nerve cells. However, it can have a significant effect on the apparent voltage shift, seen when measuring the response of a silent cell. This is because the typical membrane resistance for a silent cell is ~1 MΩ, and thus the temperature-induced change in voltage as measured across the electrode plus the membrane can be 4 to 8 times that produced by the membrane alone. Fortunately, the time constants for the voltage from the microelectrode is 1.25 s and that for the membrane plus electrode is 3.25 s. Thus, the effect of the microelectrode can be subtracted out.

The final microelectrode characterization includes a determination of the microelectrode behavior as a function of the rate at which its temperature changes with time ($\dot{T}$). A microelectrode is subject to a series of "equal energy" microwave pulses, all of different lengths (0.2 to 5 s) but all raising the temperature of the perfusate (and electrode) by ~ 3.5°C. The electrode potential shifts in response to these pulses are recorded on a chart recorder. The magnitude of the maximum shift is plotted as a function of the rate at which the temperature was changed ($\dot{T}$) in Fig. 11. $\dot{T}$ is determined by dividing the extent of temperature excursion by the length of the microwave pulse. The dashed portion of Fig. 11 is drawn in from an assumed origin. The apparent microelectrode $\dot{T}$ sensitivity indicated in Fig. 11 is surprising but may be explained by the fact that there exists a potential barrier between the perfusate medium and the 0.5-M KCl electrode solution. The ion-concentration difference between the two regions is related by the Nernst equation [4] so that $C_1 = C_2 \exp[q\phi/\zeta KT]$ and a current $I \sim \Delta T/T$ is generated by a temperature pulse ΔT [5]. C_1 and C_2 are concentrations, q is the ion charge, K is the Boltzmann constant, ϕ is the potential, ζ is a parameter on the order of unity, and T is the temperature.

VI. Some Examples of the System's Use: Microwave Effects on *Aplysia* Pacemaker Neurons

The results in Fig. 12 show the change in firing rate for a typical pacemaker cell (taken from the ganglion of an *Aplysia*) after turning on a CW microwave signal leading to a rise of ~ 2°C in 15 s. The total temperature rise is determined by the balance between the absorbed microwave power and cooling through the plastic post, with a thermal relaxation time of about 30 s. Following application of the microwave signal, the cell first slows down, and then accelerates. A similar change in firing rate can be obtained by injecting a hyperpolarizing current (which makes the interior of the cell more negative) into the cell through the sensing microelectrode [6]. The amount of pulsed current required to increase the firing rate of a typical cell is shown in Fig. 13 [7]. The amount of current required to get a given change in the firing rate is very nonlinear, and is strongly dependent on how far the natural operating point for the cell is displaced from the cutoff where the cell ceases to oscillate.

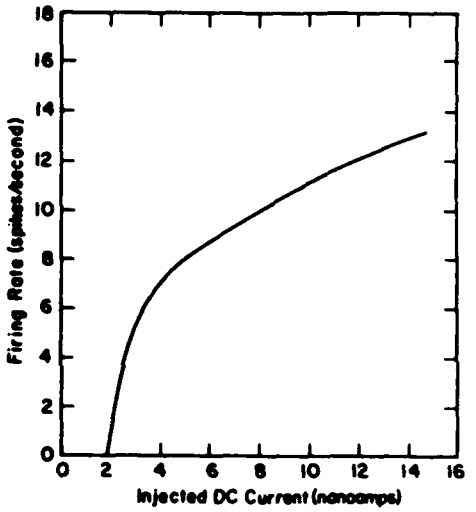

Fig. 13. Changes in the firing rate of a pacemaker cell as determined by injecting current step and noting the initial shift in the interspike interval.

VII. Conclusions

The exposure system described allows for relatively uniform exposure of isolated neural tissue at 2.45 GHz and nearby frequencies. The recording microelectrode is shown

to be sensitive to both temperature and the rate of temperature rise. Temperature rate of rise measurements as a function of the angle between the electric field and the tissue sample holder, and depth, show that a relatively uniform power density is being deposited in the cell sample with the variations in the SAR of less than 10 percent. We believe that this system is well suited for exposing a variety of tissues to RF fields, the direction of which can be varied while responses are monitored with microelectrodes. Additionally, some sample results are given which show that changes in the firing rate of pacemaker cells taken from the ganglion of an *Aplysia* are induced by microwave pulses.

References

[1] H. Wachtel, R. Seaman, and W. Joines, "Effects of low-intensity microwaves on isolated neurons," *Ann. NY Acad. Sci.*, vol. 247, pp. 46–62, 1975.

[2] M. L. Crawford, "Generation of standard EM fields using TEM transmission cells," *IEEE Trans. Electromagn. Compat.*, vol. EMC-16, pp. 189–195, 1975.

[3] S. V. Marshall, R. F. Brown, C. W. Hughes, and P. V. Marshall, "Environmentally controlled exposure system for irradiation of mice at frequencies below 500 MHz," in *IEEE Int. Symp. Electromagn. Compat.*, 1981, pp. 99–104.

[4] R. J. MacGregor and E. R. Lewis, *Neural Modeling*. New York: Plenum Press, 1977, chs. 6, 7.

[5] F. S. Barnes, "Cell membrane temperature rate sensitivity predicted from the Nernst equation," *BEMS*, vol. 5, pp. 113–115, 1983.

[6] D. O. Carpenter, "Temperature effects on pacemaker generation membrane potential and critical firing threshold in *Aplysia* neurons," *J. Gen. Phys.*, vol. 50, no. 6, part I, pp. 1469–1484, 1967.

[7] J. Forster, "Nonlinear microwave bioeffects on isolated neurons of *Aplysia*," Masters thesis, Dept. Elec. Eng., Univ. of Colorado, 1981.

Joseph D. Forster (S'75–M'81) received the B.S. degree in engineering science in 1978 from New Jersey Institute of Technology, Newark, NJ, and the M.S.E.E. degree in 1981 from the University of Colorado in Boulder, CO.

From 1981 to 1983, he was a Staff Engineer at Baylor College of Medicine, where he became involved with NMR studies of biological systems and NMR whole body imaging. In 1983, he joined Fonar Corporation, Melville, NY, where he became Project Engineer for the Fonar Mobile NMR and is now Assistant to the Vice President of Operations in Manufacturing.

Mr. Forster is a member of Sigma Xi and the Bioelectromagnetic Society.

Frank Barnes (S'54–M'58–F'70) received the B.S. degree from Princeton in 1954, and the M.S. and Ph.D. degrees from Stanford in 1955 and 1958, respectively.

From 1957 to 1958, he taught at the College of Engineering in Baghdad, Iraq, on a Fulbright. In 1958, he joined the Colorado Research Corp. as a Research Associate. He joined the Department of Electrical Engineering at the University of Colorado, Boulder, in 1959, where he is a Professor. He served as Department Chairman from 1964 to 1980.

Dr. Barnes has been involved in the study of lasers, microwave devices, and their applications to biological materials. He is a fellow of AAAS and has received the Curtis McGraw Award for Research from ASEE in 1965. He is also a member of the American Physical Society and the Biolelectromagnetic Society.

Howard Wachtel, photograph and biography unavailable at the time of publication.

Ronald R. Bowman, photograph and biography unavailable at the time of publication.

James W. Frazer received a degree in basic medical sciences (State University of New York, College of Medicine, Syracuse, NY, 1965) with expertise in biochemistry, pharmacology, physiology, and biophysics. His interests for many years have been in examination of the electromagnetic behavior of biomacromolecular systems with experimental approaches utilizing optical spectroscopy (absorbance and light scattering) resonance spectroscopies, nuclear magnetic resonance (NMR), electron spin resonance (ESR), resonant Raman spectroscopy, Raman spectroscopy, and a variety of EM-wave applicators to biological systems. His present efforts include NMR examination of tumor cells and the use of electromagnetically induced hyperthermia in tumor treatment.

Rich Chalker, photograph and biography unavailable at the time of publication.

PROGRESS REPORT

Over the past two years our research into the effects of wide microwave pulses (WMP) on neural function has progressed along four parallel lines:

1) Effects of WMP on Isolated Aplysia pacemaker neurons studied with intracellular recording techniques.
2) Effects of WMP on evoked potentials elicited in rat brain (hippocampus) slices.
3) Physiological effects on intact mice exposed to low level WMP and monitored via evoked kinetic responses (EKR) and EEG changes.
4) Physiological and pathological effects of higher level WMP on intact mice studied in collaboration with Dr. William Stavinoha at his laboratory in San Antonio.

Although these four phases span a vast phylogenetic and organizational range, the basic experimental approaches are similar. In each case we have exposed the nervous system (or sub-system) to wide microwave pulses and characterized the electrophysiological or behavioral response seen. We have also attempted to quantify the responses seen when WMPs of varying duration, but constant energy, are presented. In this way we have been exploring the "optimal" pulse parameters for each system and so far, have obtained comparable results in each phase.

1. Results of Aplysia pacemaker cell exposures to WMP

This facet of our study was already underway when the ONR contract began and its support overlapped with our previous E.P.A. contract. Most of these results were presented by us at the 1982 B.E.M.S. meetings in Los Angeles and is expostulated in great detail in Mr. Richard Chalker's M.S. thesis which is appended to this report.

Using a somewhat modified version of the stripline exposure cell system developed over the previous decade (Wachtel, et al 1975, Seaman & Wachtel, 1978, Forster, Wachtel & Barnes, 1983) we isolated the abdominal ganglion from the sea hare (ophistobranch mollusc) Aplysia Californica and impaled certain identified pacemaker neurons (R3-R13) with glass intracellular microelectrodes. The ganglion was exposed to very wide 2450 MHz microwave pulses (0.1 to 10 secs.) that led to only moderate temperature rises (less than 2°C) compared to the animals' normal range of thermal variation (10°C or more). A rapid perfusion temperature control system was developed specifically for this study which allowed us to mimic microwave temperature rise profiles with the field off or, alternatively, to suppress microwave induced temperature rises when the field was on.

As in previous studies (Seaman & Wachtel, 1978, Foster et. al, 1983) we observed a two phase response to these WMP exposures--a brief hyperpolarization and inhibition of firing followed by a longer lasting period of excitation (increased firing rate) as is illustrated in Fig. 1. The inhibitory phase would only be seen

however, when the rate of temperature rise was relatively fast (greater than 2°C/sec.). When similarly rapid temperature rises were produced by our "hot flushing" (perfusion) technique the response was quite comparable to the microwave effect as is illustrated in Fig. 2. Furthermore when the perfusion system was used to suppress the rapid temperature rise in the presence of the microwave field the response (change in firing rate) largely vanished, as is illustrated in Fig. 3. This set of experiments led us to the conclusion that it was a sensitivity to the temperature rate of rise ($\dot{T}$) that was the primary "membrane detector mechanism" involved in these Aplysia pacemaker neuron responses.

The precise relationship between $\dot{T}$ and the inhibitory response magnitude (as measured by the relative decrease in firing rate) was quantified in a series of "equicaloric" WMP exposure experiments. Pulses ranging in width from 0.1 to 10 sec., but all leading to the same total temperature rise (as measured with a Vitek probe) were seen to give significantly different effects as is illustrated in Fig. 4. Very wide pulses leading to $\dot{T}$ values less than about one degree per second, produced little or no inhibition whereas increases in $\dot{T}$ beyond 3°C/sec., or thereabouts, produced no further increase in the inhibitory effect. A continuous curve drawn from such results, as shown in Fig. 5, is quite consistent with the predictions of our theoretical model and suggests that the "optimal pulse" duration (at which the greatest effect is obtained for a given pulse

energy content) is about 0.5 seconds. This time is of the same order as the membrane time constant for these Aplysia pacemakers and is, of course, much longer than mammalian neural membrane time constants (which are about 1 to 10 msec.).

An exploration into the biophysical mechanism underlying the inhibitory effect was carried out by estimating the "reversal potential" for the hyperpolarizing phase. This was done by passing "biasing" currents through the microelectrode and noting changes in the size, and polarity, of WMP induced membrane potential shift. After appropriate corrections for electrode artifacts were made, data such as that illustrated in Fig. 6 were obtained. It is seen that the WMP induced hyperpolarization diminishes in size and clearly reverses when the ambient membrane potential is made more negative by the "biasing" current. Such a clearcut reversal pattern, which follows an essentially linear relationship when plotted (Fig. 7) is indicative of a specific ionic conductance increase mechanism, rather than other proposed mechanisms such as electrogenic pumps (which could not easily be reversed). Based on the estimated reversal potential (about -70 Mv.) and comparison to other well studied phenomena (such as inhibitory post synaptic potentials) in this ganglion, these results suggest that an increase in potassium conductance (G_K) is the primary inhibitory mechanism. Similar changes in G_K are known to be produced by the influx of calcium ions (Meech 1974, Carnevale & Wachtel, 1982) which suggests that, as in other well known cases Bawin&Adey,1974,Blackman, 1977) microwave induced movements of

calcium ions may be an important mediator in the case of the Aplysia pacemaker neurons.

2. Changes of Electrical Evoked Potentials in Rat Hippocampal Slices Produced by WMP

In recent years the rodent brain slice (mainly from the hippocampus) has been exploited as a neurophysiological "testing ground" in much the same way that isolated Aplysia (or other invertebrate) neurons had previously been used. Mr. Geoffery Adey, a graduate student in our laboratory, spent about a year and a half adapting this very useful, but difficult, neuro-technology to a microwave exposure system and obtaining some preliminary results. Unlike isolated Aplysia ganglia which function quite well with only minimal attention to perfusion or temperature control, the isolated rodent brain slice will survive only under very carefully controlled and balanced conditions of temperature, oxygen and carbon dioxide concentration, perfusate level and chamber humidity. These constraints necessitated the development of an entirely different life support and microwave exposure system from that used for the Aplysia experiments. This system and the initial results obtained using it were presented at the 1983 BEMS meeting in Boulder and will be the basis for Mr. Adey's M.S. thesis to be completed this year.

The electrophysiological signal that was used as a microwave response indicator was the electrically evoked potential recorded and elicited using extracellular glass electrodes

filled with physiological saline in an agar base. Such electrodes, like the intracellular versions used in the Aplysia studies, produce only minimal microwave artifacts which can readily be separated from the electrophysiological signal. The evoked potential consists of several components which are demarcated in Fig. 8. It was the post synaptic phases of this response (the EPSP and "Pop Spike") which were especially sensitive to wide microwave pulses of rather low intensity. For example, a single 4 msec. long pulse having peak S.A.R. of 30 watt/gm (which would cause temperature rise of only 0.03°C) led to the prolonged changes shown in Fig. 9. Here the postsynaptic phase which is quite stable in control experiments grows markedly (almost three-fold) after a single 4 msec. pulse. An even more interesting response is shown in Fig. 10 in response to a somewhat more intense pulse (4 msec. at 50 w/gm leading to a temperature rise of 0.05°C). Here there is a brief period of complete inhibition (no postsynaptic response) immediately following the WMP. Soon thereafter there is a recovery and even an appreciable increase in the postsynaptic response. This response pattern of early, but short lived, inhibition followed by longer lasting excitation is quite reminiscent of the Aplysia response pattern but the overall response (prolonged excitation phase) lasts far longer--sometimes for several hours! The time courses for the responses shown in Figs. 9 and 10 are compared graphically in Fig. 11.

The exploration of the "optimal pulse" for eliciting these changes in mammalian brain slice evoked responses was pursued by

carrying out the "equicaloric pulse" experiments previously described for the Aplysia. Fig. 12 shows the immediate effects of widening the microwave exposure time from 4 to 16 to 32 msec. while proportionately reducing the intensity so as to produce a constant temperature rise of 0.05°C. The inhibitory effect (on the post synaptic response) is almost total at 8 msec., about 70% at 10 msec., and only 40% at 32 msec. This result is consistent with predictions of our model and the Aplysia results. However, when longer term (excitatory) response, taken 40 minutes after the microwave pulse, is examined, as shown in Fig. 13, the results show a somewhat opposite trend.

From this sort of preliminary data we would tentatively suggest that the immediate inhibitory response could have a similar biophysical basis (i.e. a calcium controlled G_K increase) to that in the Aplysia pacemakers. We have, however, a much poorer understanding of (and less data for) the longer term response.

3. Physiological responses of intact mice exposed to low levels of WMP

We have devised two ways of quantifying the neurological response of an intact mouse to wide microwave pulses comparable to those used in the brain slice experiments. The exposure system in both cases is the same and derives from the "microwave brain inactivator" configuration developed and used in Dr. William Stavinoha's laboratory at the Southwest Texas Medical Center

in San Antonio. As illustrated in Fig. 14 the mouse is constrained within a plastic cage (fashioned from a 60 cc. syringe) so that its head is at an H-field maximum within the waveguide. This sort of coupling, which is abetted by use of an E-H tuner has previously been shown (Stavinoha et al, 1978) to be most effective in depositing microwave energy selectively and fairly uniformly in the animal's brain.

In some studies preliminary to the present project we utilized Stavinoha's setup to induce "hypokinesis" (inhibition of cage exploratory movements) with fairly intense microwave pulses (leading to a 2 or 3° brain temperature rise). We found that, in general agreement with our model's predictions, narrower pulses were far more effective than wider pulses of the same total energy content. (These results were presented at 1981 BEMS conference in Washington, D.C., and appended to our original ONR proposal). These hypokinesis effects were moderately interesting (and gave us some initial confidence in the model) but rather crude and limited in quantifiability.

From the hypokinesis results, which are really only "after-effects," we reasoned that the mice should show immediate kinetic responses to substantially lower levels of WMP. To test this notion we devised an apparatus, illustrated in Fig. 15, for recording body motions via a transducer clamped to the tail. This device is quite sensitive to any body motion (not just "tail flicks") and can even be used to record respiration. Mr. Ross Jacobson, another of our current graduate students, has used

this device as part of a system shown in Fig. 16, to record the "Evoked Kinetic Responses" (EKR) to WMP. Some of his initial findings along with the methodological aspects were presented at the 1983 BEMS meetings and will be the basis for his M.S. thesis.

Several aspects of the EKR have been examined but the parameter that is most reliable is the delay from the end of microwave exposure to the onset of the movement response. Because of inherent limitations (constraint induced torpor and temperature recovery times) each mouse can only be exposed to about 9 pulses (in about a 30 minute experiment). When a "three by three" equicaloric pulse experiment is carried out (by using 3 different durations three times each in random sequence) the delay is seen to clearly decrease as the same energy is delivered in narrower pulses (as illustrated in Fig. 17 which shows the z-scored averages and deviations from a set of 3 mice). The results of a control series in which the pulse duration was not changed (nine identical pulses in each experiment) are shown in Fig. 18. Here the delays are not significantly different when the responses are grouped and averaged in the same sequence used for the "3 by 3" experiment. This shows that the results illustrated in Fig. 17 cannot be explained by some sort of coincidental change in the response with time.

A similar trend, wherein narrower microwave pulses having a given energy content are more effective, is also seen when the "magnitude" of the EKR is used as the effect indicator.

However, the effects in these cases, as illustrated in Fig. 19, are not significant viewed in the light of the variance seen for each of the three pulse duration groups. This is not surprising since the "magnitude" of the complex EKR signal is much harder to define and quantify than the delay time to response onset.

The estimated brain temperature rises (which must be measured in separate experiments using anesthetized mice) associated with EKR-inducing microwave pulses are in the order of 0.5°C--much lower than those required to produce hypokinesis but still an order to magnitude greater than S.A.R. levels effective in the brain slice. Again, this is to be expected since electrophysiological responses to external stimuli can generally be detected at much lower levels than kinetic response. This suggested to us that changes in the EEG might be observable, and useful as effect indicators, at lower microwave exposure levels. Some very preliminary experiments, using implanted carbon loaded teflon electrodes beneath the skull of mice, indicate that this may very well be the case. Using a recently acquired microprocessor system (Apple IIe with AD/DA capability) we are presently developing techniques for spectral analysis and other signal processing paradigms that can "suck out" subtle, but still significant, changes in the intact mouse EEG in response to fairly low level WMP.

4. Physiological and Pathological Responses of Intact Mice to Higher WMP Levels.

As part of our continuing collaboration with Dr. Stavinoha and his associates, we have tried to "bridge the gap" between the very high level lethal exposures that he uses to rapidly sacrifice mice for neurotransmitter analysis and the much lower levels we use for our purposes to simply perturb neural function in a reasonably reversible manner. One reason for doing this is to determine how much of a "margin" there is, in terms of absorbed energy, between the neuro-physiological effect levels we are studying and clearly pathological levels.

In addition to the aforementioned techniques for looking at post-exposure behavior (as in the hypokinesis experiments) and immediate responses (using the body motion detector as per the EKR registration) we also included heart rate changes in this sub-study. Heart rate was obtained from an EKG signal that was recorded from the hind quarters of the mouse which are essentially outside the microwave field. A 100 msec. pulse of increasing intensity (but only one pulse per mouse) was used and the three indices of response noted. These results are summarized in Fig. 20 which also shows the estimated brain temperature rise associated with each absorbed energy level. From these results it can be concluded that the sort of neurophysiological responses to WMP that we are primarily studying lie at least an order of magnitude (perhaps two orders) below exposure levels at which "pathological" effects become manifest. This result is consistent with earlier findings using Aplysia in which we deliberately

tried to permanently damage isolated neurons using high level WMP. As long as the temperature rises were not allowed to accumulate, we found that we could not define a clear threshold for "damage" even at levels up to 100 times that needed to perturb firing patterns.

A rather interesting "spinoff" study has also come out of our collaboration with Stavinoha's group. We were interested in ascertaining what, if any responses, a mouse would manifest initially when sacrified with the microwave "brain inactivating" technique (which raises brain temperature about 50°C in roughly 200 msec.). Ideally, for the purposes of the neurotransmitter assay, all neural activity should abruptly cease and therefore no kinetic or electrophysiological response should be seen. In actuality this proved not to be the case. When the mouse was sacrificed not only did it respond with a massive body movement midway into the brief exposure period (as shown in the top trace of Fig. 21) but it still gave some residual kinetic responses to a second, and even a third "lethal" exposure administered two minutes later. When implanted agar filled electrodes were used to monitor the EEG before, during and after the lethal exposure it was noted, as shown in Fig. 22 that a period of <u>increased</u> activity (seizures?) ensued after the exposure and the EEG then decayed away rather gradually (taking a minute or more to "go flat"). Those results suggest that neural activity is actually heightened in response to these lethal

microwave pulse exposures before slowly subsiding. This would make it seem likely that neurotransmitter levels are going to be appreciably changed during the sacrifice process--which sheds some doubt on the efficacy of the technique.

Figs. 23 and 24 summarize this "spinoff" study by comparing what many proponents of the "microwave brain inactivation" technique presume is happening with what we believe is a more likely scenario.

A summary of this progress report appears in Table II. By comparing this table with Table I (taken from our 1981 proposal) it can be seen that a number of our objectives have been reached and that we are progressing towards several others. A notable exception of course, is line D of Table I wherein we proposed to study effects on unconstrained animals. We have chosen to defer this aspect of the project in favor of other endeavors. We have proven fruitful. It can be seen from a comparison of Tables I and II that we have explored areas not originally proposed (or even envisioned) and this is a natural outcome of scientific research.

TABLE II

SUMMARY OF PROGRESS REPORT

Neural System	Methods Used	Results and Conclusions
Aplysia Pacemaker Neurons	Perfusion simulation or suppression of microwave temperature rise. Equicaloric pulses. Reversal Potential Measurement	"Hot Flushing" mimics microwave response. Temperature clamping eliminates microwave response. Detection mechanism related to T sensivity. Optimal pulse about 0.5 sec.--curve fits with model. Hyperpolarizing phase reversible--indicates G_K mechanism.
Rat Hippocampal Slice	Extracellular Recording Evoked Responses Equicaloric Pulses	Single WMP with temp. rise of 0.01 to 0.1°C sufficient to give effects. Immediate inhibition, followed by very long lasting execution. Inhibition not seen at lowest WMP levels. Short term response greater for shorter responses, but not long term.
Intact Mice Low Level WMP	Evoked Kinetic Responses (EKR) Equicaloric Pulses EEG Changes	EKR produced with temp. rises of about 0.5°C. Onset delay of EKR most reliable parameter. Delay decreases with narrower pulses of equal energy. Results to date fit model. Preliminary EEG data indicates lower level effect.
Intact Mice High Level WMP	Use of Stavinoha's "Brain Inactivator" Compare immediate response, post exposure behaviour and heart rate Response to "Lethal" Exposures	Large separation between these neurophysiological perterbations and definite pathologies. "Lethal" microwave exposures appear to accelerate neural activity prior to extinguishing it.

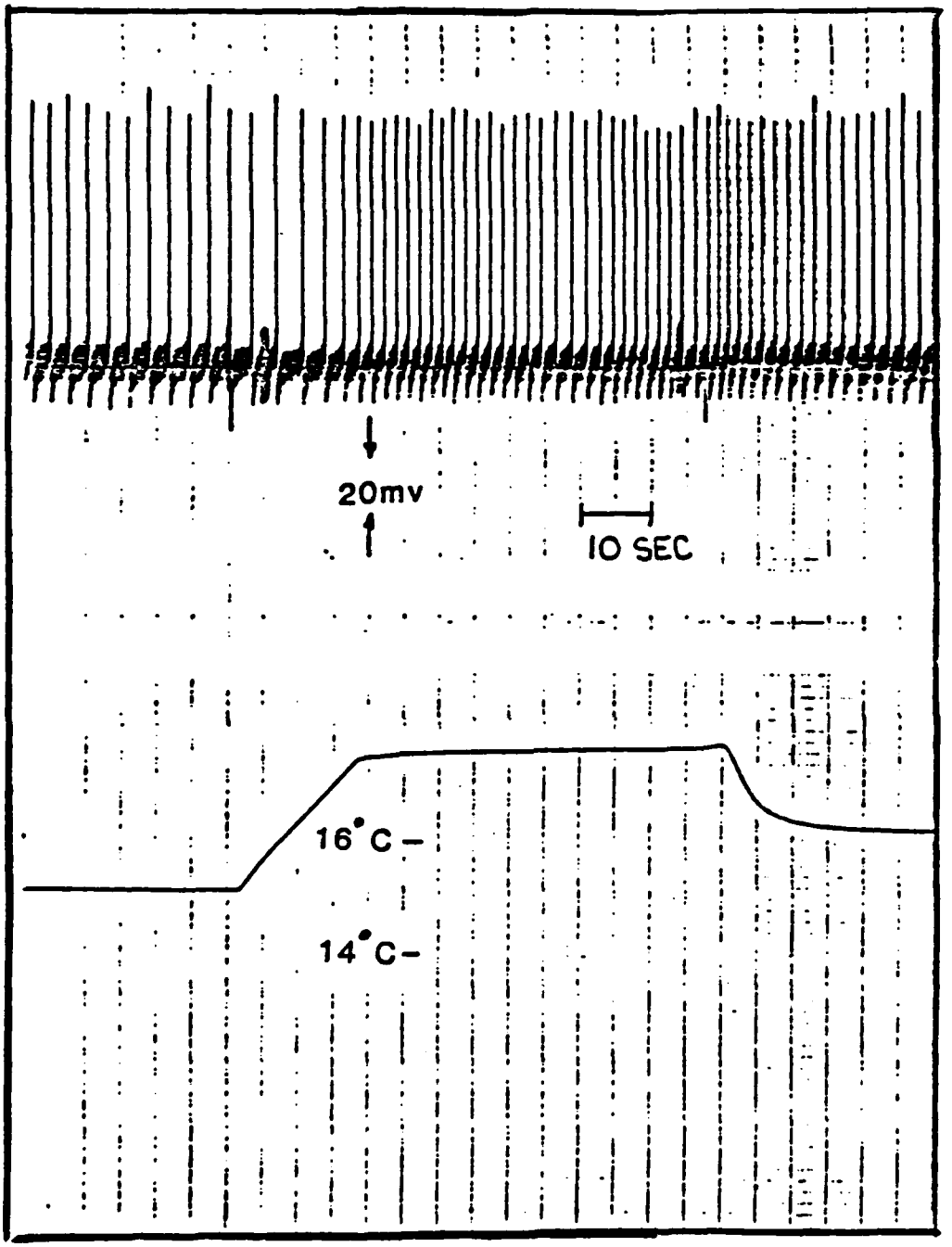

A microwave-induced temperature and firing rate profile.
F = 2.45 GHz; P ≅ 15 watts.

FIG 1

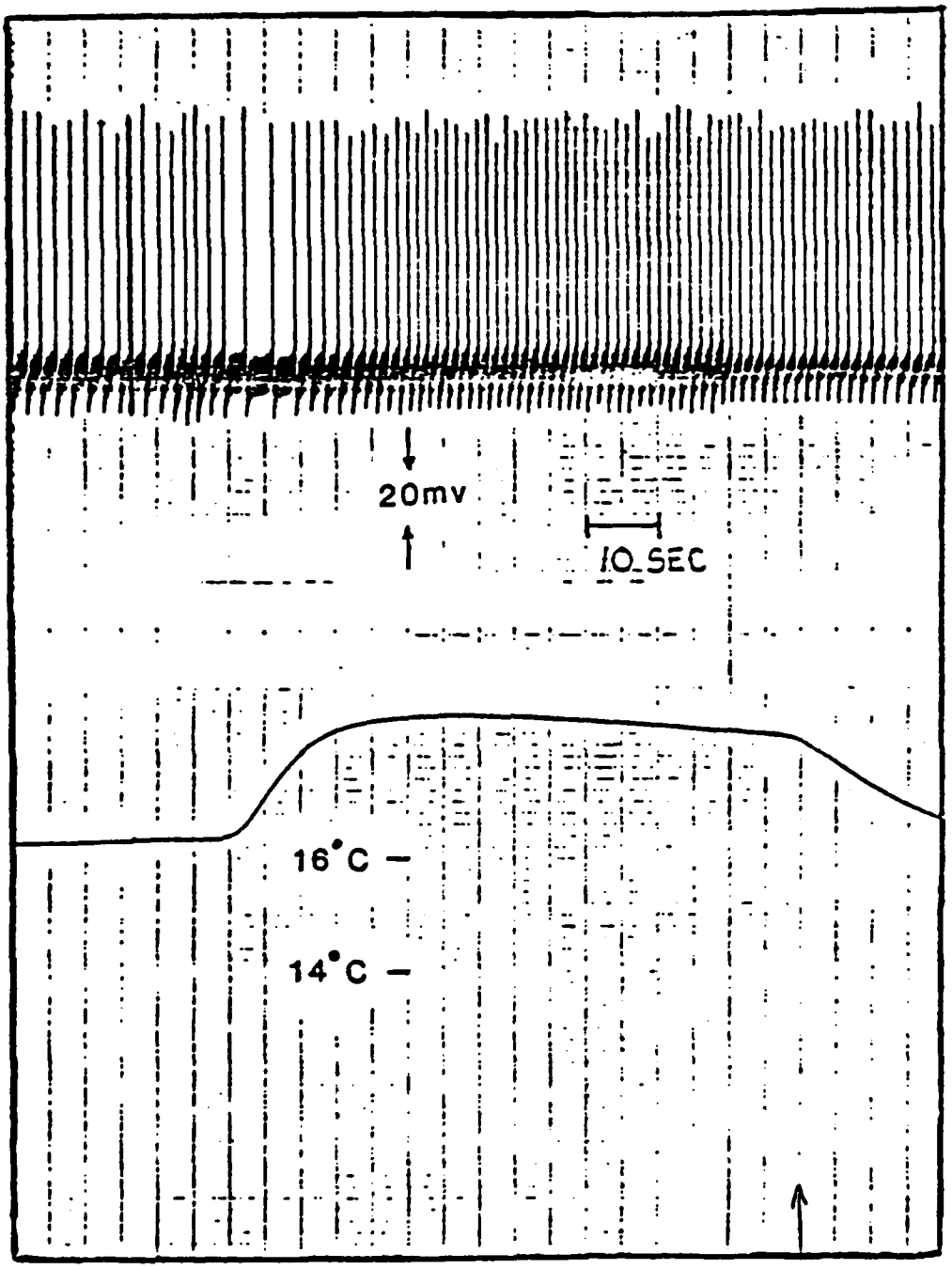

A perfusion mimic of a microwave-induced temperature profile with associated firing rate profile.

FIG. 2

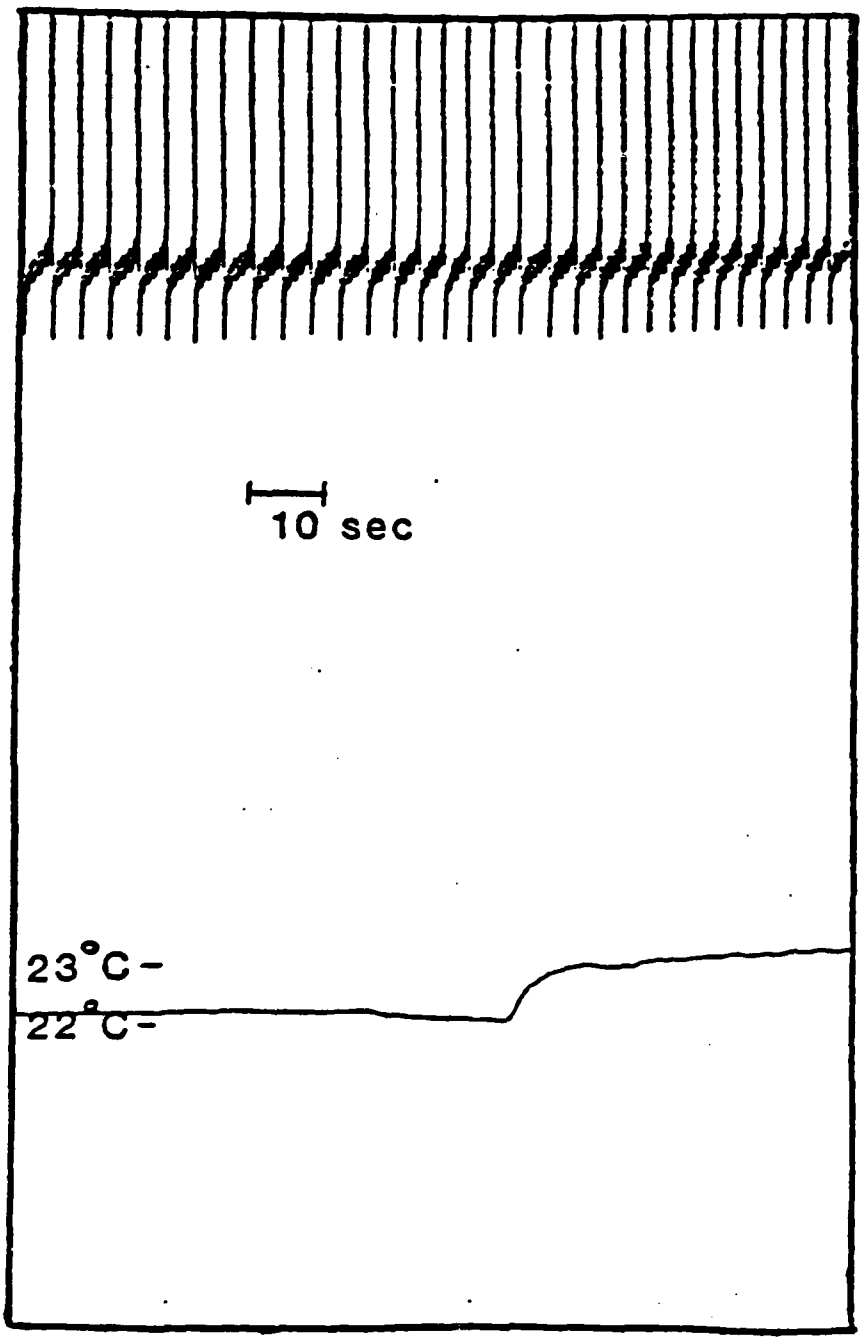

A very suppressed, continuous 15 watt application of microwave power.

FIG 3

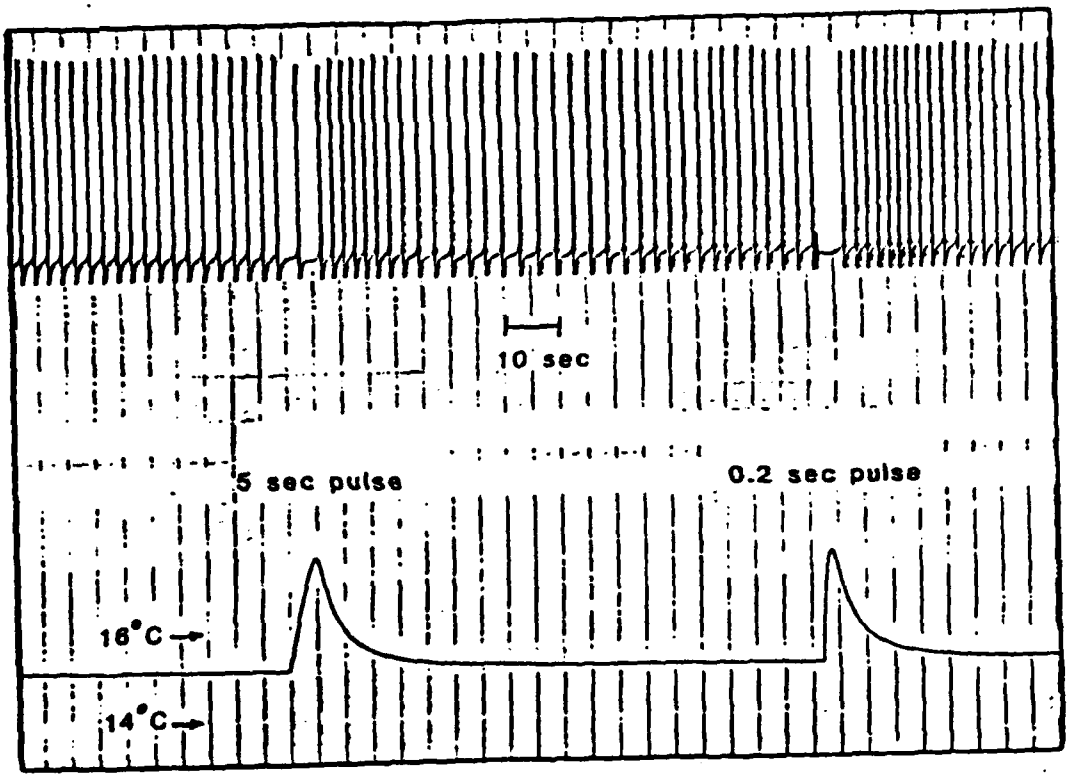

FIG. 4

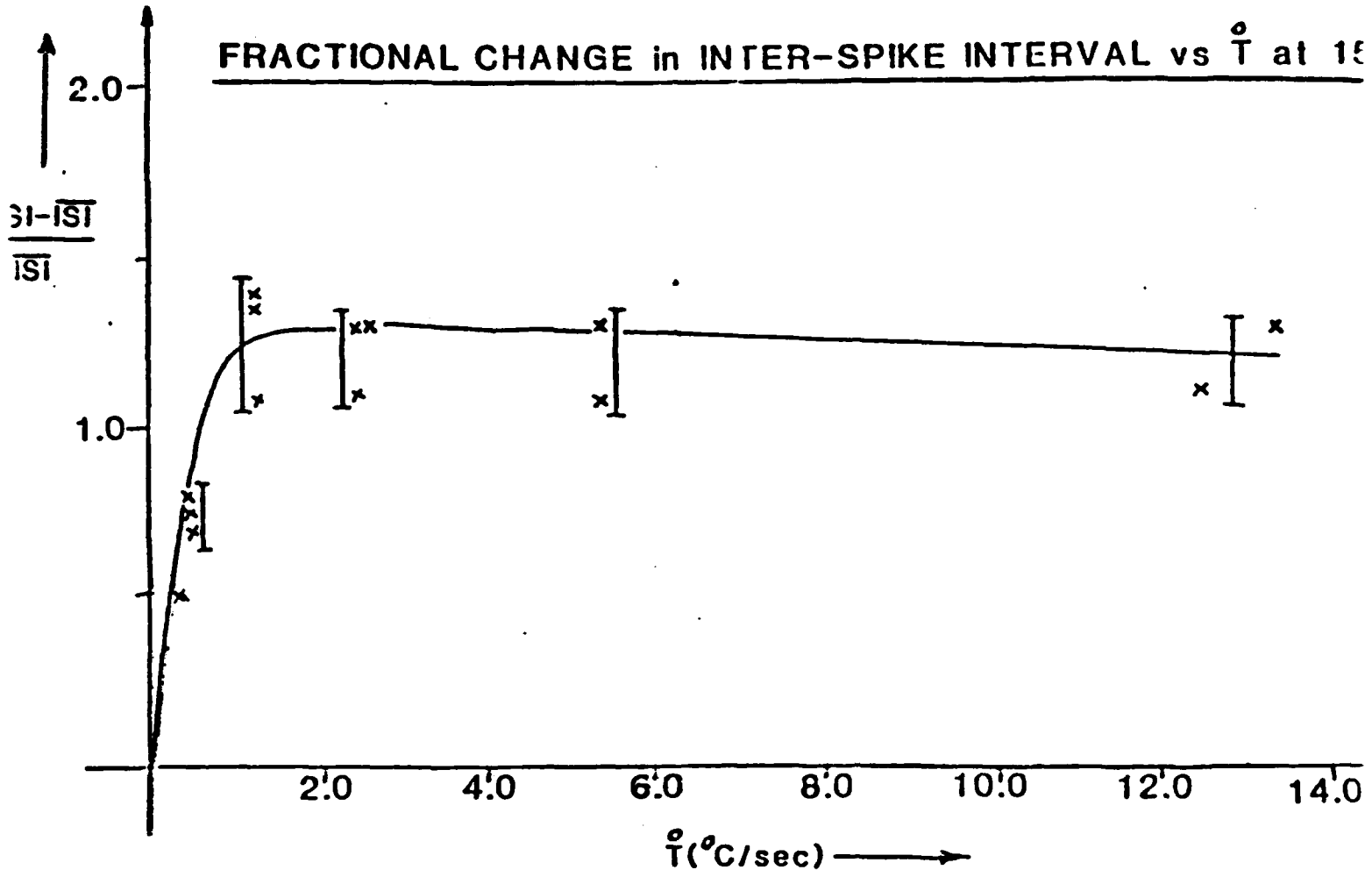
FRACTIONAL CHANGE in INTER-SPIKE INTERVAL vs $\dot{T}$ at 1
2.0
1.0
SI-ISI
ISI
2.0
4.0
6.0
8.0
10.0
12.0
14.0
$\dot{T}$(°C/sec)

FIG 5

(corrected) CELLULAR VOLTAGE RESPONSE to 150msec PULSE
at 5 DIFFERENT LEVELS of CURRENT INJECTION.
T≅ 22°C. ΔT≅ 2.1°C. F= 2.45GHz.

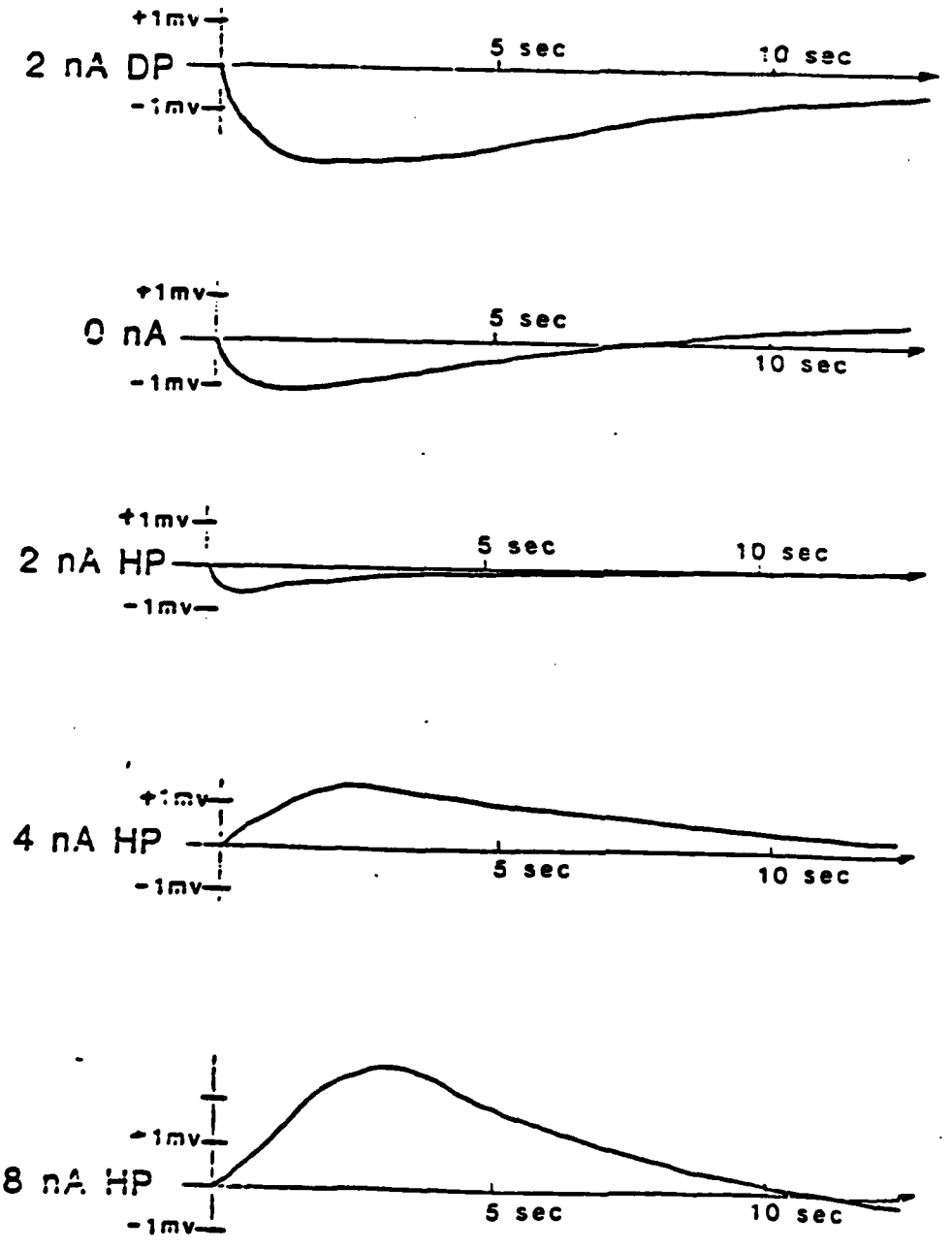

FIG 6

PEAK CORRECTED CELLULAR VOLTAGE RESPONSE vs CURRENT INJECTION LEVEL

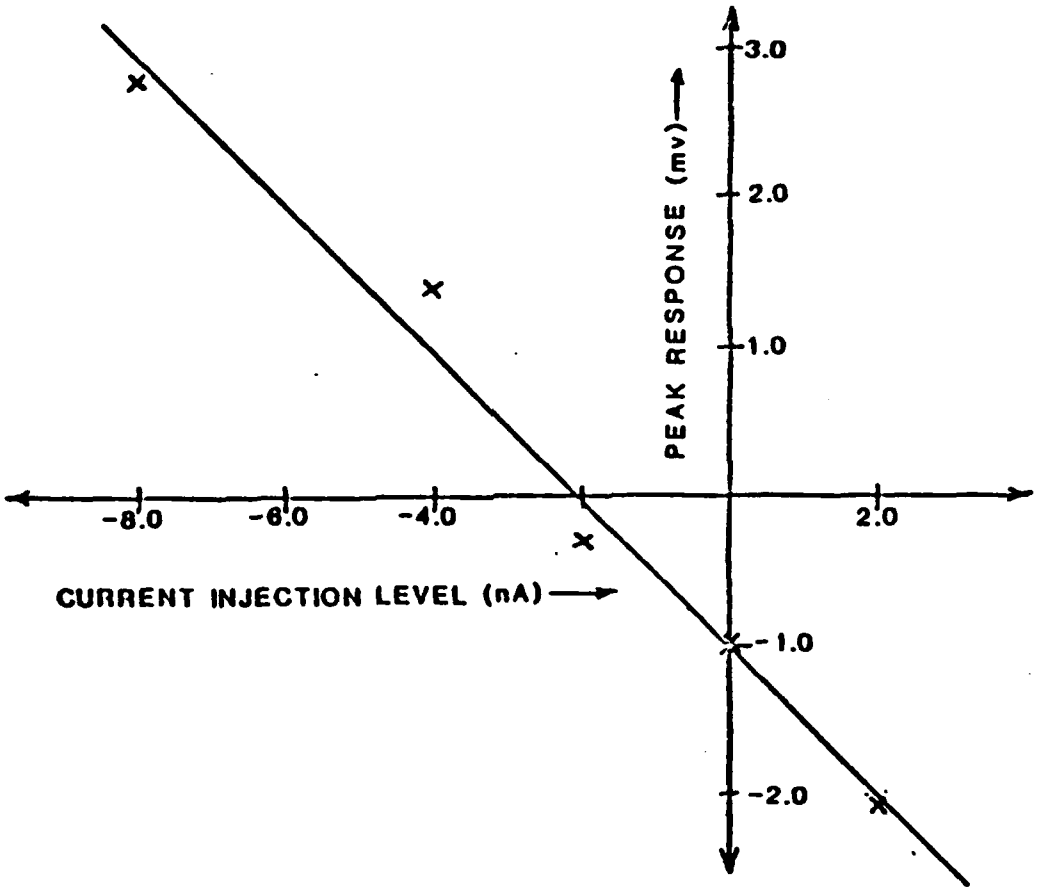

FIG 7

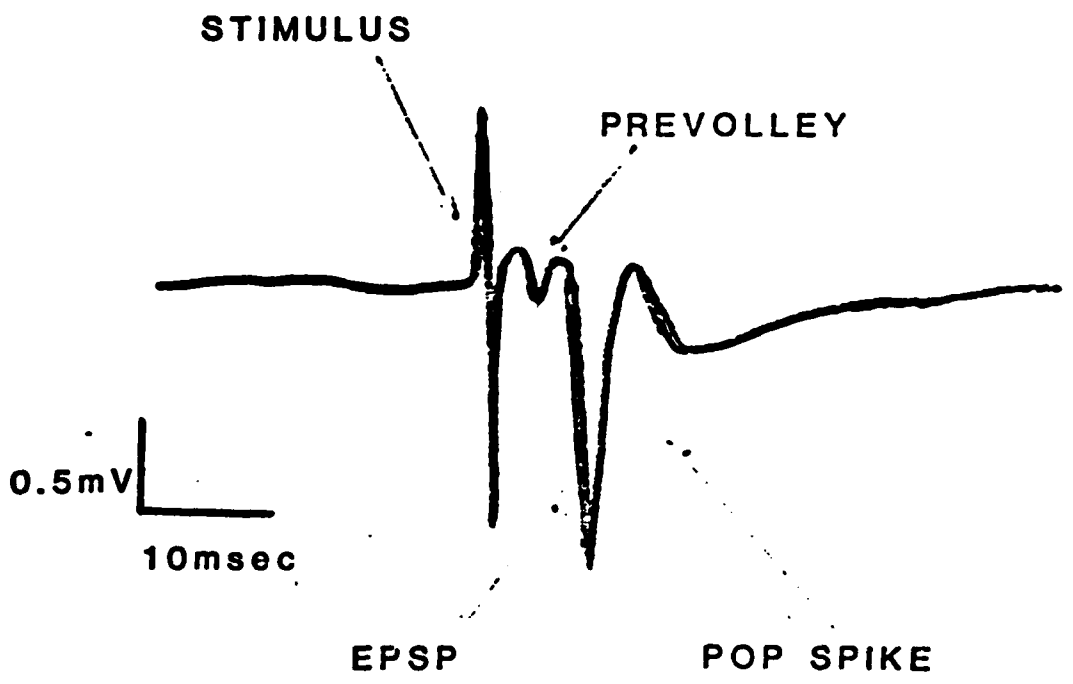

COMPONENTS OF THE EVOKED RESPONSE

FIG. 8

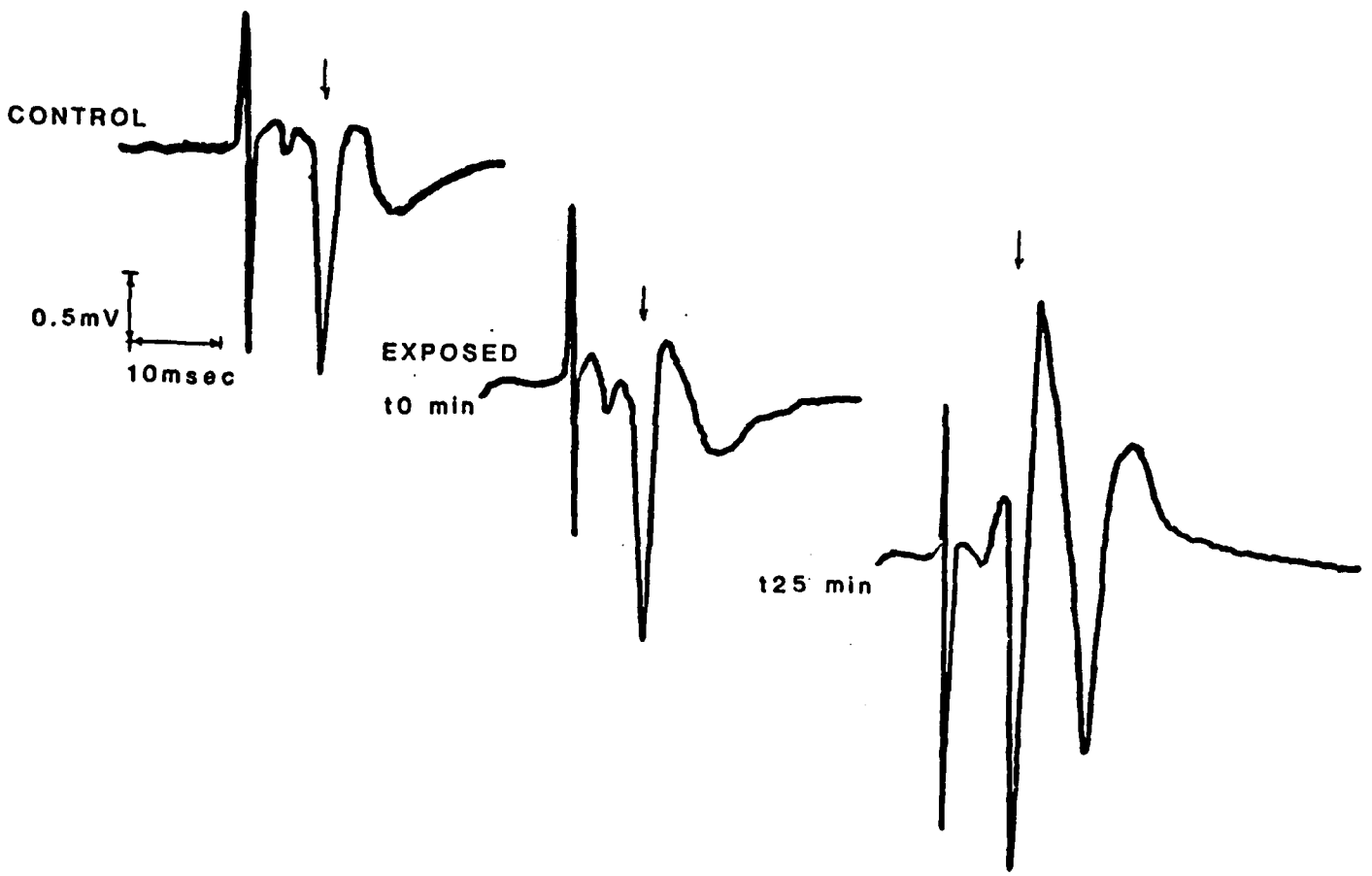

EFFECT OF EXPOSURE TO 4msec PULSES AT 30W/cc SAR

FIG. 9

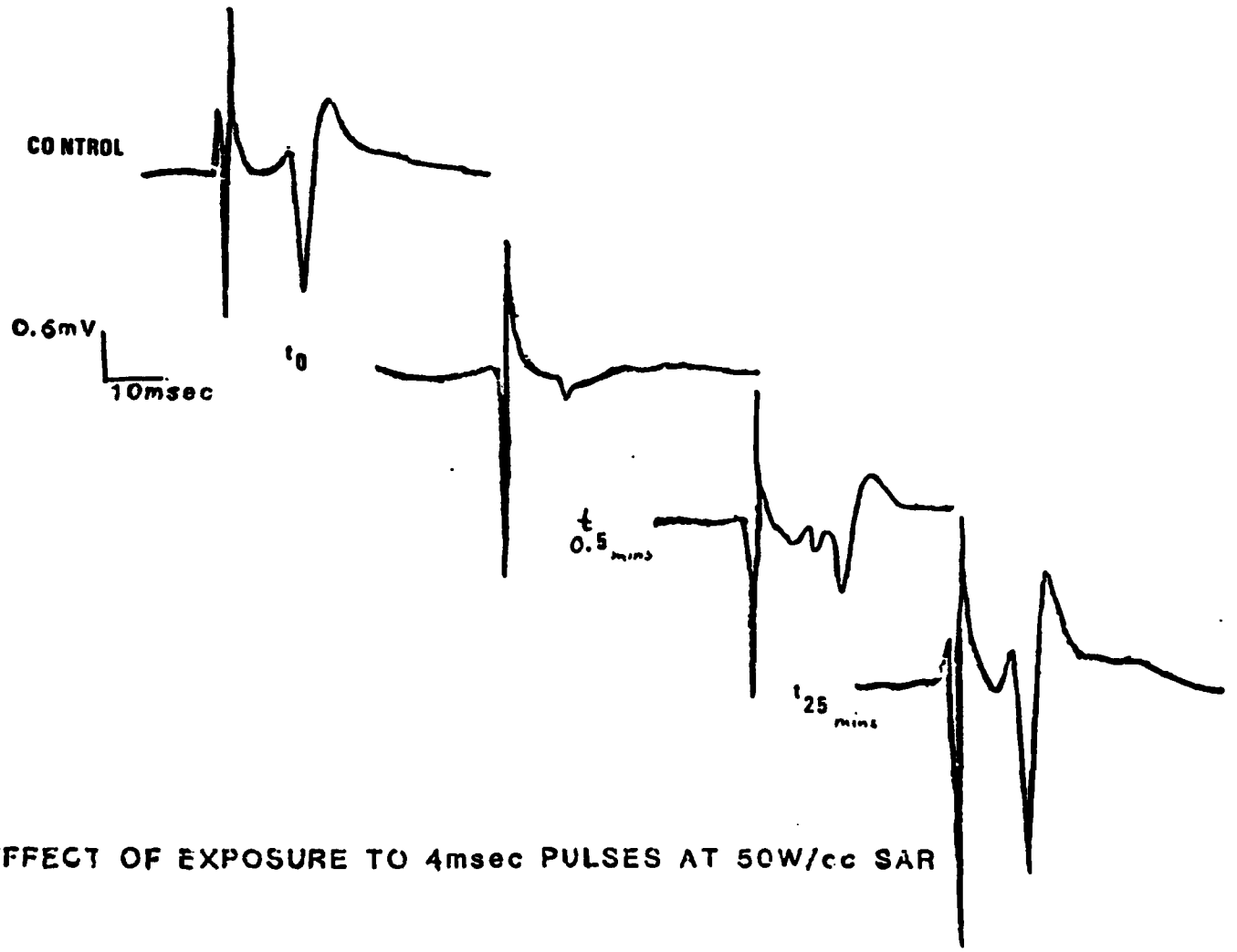

EFFECT OF EXPOSURE TO 4msec PULSES AT 50W/cc SAR

FIG. 10

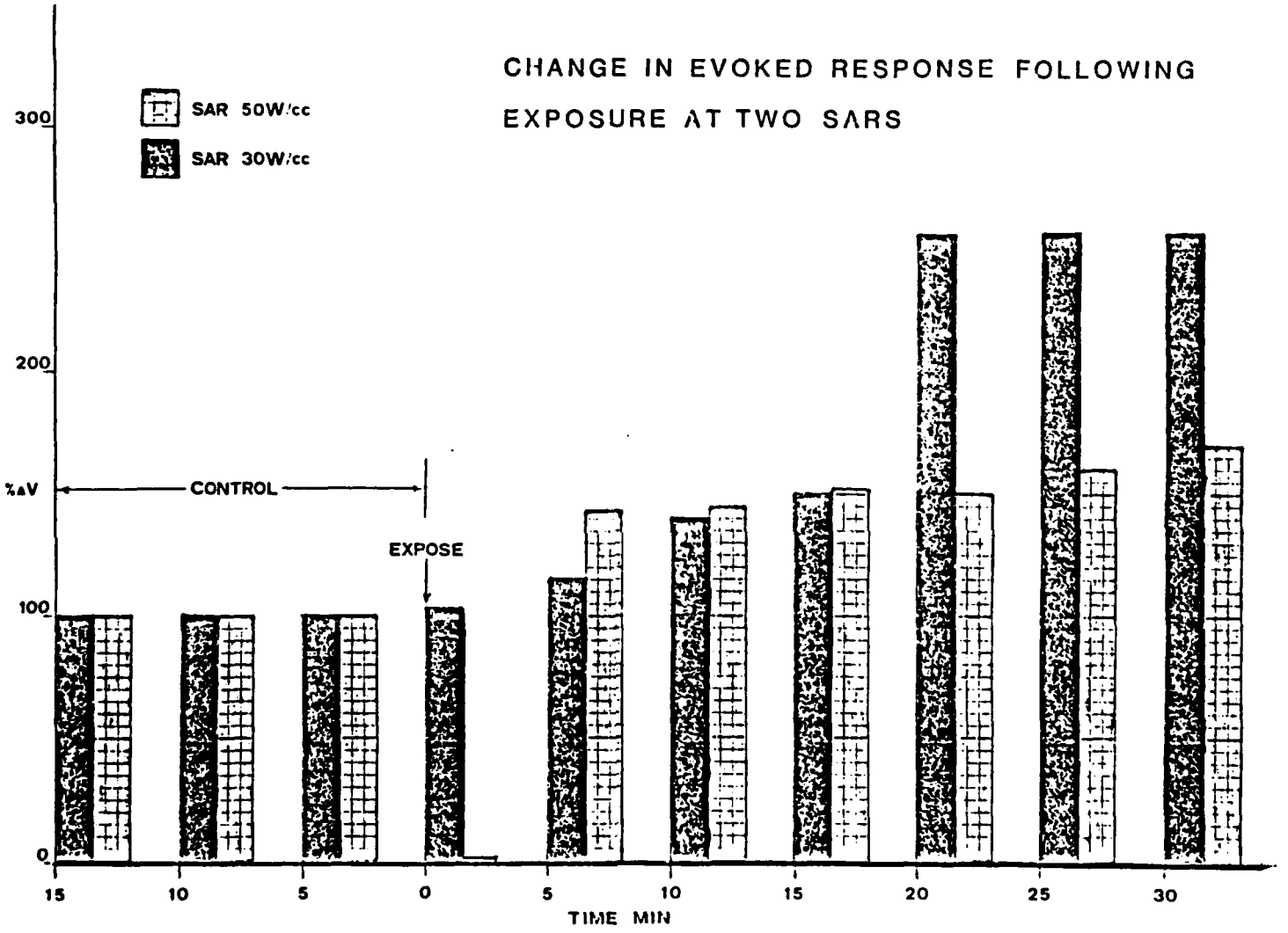
CHANGE IN EVOKED RESPONSE FOLLOWING
EXPOSURE AT TWO SARS
SAR 50W/cc
SAR 30W/cc
300
200
100
0
%ΔV
CONTROL
EXPOSE
15
10
5
0
5
10
15
20
25
30
TIME MIN

FIG 11

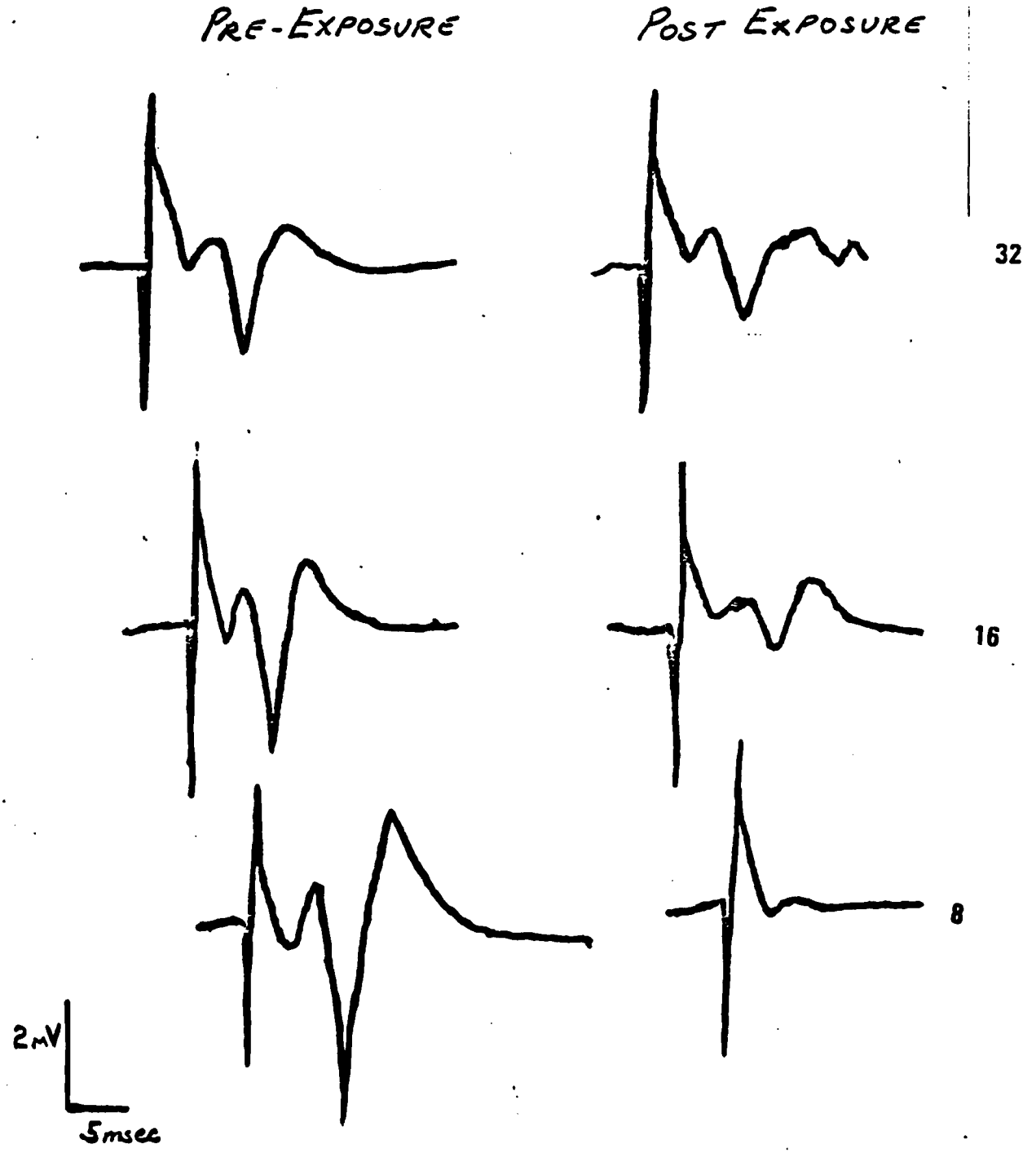
PRE-EXPOSURE
POST EXPOSURE
32
16
8
2mV
5msec
SAR 50W/g
PULSE WIDTH (msec)

FIG 12

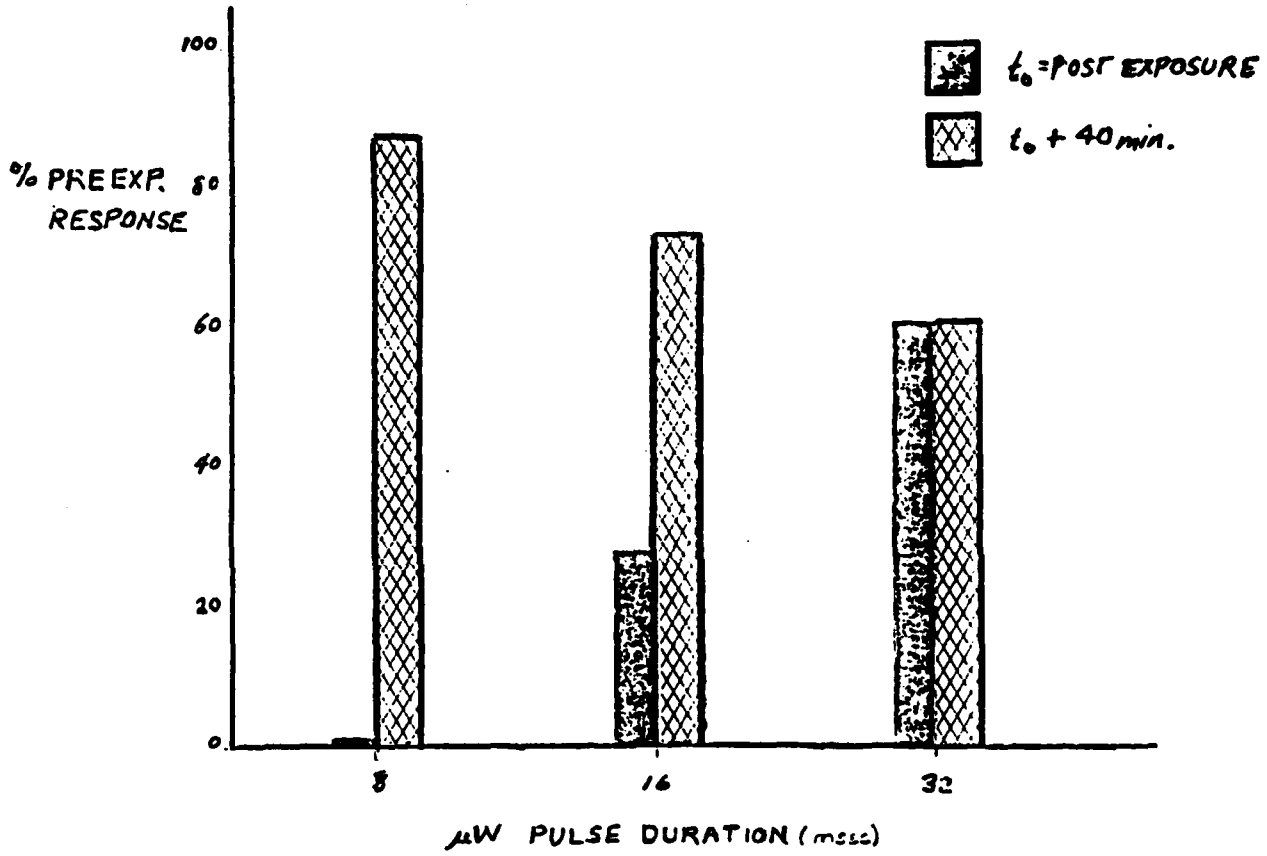
100
80
60
40
20
0
% PRE EXP. RESPONSE
t_o = POST EXPOSURE
t_o + 40 min.
8
16
32
μW PULSE DURATION (msec)
ΔT = 0.05C°

FIG. 13

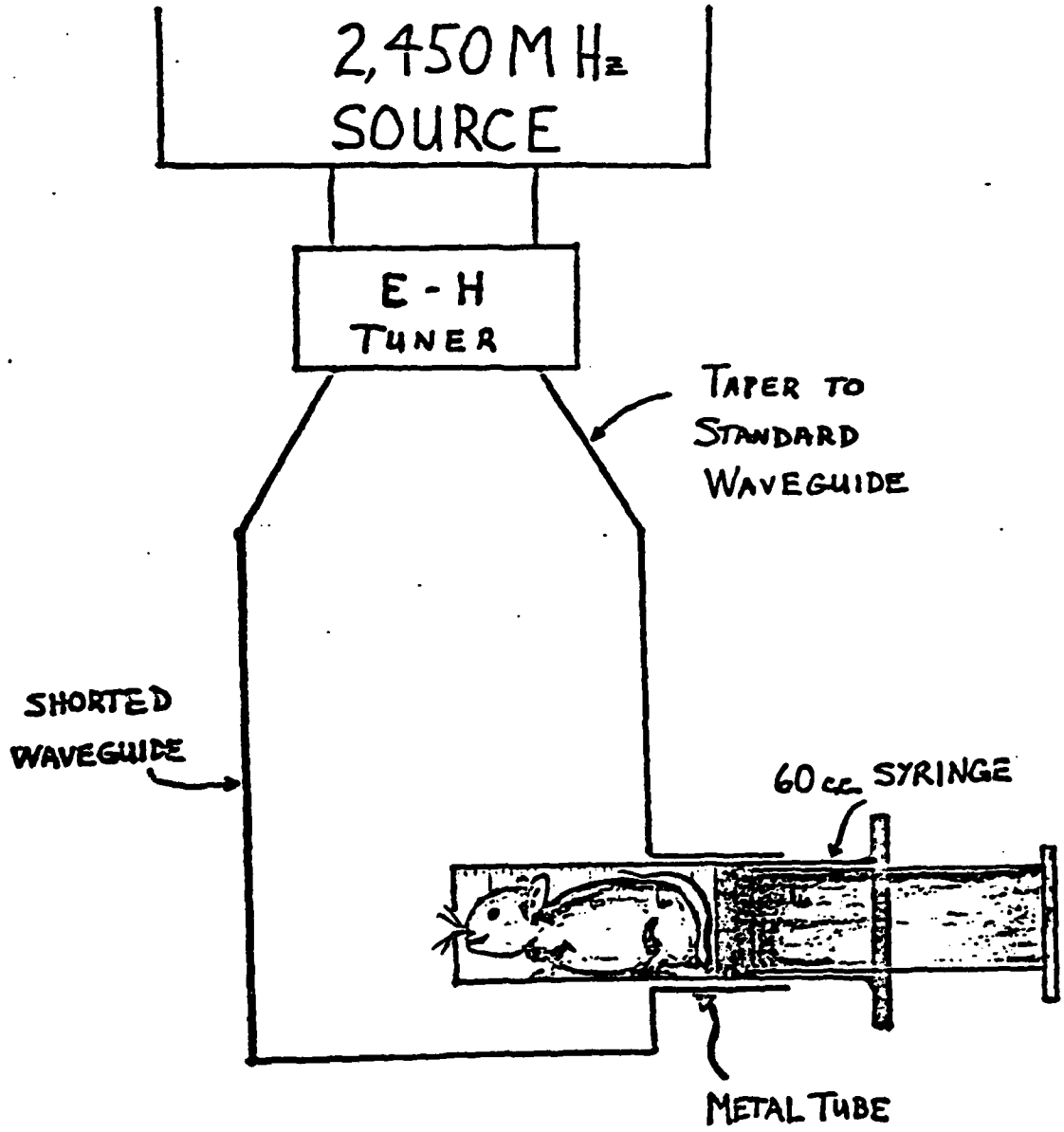
2,450 MHz
SOURCE
E - H
TUNER
TAPER TO
STANDARD
WAVEGUIDE
SHORTED
WAVEGUIDE
60 cc SYRINGE
METAL TUBE

FIG 14

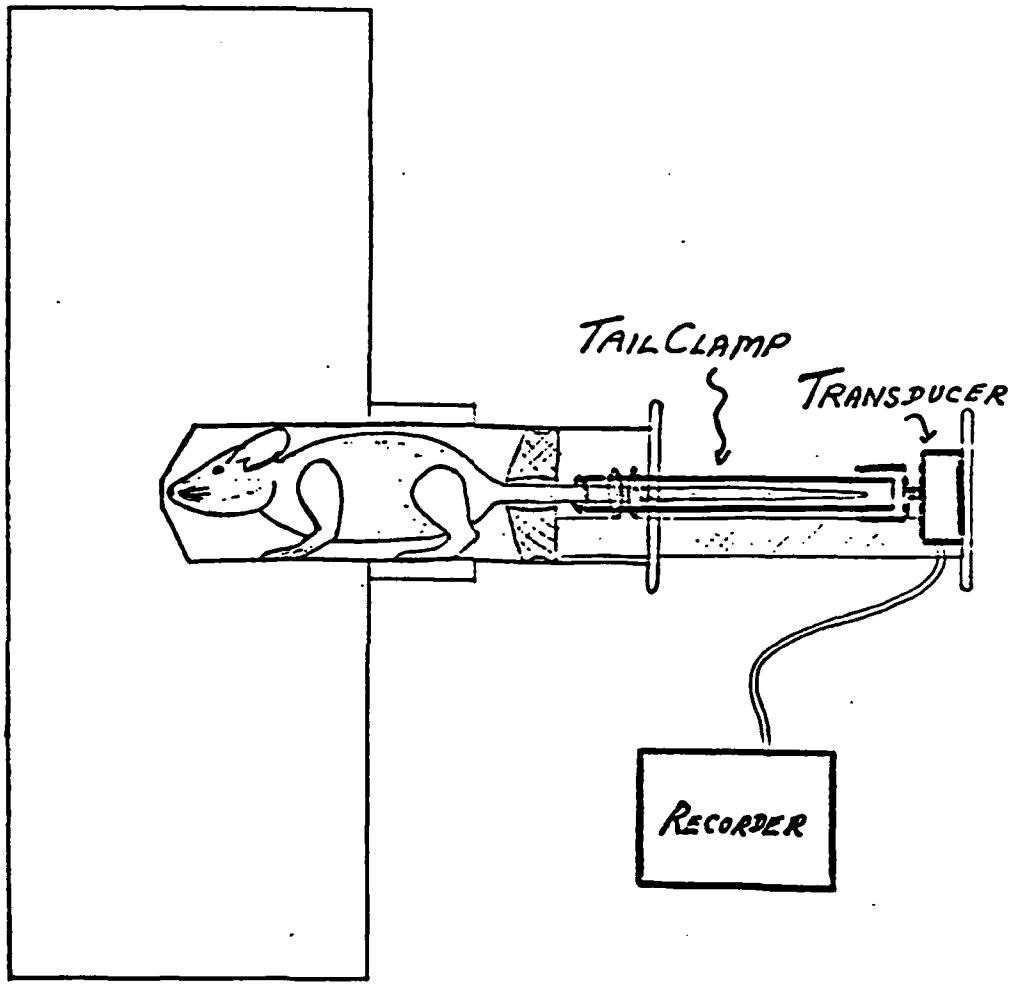

FIG 15

EKR EXPOSURE AND RECORDING SYSTEM

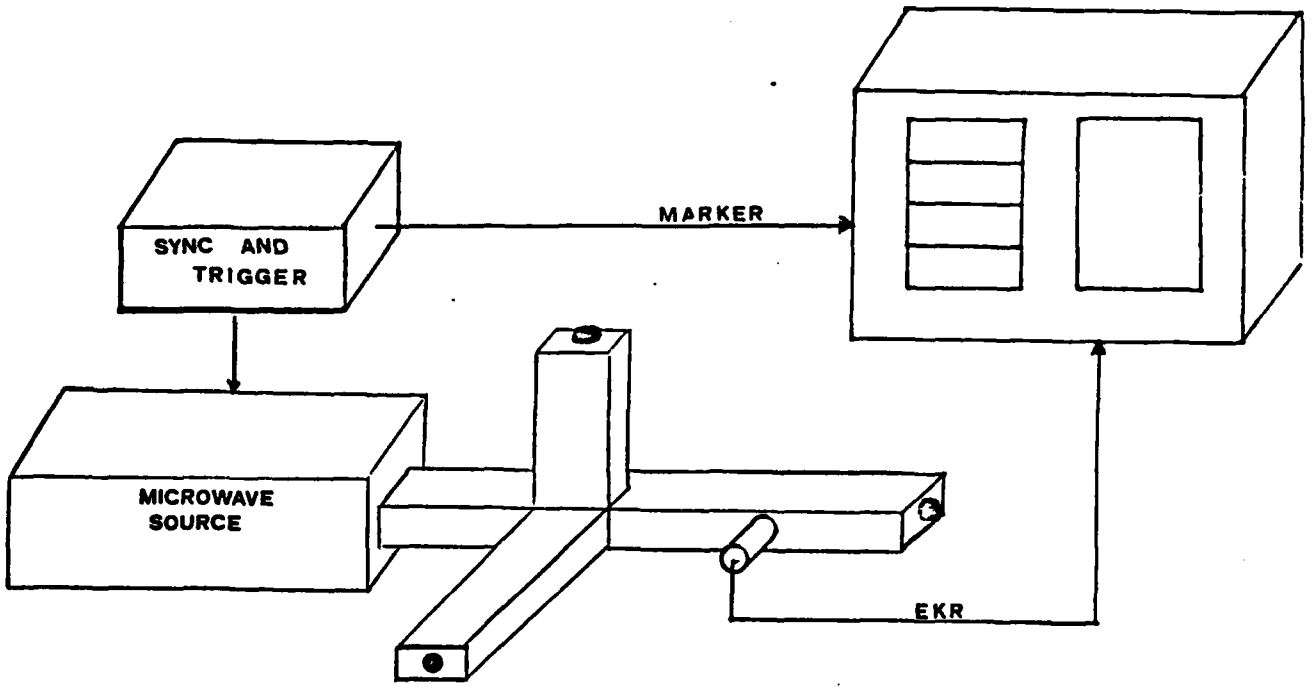

FIG 16

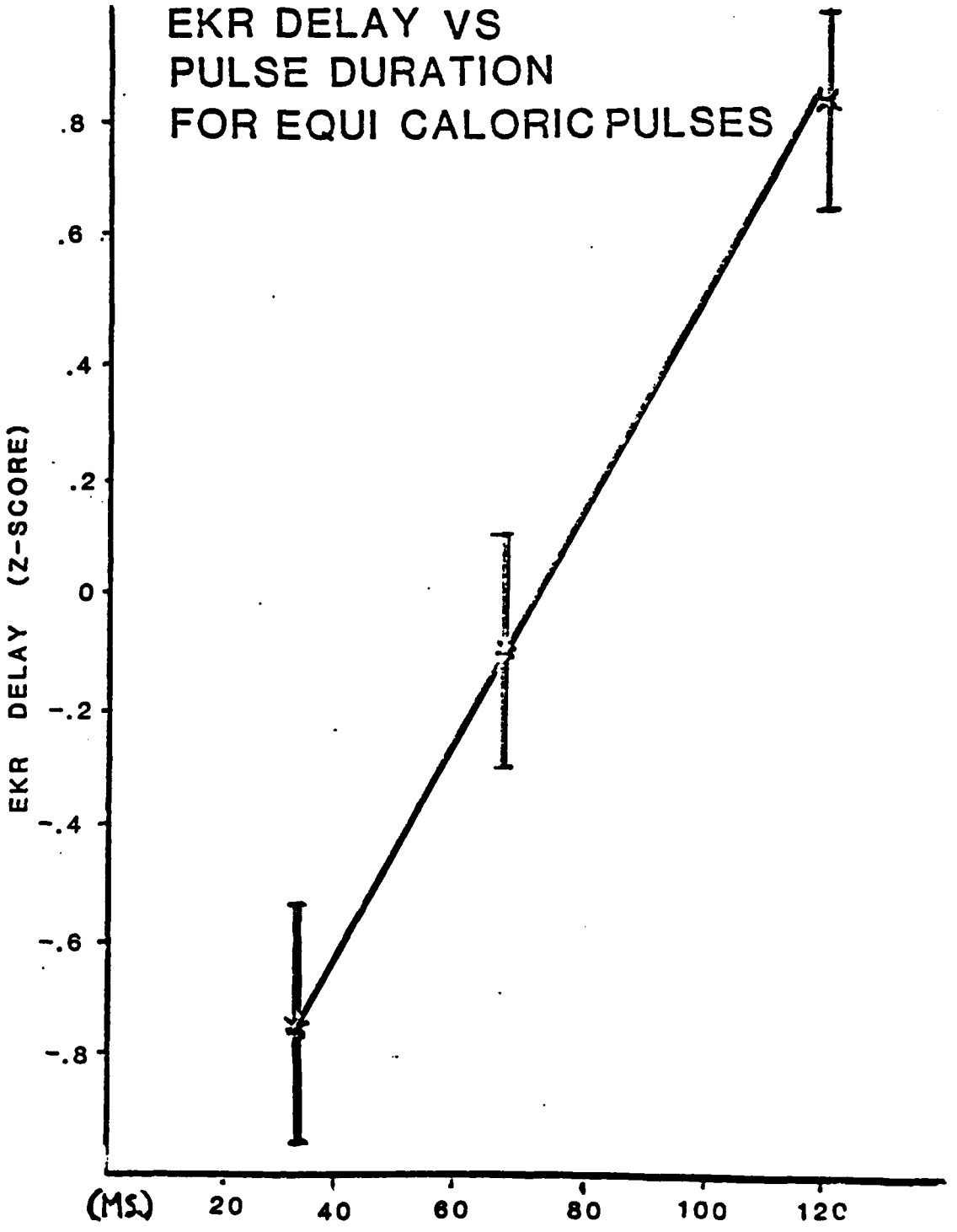
EKR DELAY VS
PULSE DURATION
FOR EQUI CALORIC PULSES
EKR DELAY (Z-SCORE)
.8
.6
.4
.2
0
-.2
-.4
-.6
-.8
(MS)
20
40
60
80
100
120

FIG 17

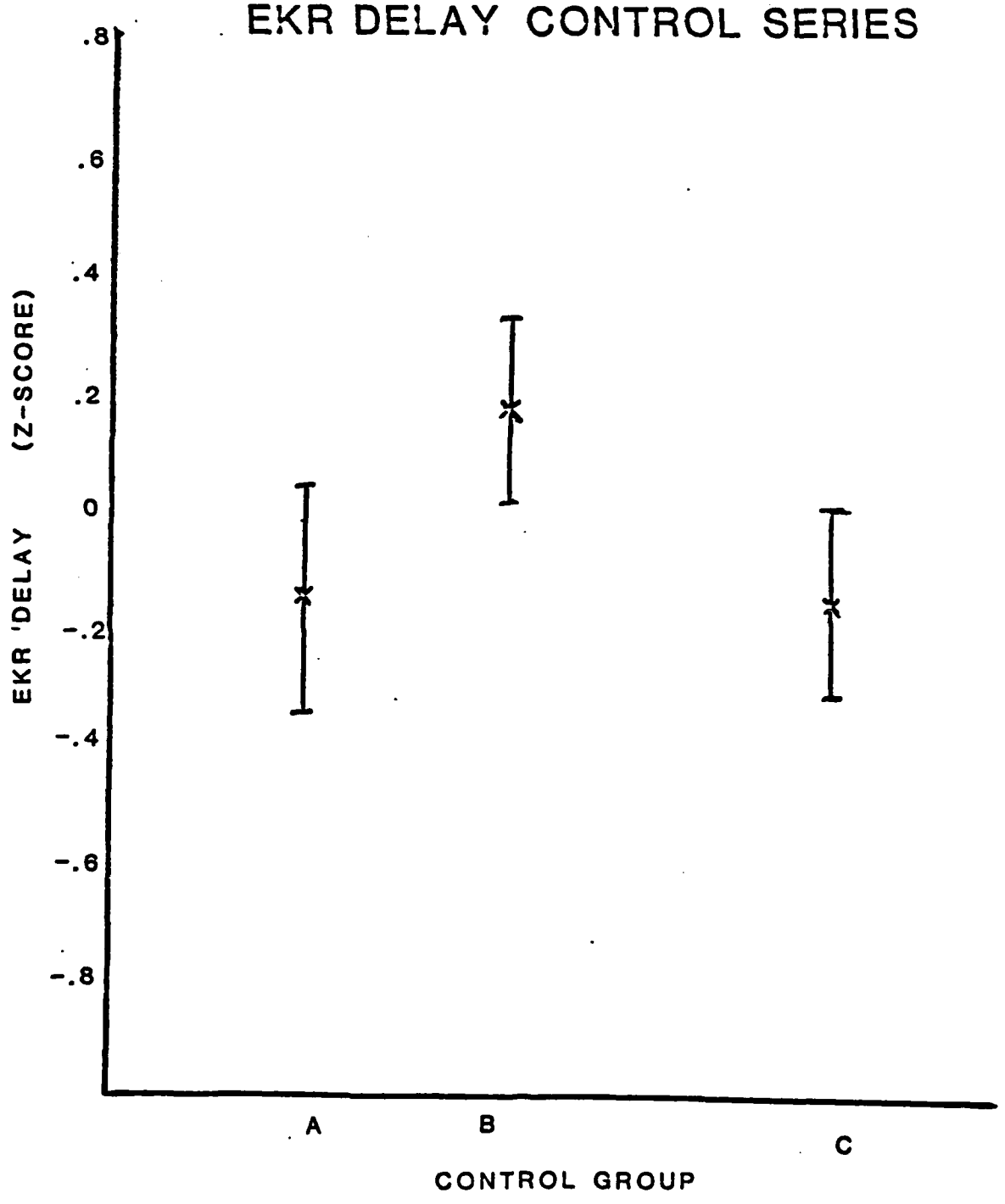
EKR DELAY CONTROL SERIES
EKR 'DELAY (Z-SCORE)
.8
.6
.4
.2
0
-.2
-.4
-.6
-.8
A
B
C
CONTROL GROUP

FIG 18

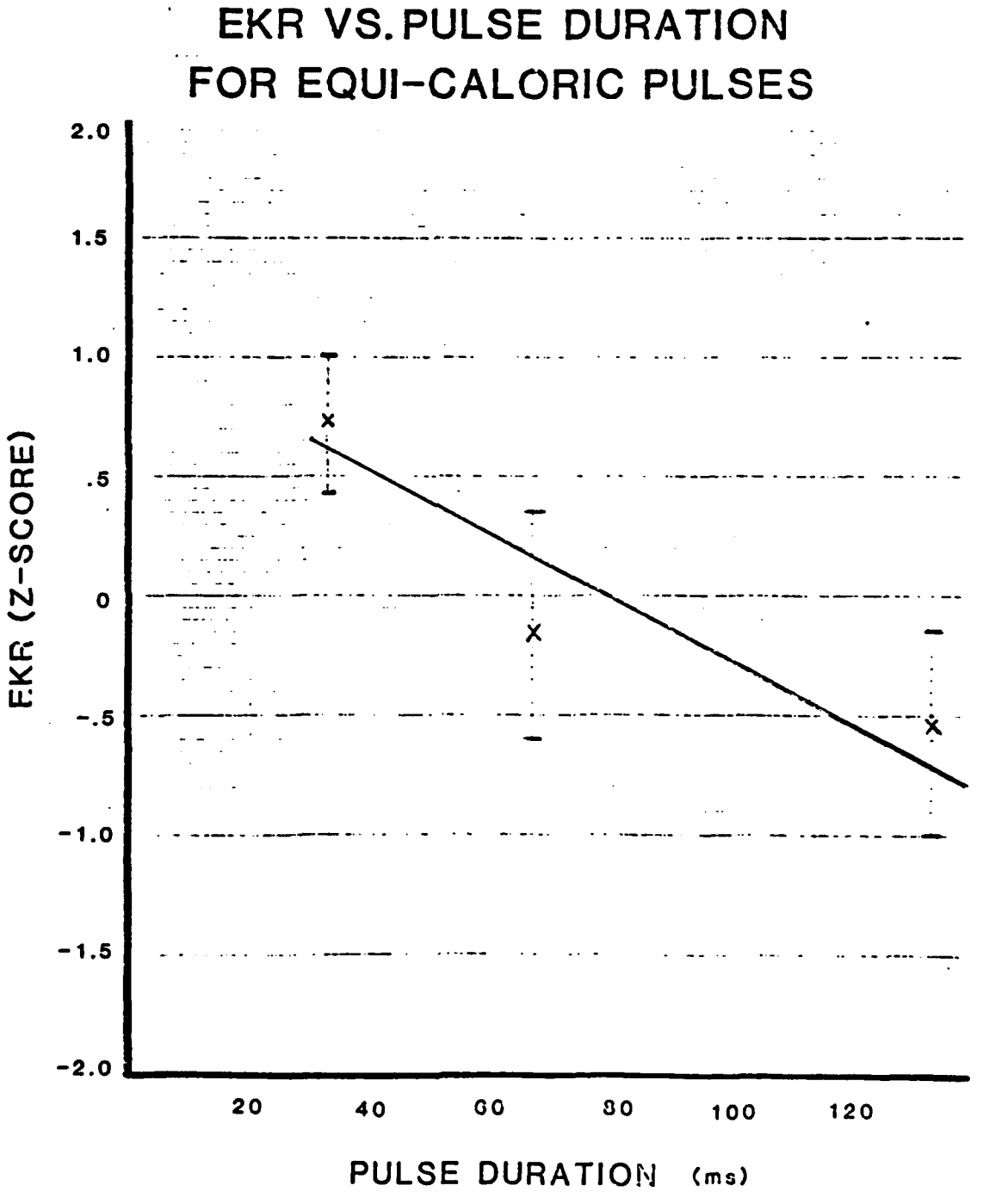
EKR VS. PULSE DURATION
FOR EQUI-CALORIC PULSES
2.0
1.5
1.0
.5
0
-.5
-1.0
-1.5
-2.0
EKR (Z-SCORE)
20
40
60
80
100
120
PULSE DURATION (ms)

FIG 19

KINETIC RESPONSES TO A SERIES OF "BRAIN INACTIVATING" MICROWAVE EXPOSURES

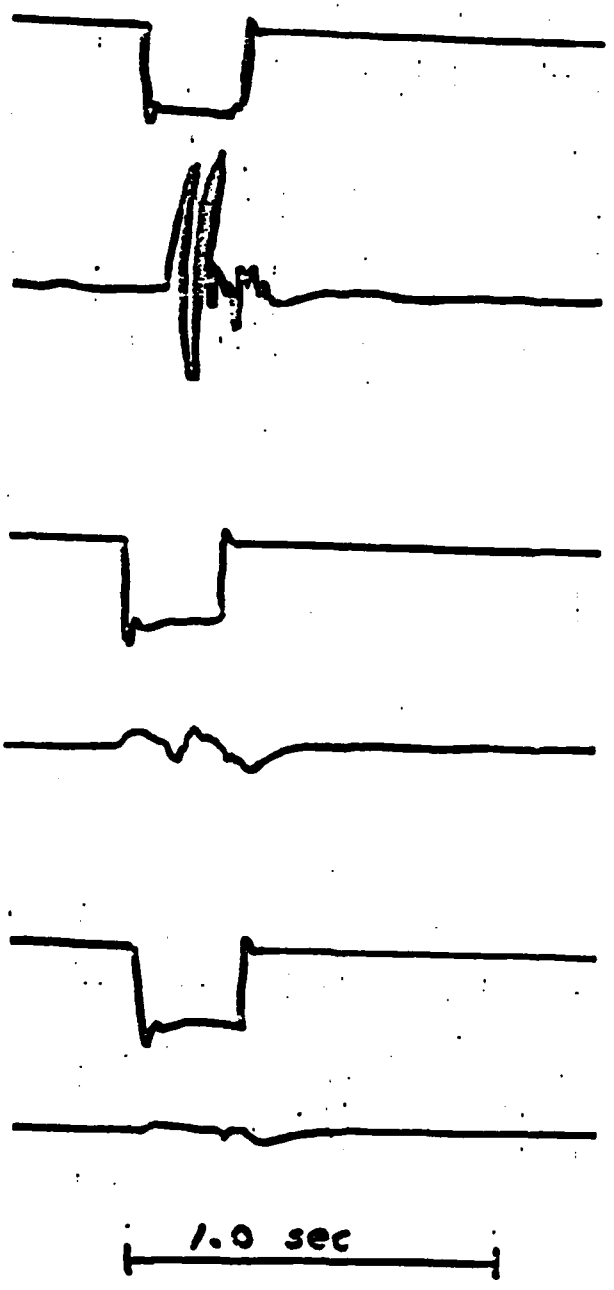

FIG 20

EEG Recording Following "Brain Inactivating" Microwave Exposure

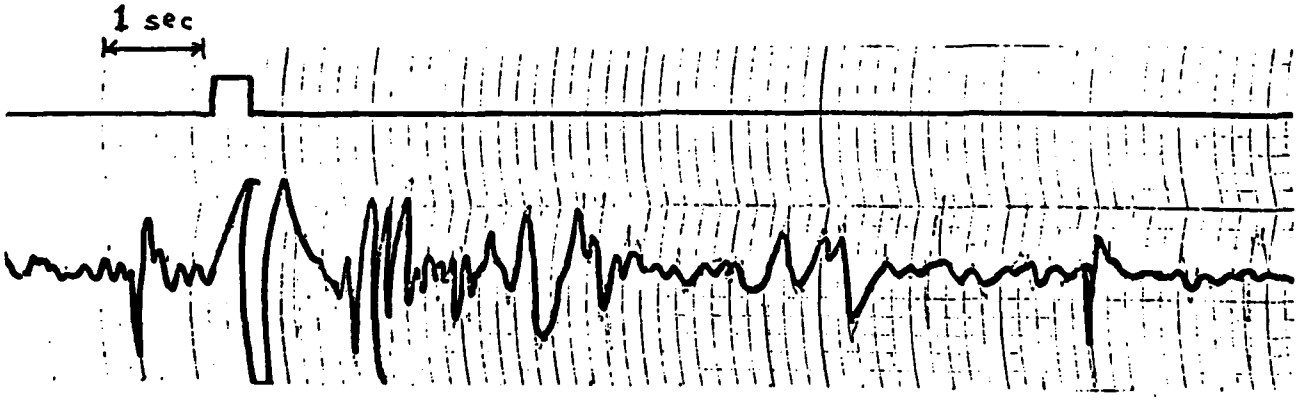

Fig 21

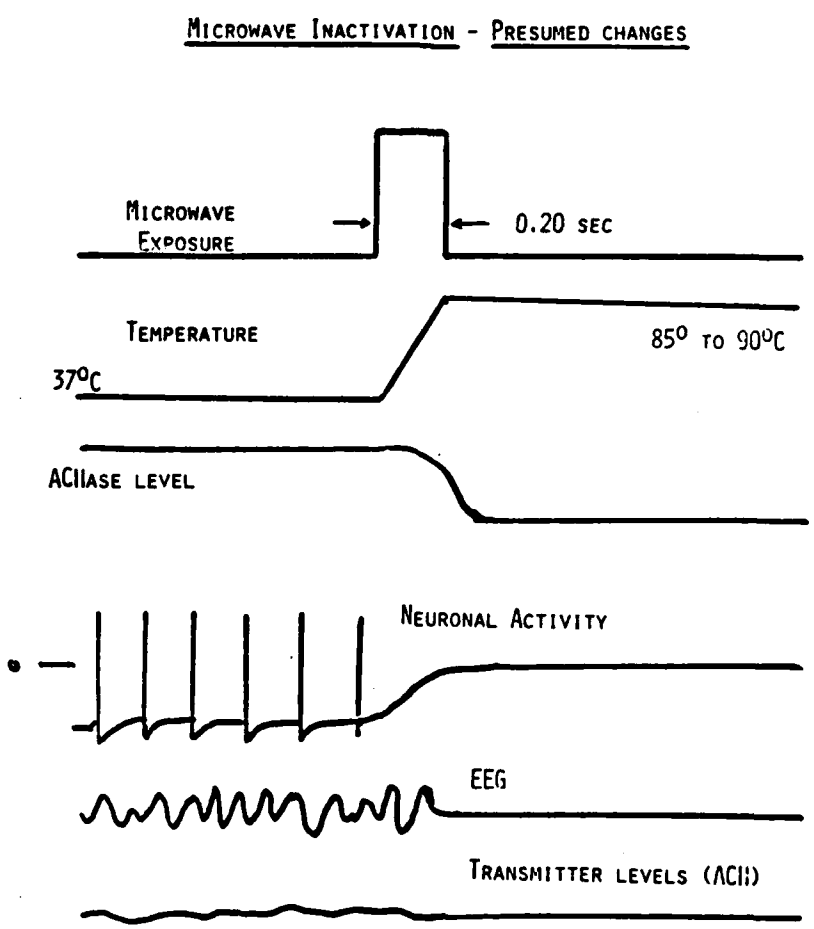
MICROWAVE INACTIVATION - PRESUMED CHANGES
MICROWAVE EXPOSURE
0.20 SEC
TEMPERATURE
37°C
85° TO 90°C
ACHASE LEVEL
NEURONAL ACTIVITY
EEG
TRANSMITTER LEVELS (ACH)

FIG 22

MICROWAVE "INACTIVATION" - MORE LIKELY SCENARIO

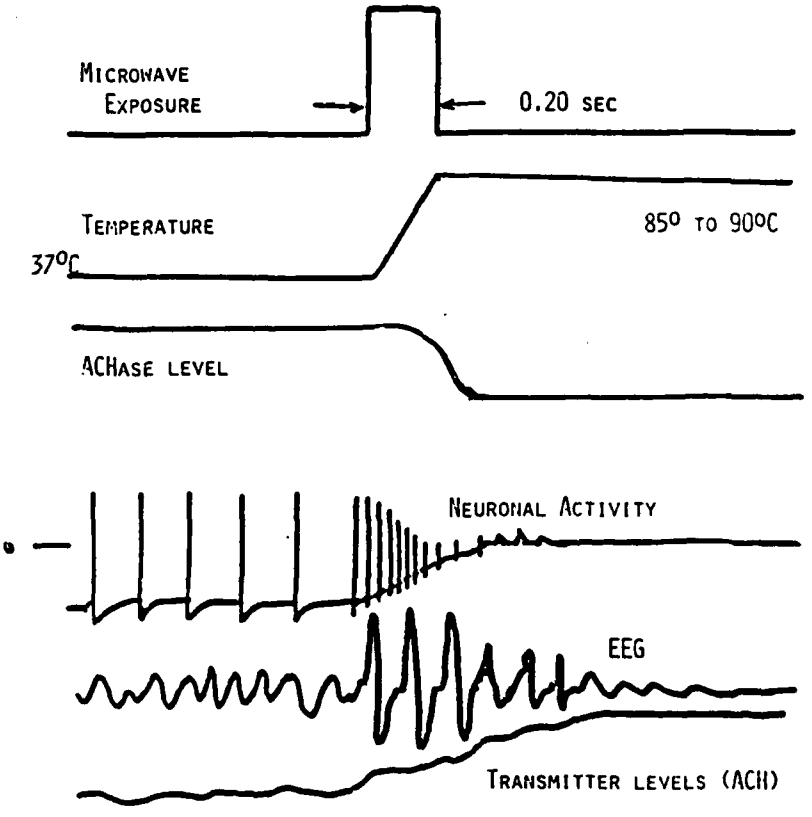

FIG 23

MODULATION OF NEURAL ACTIVITY USING WIDE MICROWAVE PUSES AND PULSE TRAINS

by

Abdelkrim Aitarkoub

Diplôme d'Ingenieur,
Ecole Nationale Polytechnique d'Alger,
1982

A thesis submitted to the

Faculty of the Graduate School of the

University of Colorado in partial fulfillment

of the requirements for the degree of

Master of Science

Department of Electrical Engineering

1985

This thesis for the Master of Science degree by

Abdelkrim Aitarkoub

has been approved for the

Department of

Electrical Engineering

by

Frank S. Barnes

Howard Wachtel

Date 7/18/85

Aitarkoub, Abdelkrim (M.S., Electrical Engineering)

Modulation of Neural Activity Using Wide Microwave Pulses and Pulse Trains

Thesis directed by Professor Frank S. Barnes

Previous studies on the effects of pulsed microwave exposure on the central nervous system of mice showed that the EEG power in the 4 to 8 Hz range was reversibly depressed immediately after exposure, recovering within a few minutes. These studies were extended to include determination of the threshold for the effect induced by a single microwave pulse and effects of wide microwave pulse trains on the EEG of intact, conscious mice.

Cortical electroencephalograms were recorded before and after exposure. Spectral power densities were calculated and EEG power shifts due to microwave exposure were quantified. In the threshold experiments, the energy content of the pulse was reduced by shortening the duration of the pulse. Animals were subjected to a series of microwave pulses lasting from 32 to 2 ms, yielding cortical temperature rises from 1° C to 0.05° C. The pulses peak power was kept constant producing an SAR of 130.6 W/g. The threshold for the effect of a single pulse is low. Effects were elicited by pulses whose energy content yielded a cortical temperature increase of 0.1° C. In the repetitive pulse train experiments, animals were subjected to a series of equi-caloric trains of microwave pulses, all yielding a total cortical temperature increase of 1° C. The trains had the same energy content and the same duration (6 seconds). The pulses peak power was kept constant producing an SAR of 43.5 W/g. These exposures differed in the pulses

repetition rate (PRR), with repetition frequencies from 4 to 12 Hz. The energy content of a single pulse within the trains was below the threshold for the detection of a single pulse. The EEG changes produced by these microwave pulse trains were quite different for all PRRs than that ellicited by a single wide microwave pulse which yields the same temperature increase and the same $\dot{T}$. In general, the EEG shift was smallest in the frequency bin at the PRR, which suggests an "Anti-Resonance" effect.

This study shows that the brain can resolve pulse patterning and this could be a way of sending signals into the brain.

ACKNOWLEDGEMENTS

Special thanks to my adviser, Frank Barnes, and to Howard Wachtel for their support and advice during the creation of this thesis.

I would like to thank Ross Jacobson for his invaluable assistance in the lab in the begining stages of this thesis.

I would also like to express my appreciation to everyone who helped in the creation of this thesis. This includes : Marvin Luttges, Kurt Schlesinger, Brahim Lekmine, Edouard Srenger, and Brad Lister.

CONTENTS

TABLES

Table

FIGURES

Figure

Figure

CHAPTER 1

INTRODUCTION

Our concern over the mechanisms of interaction of electromagnetic waves with living tissue was prompted by the numerous applications of this portion of the electromagnetic (EM) spectrum by private, industrial, commercial, and military users; and by the large and growing scientific evidence of the effects of microwave fields on living organisms. This concern is directed at human safety, at regulatory standards, at controlling radiation leakage and viability of radiating systems, at the dangers of present and proposed therapeutic applications of these frequencies, and at the unclarified mechanisms of microwave-biological effects.

During World War II, suitable microwave generators were invented for radar. Since, there has been extensive development of microwave equipment. Microwave-generating devices have been used in an increasing variety of applications: for systems of communication, surveillance, navigation, detection and weapons control; and for heating such as microwave diathermy in medical treatment and microwave ovens for household and commercial cooking. Other low frequency sources of EM radiation in our environment are associated with common electrical house wiring and at a much higher power level with thousands of miles of high voltage power lines. As uses multiply, and power output increases steadily, man is

increasingly exposed to EM radiation at work and elsewhere in his daily life. Workers exposed for long periods of time in their occupational environment made the first reports of possible adverse effects of exposure to EM radiation. The symptoms reported include: typical frontal headache, increased fatigability, increased irritability and nervousness [1]. The health implications of exposure to this type of non-ionizing radiation need to be known so that protective standards will have a firm and clearly understood biologic basis.

There are large disparities between international RF safety standards. In the USA and western European countries, the safety guidelines were based on the capacity of microwaves to produce a measurable temperature rise in irradiated tissue. The recommended maximum permissible power density for occupational exposure is 10 mW/cm^2. In the USSR and other eastern European countries, the criteria used in setting the maximum permissible limits were the so-called non thermal effects insufficient to cause an appreciable temperature rise. The official standard in the USSR was set at 10 $\mu W/cm^2$, which is in most situations about 1000 times lower than the permissible level in the United States [2,3]. This discrepancy led researchers to further exploration.

Other magnetic and electric sources are the natural fields intrinsic to the terrestrial environment. As a result of the spherical capacitor formed by the earth and the ionosphere, there is an average electric field of about 130 V/m at ground level. Under particular conditions fields up to 3000 V/m have been measured [4]. Slow oscillations of these fields at frequencies that

may be physiologically significant occur naturally due to resonances between the ground and the atmosphere [5]. Geomagnetic fields do vary in time and space and complete reversals of these fields have been observed periodically. Some species have developed some extraordinary sensitivities to these naturally existing fields. In 1917 Parker and Van Heusen first reported sensitivity of the catfish to environmental electric fields [6]. Since then, specialized sensing organs have been found in fish, insects, and birds. These natural fields may have other unknown yet influences on biological processes.

The use of electromagnetics in medicine was established by d'Arsonval in 1890 [7]. The use of EM radiation in diathermy and in bone fracture repair are well established [8,9]. New exciting medical applications are: noninvasive biomedical imaging, and use of EM hyperthermia in cancer therapy.

1. Microwave Biological Effects

Historically, the interaction of microwaves with biological systems has been considered to be with water and dissolved ions producing heat. Today, the bioeffects associated with this non-ionizing radiation are divided into thermal and athermal effects. The thermal effects due to exposure to EM radiation are the result of heating in the biological conductive material. These effects can be produced alternatively through heating the system in different ways. Athermal (or non-thermal) effects are changes, under the influence of a field, of the properties of a biological system that cannot be achieved by heating. Athermal effects have been observed at intensities far

below those that can give rise to thermal effects [10,11,12].

Effects of EM radiation on biological systems are difficult to assess, particularly at low levels because of the complexity of biological material, and because of the negative feedback intrinsinc to biological systems that tends to null out perturbations which would damage them or change their properties. Power absorption of EM radiation is very sensitive to the geometry and the physical properties of the material irradiated. Biological tissue consists of cells of different shapes and orientations. Besides, intracellular fluid, cell membrane, and extracellular fluid have different dielectric properties. Because of these inhomogeneities in biological material, large temperature increases can occur at the microscopic level, while no significant heating is measured macroscopically.

Investigations of the interaction of these external fields with the central nervous system developed because the adverse effects reported by workers continuously exposed to microwaves are thought of being of neurological origin, and because of the electrical nature of neural signals.

The signals used by nerve cells to transmit information consist of potential changes produced by electrical currents flowing across their surface membranes. The electrical potential difference across the cell membrane results from the differences in the concentration of ionic species in the intracellular fluid and in the extracellular fluid. There is a relatively high concentration of potassium and low concentration of sodium in the intracellular fluid with respect to the extracellular fluid. A metabolically dependent process, known as the sodium-potassium pump, is responsible for the long

term maintenance of the ionic concentration gradients for sodium and potassium. The resting membrane potential in nerve cells is usually in the vicinity of −60 mV. This electrical potential difference between the inside and the outside of a nerve cell membrane depends also on the relative permeability of the membrane to the ions present. Dynamic changes in the membrane permeability to these ions lead to an electrical current flow across the membrane and thus to electrical signals known as action potentials. The molecular basis for these changes in membrane permeability is not well understood [13,14]. It has been shown that cell functioning can be greatly affected by extremely small currents flowing across the cell membrane [15].

1.1. Thermal Effects

Extensive investigations into microwave bioeffects during the last 30 years indicate that exposure to microwave radiation can result in manifestations of a thermal nature. Relatively high power levels which cause large and rapid increases in temperature (4 - 5° C) might result in cellular damage and destruction [16]. Lower levels (1 - 3° C) result in changes in the chemical equilibrium, which may affect membrane and synaptic functioning [17].

Because of the inhomogeneous nature of biologic materials,temperature elevation during exposure to microwaves is quantitatively an important aspect of microwave interactions with biosystems, and depends on: the specific area of the body exposed and the efficiency of heat elimination, the intensity or field strength, the duration of exposure, and

the specific frequency or wavelength. In partial body exposure, the body acts as a cooling reservoir. This temperature stabilization is due to heat dissipation via conduction to the surrounding tissue, and to increased blood flow to cooler parts of the body. Power absorption of EM radiation is highly sensitive to the geometries and physical properties of the irradiated material. Biological material consists usually of different layers with different dielectric properties, and of cells of different orientations causing differential power absorption. Exposure time-intensity factors are also important. A temperature elevation of a few degrees over a period of minutes may produce no damage, while the same increase over a period of milliseconds may result in local tissue destruction. Another physical factor that must be considered is the size of the irradiated portion of the body with respect to the wavelength. For these reasons, even with acurate dosimetry, there are large areas of confusion, uncertainty, and misinformation.

Neural cell functioning is affected in several ways by temperature elevation. These effects concern the ability of the cell membrane to maintain the ionic concentration gradient necessary for neural functioning. Since the ionic concentration varies from one side to the other of the semipermeable membrane, it is necessary that the field driven drift current balance the diffusion current so that a potential barrier is formed to maintain the concentration difference. The relation between the electrical voltage across the membrane and the concentration of a given ionic species is given by the Nernst equation:

$$V = \frac{RT}{ZF} \ln \frac{C_1}{C_2} \qquad (1)$$

where

V voltage across the membrane

R gas constant

T absolute temperature

Z valence of ion C

F Faraday's constant

C_1 concentration of ion C on one side of the membrane

C_2 concentration of ion C on the other side of the membrane.

Three major small ion species (K^+,Na^+,Cl^-) contribute to the potential gradient across the membrane of a nerve cell. The relation between the membrane potential and the concentrations of these ions is given by the Goldman equation:

$$V_m = \frac{RT}{F} \ln \frac{P_K\left[K^+\right]_o + P_{Na}\left[Na^+\right]_o + P_{Cl}\left[Cl^-\right]_i}{P_K\left[K^+\right]_i + P_{Na}\left[Na^+\right]_i + P_{Cl}\left[Cl^-\right]_o} \qquad (2)$$

where

P_K, P_{Na}, P_{Cl} are the permeabilities of K^+, Na^+, Cl^-

$\left[K^+\right]_o$, $\left[Na^+\right]_o$, $\left[Cl^-\right]_o$ the extracellular concentrations of K^+, Na^+, Cl^-

$\left[K^+\right]_i$, $\left[Na^+\right]_i$, $\left[Cl^-\right]_i$ the intracellular concentrations of K^+, Na^+, Cl^-.

It is evident from equation (2) that changes in the permeability of the membrane to the different ions will lead to changes in the membrane poten-

tial. The permeability ratio P_{Na}/P_K has been found to have a significant dependence on temperature. Gorman and Marmor [18] found that the sodium-potassium permeability ratio of a molluscan giant neuron increases from 0.028 at 4° C to 0.068 at 18° C.

Equation (1) predicts that the membrane should hyperpolarize slightly with increasing temperature (0.2 mV/° C) [16]. This prediction was not confirmed by experimental results. Warming of the cell produced a depolarization instead of the expected hyperpolarization. This contradiction is possibly due to changes in the sodium-potassium permeability ratio, or to other membrane metabolic processes that the Nernst equation does not account for.

Neural cell functioning is also affected by rapid temperature changes as observed by Chalker [32]. Barnes showed that cell membranes have a temperature rate sensitivity predicted from the Nernst equation [18a]. A hyperpolarized current is predicted from the Nernst equation for conditions of positive temperature derivatives with respect to time. The Nernst equation for the potassium concentration between the inside and outside of a cell is given by :

$$C_1 = C_2 \exp\left[\frac{q\phi}{kT}\right] \tag{3}$$

where C_1 and C_2 are the concentrations of potassium inside and outside the cell, q is the charge on the electron, ϕ is the voltage across the membrane, k is Boltzmann's constant, and T is the absolute temperature. The contribution of the potassium to the membrane current is given by :

$$I = q\frac{d(C_1V_1)}{dt} = -q\frac{d(C_2V_2)}{dt} \tag{4}$$

where V_1 is the volume of the cell, V_2 is the volume of the extracellular fluid, and t is time. Taking the derivative of equation (3), substituting from equation (4), and assuming that V_2 will be large compared to V_1 yields :

$$I = -qV_1C_1\left[\frac{\phi}{\phi_T}\right]\left[\frac{\phi}{\phi} - \frac{T}{T}\right] \tag{5}$$

where

$$\phi_T = \frac{kT}{q} \qquad \phi = \frac{d\phi}{dt} \qquad T = \frac{dT}{dt}$$

Using some approximate values for a pacemaker cell from *Aplysia* and taking $\phi = 0$ and $T = 0.1°$ C/s; equation (5) yields a current of approximately 0.5 nA. Experimentally, it has been shown that currents as small as 2 nA injected through a microelectrode will bias a pacemaker cell from cutoff to saturation, and currents of a few tenths of a nanoamp will change the firing rate.

Another membrane process that is temperature sensitive is the sodium-potassium pump [19]. This metabolically dependent process is responsible for the long term maintenance of the ionic concentration gradients for Na^+ and K^+. It actively transports Na^+ against a concentration gradient from inside to out, and K^+ from outside to in. Its action is equivalent to a hyperpolarizing current. The rate of operation of the pump is temperature sensitive. Temperature elevation leads to an increased pump action, and thus to a more hyperpolarized cell.

The ability of the membrane to maintain the ionic concentration gradient necessary for neural functioning is affected by temperature changes in three different ways. It is affected through the temperature rate sensitivity of the cell membrane, through the dependence on temperature of the permeability of the membrane to the different ions present, and through the temperature sensitivity of the sodium-potassium pump. These three phenomenon take place with different time constants. This difference in their onset times may explain some of the contradictions observed experimentally.

1.2. Athermal Effects

There has been considerable controversy for some time about the possible non existence of nonthermal effects of microwave fields on biological materials. There is a large and growing scientific evidence to counter objections that such low level effects are physically impossible. An effect is athermal when, under the influence of a field, the system changes its properties in a way that cannot be achieved by simple heating, i.e., when its response is non-linear. Nonthermal biological effects of microwaves have been reported at intensities far below those that can give rise to thermal effects. This clearly imposes the interpretation that most of the energy required to produce the effect is supplied by the biological system itself, with the externally applied field acting as a trigger. Several mechanisms of athermal microwave biological effects have been postulated. No general theory has yet been verified experimentally. As far as microwaves are concerned, cell membranes have now been identified experimentally as a prime suspect for

the site of athermal interactions.

Coherent oscillations provide a model on which athermal microwave-biological effects could be based on. Biological material has a molecular structure, and nonlinear interactions do exist in the molecular lattice. In the presence of nonlinearities, it is reasonable to assume that a coherent excitation of the lowest modes of an oscillating polar system can result from energy supplied from the surrounding heat bath [23]. According to Fröhlich [21-23], long-range coherent interactions of such modes are an essential feature of biological systems, including biological membranes, for control of different mechanisms. Microwave energy that is absorbed by the system by excitation of some mode could be selectively channeled into the dipolar mode by nonlinear interactions and thus trigger the presumed biological actions that accompany these long-range interactions without being the principal source of energy to the entire system. This process is characterized by both time and amplitude thresholds and is strongly frequency dependent [24].

The soliton behavior provides another model on which athermal effects could be based. A soliton is a pulse-like wave that can propagate through a nonlinear lattice, retaining its shape and speed despite disturbances [25]. Because of the nonlinearities, the molecular vibrations will propagate and amplify. Microwave energy will not necessarily be thermalized, but can be stored in a group of modes and then pumped periodically back into one mode. This could explain how radiation at levels many times weaker than naturally occuring mechanisms could affect cell function.

Another possible mechanism can be postulated as a membrane phenomenon. In the fluid mosaic model of membrane structure [26], the membrane consists of a lipid bilayer into which protein macromolecules are inserted or attached to the surface. These macromolecules serve as the gating channels that allow selective transport of ions across the membrane. It is believed that conformational changes of membrane protein molecules are involved in this process [27]. The microwave energy absorbed could be transferred from the EM field to the vibrational modes of these macromolecules, altering mode structure and molecular conformation, and thus altering cell functioning. Adey et al [17,28] observed an increased calcium efflux from both in vivo and in vitro brain tissue exposed to 147 and 450 MHz fields down to 0.05 mW/cm^2. It is known that changes in Ca^{2+} affect axonal excitability and synaptic transmission. This establishes a possible link to the behavioral effects resulting from low-level microwave exposure.

Barnes and Hu [29] have proposed another mechanism based on the rectifying properties of a cell membrane. Because of the nonlinearity in the Boltzmann or Nernst equation, the imposition of an RF field may result in a transmembrane current. Starting with the Nernst equation in a different form than in equation (1):

$$C_1 = C_2 \exp\frac{V}{\zeta V_T} \qquad V_T = \frac{kT}{q} \tag{6}$$

where

V_T thermal voltage

k Boltzmann's constant

q . charge of an electron

ζ a constant of the order of unity which takes into account recombination or generation at the barrier and possible geometric variations with voltage.

An external EM field will induce an oscillating voltage across the membrane. The membrane potential is expressed as the sum of the normal membrane resting potential and the superimposed ac potential.

$$V = V_o + V_m \cos\omega t \tag{7}$$

where

V_o normal membrane resting potential

V_m peak value of the ac voltage induced across the membrane

Substituting (7) into (6) and expanding in a power series yields

$$C_1 = C_2\left[\frac{V_o}{\zeta V_T}\right]\left[1 + \frac{V_m^2}{4\zeta^2 V_T^2} + \frac{V_m}{\zeta V_T}\cos\omega t + \frac{V_m^2}{4\zeta^2 V_T^2}\cos 2\omega t \cdots\right] \tag{8}$$

This rectification process leads to a depolarizing current proportional to $V_m^2/4\zeta^2 V_T^2$. This process is limited in frequency by two factors: the ionic transit time, and the decrease of the induced voltage as frequency increases due to the complex impedances of biological materials. Barnes has demonstrated that currents sufficient to affect cell functioning may result from exposures as low as 10 mW/ cm^2 for a few seconds. Picard [29a] showed that this rectification process becomes insignificant above 10 MHz as a result of the transit time limitation for the motion of the ions.

2. Present Investigation

In this study effects of high intensity microwave pulses on the electroencephalogram (EEG) of mice were examined. Intact unanesthetized animals were utilized. It was a continuation of a previous study [29] in the Electrical Engineering Department of the University of Colorado at Boulder, looking at the effects of single wide microwave pulses on the central nervous system of mice. Two sets of experiments were performed. The first one was a determination of the threshold of the effect of a single pulse with respect to the energy content of the pulse. In the second set of experiments, the effects of microwave pulse trains on the EEG were examined. The first difficulty was due to the constantly changing conditions of the animal. Handling and constraints could have big effects on the animal, and alter the reactions caused by the same stimulus. Accurate evaluation of the effect of a stimulus on a conscious animal was another problem.

A source of microwave radiation at a frequency of 2.45 GHz was used for exposure. The choice of this frequency was based on commercially available equipment. Recent studies [30] showed that microwave radiation, amplitude modulated below 100 Hz, showed the same results as exposure at very low frequencies. The carrier frequency is unimportant. At 2.45 GHz there is significant penetration of tissue [31]. For the threshold determination, the energy content of the pulse was reduced by shortening the duration of the pulse. For the repetitive pulses, the pulse duration, its amplitude, and the repetition frequency were varied to create a multitude of exposure conditions. The trains of pulses had the same energy content and

the same duration. The pulse repetition frequency was varied within the lower EEG band. This pulsed exposure was accompanied by small temperature increases while the cortex experienced relatively high intensity fields.

Previous studies on bioeffects of pulsed microwave radiation carried out in the bioengineering laboratory of the University of Colorado at Boulder were the main motivation behind this investigation. Exposure of pacemaker neurons of *Aplysia Califonia* to a single microwave pulse at 2450 MHz caused a decrease in the spontaneous firing rate of the cell [32]. The effect lasted for several seconds and was followed by a minute or more of excitatory rebound prior to a return to the normal firing rate. This effect was accompanied by a temperature increase of about 1° C and was attributed to a mechanism based on the rate of temperature increase. Analogous effects were observed with comparable microwave pulses [33]. The depression of the electrically evoked signals observed lasted for a few seconds and was followed by a rebound excitation which lasted for many minutes or even hours. The pulses were shorter than in the *Aplysia* case (about 4 msec). The SAR's were comparable (25 to 50 W/g). The temperature elevation accompanying the effect was as low as 0.02° C but the rate of temperature rise was similar. Investigations on the effects of comparable pulses on the central nervous system of intact mice have also been carried out [29]. After exposure the EEG components in the frequency range of 4 to 12 Hz showed a sizeable depression which lasted for a minute or so and was followed by a prolonged period of elevated activity.

Experiments have been also conducted at the University of Texas in

the laboratory of W. Stavinoha in which mice were exposed to large high intensity microwave pulses [34]. These exposures induced large and rapid temperature increase in the cortex and resulted in a hypokinesis during which the animal ceases or slows its movements. The effect was reversible and lasted only a few minutes. Other experiments have been conducted by A.W. Guy and C.K. Chou [35] in which the head of a rat was selectively exposed to single 915 MHz pulsed magnetic field. The reaction consisted of seizures lasting for 1 minute after exposure, followed by a 4 to 5 minute unconscious state. The effect was accompanied by a maximum temperature rise of 8° C. The animals began moving when the brain temperature returned to within 1° C of its normal value. The rats recovered, after a period of unconsciousness, without apparent effect from the exposure.

It is with this experimental and theoretical background that this investigation was carried out. Answers to the following questions were sought :

1) At what power level, using a single wide microwave pulse, would a change in the EEG acivity be elicited ?

2) Would a fairly brief microwave pulse train (6 seconds in duration) that gave rise to 1° C temperature increase, significantly alter EEG activity?

3) If so, would the EEG changes seen be more or less the same as those previously seen for single microwave pulses of equivalent energy content (i.e. giving rise to 1° C temperature increase) ?

4) Would such EEG changes be sensitive to the pulse repetition rate used, for constant train duration and constant temperature rise rate ?

5) Would EEG patterns indicating "Resonance" between the pulse repetition rate and the EEG frequency component shifted be seen ?

6) Could microwave pulse trains be used to selectively affect different neural activity patterns ?

CHAPTER 2

METHODOLOGY

Two series of experiments were performed where correlations between shifts in EEG frequencies and exposure parameters were sought. The first study was a look for the threshold of the effect of a single pulse exposure with respect to the energy content of the microwave pulse. In the second set of experiments, the effects of microwave pulse trains on the EEG were examined for different pulse repetition frequencies. In both studies adult mice were used. Cortical EEGs were recorded via chronically implanted electrodes before and after pulsed microwave exposure.

This chapter will consist of the following parts :

1) a detailed description of the aparatus and equipment used in our investigation.

2) a look at the animals used.

3) a description of the experimental protocol in both the threshold study and the repetitive pulses study.

4) an outline of the data transformations.

1. Aparatus and Equipment Used

The aparatus was common to both sets of experiments and consisted of

a pulsed microwave source, an exposure chamber, an EEG amplifier, and a microcomputer.

1.1. The Microwave Source

The microwave source was designed and built by the Instrument Development Laboratory within the Department of Electrical Engineering at the University of Colorado, Boulder. It consisted of a pulsed CW 2450 MHz magnetron. A tetrode vacuum tube was used to pulse the magnetron on and off. The magnetron high voltage supply was derived from a capacitive storage system connected to the magnetron via the tetrode. Pulsed operation was attained by pulsing the grid voltage of the tetrode, allowing the high voltage to appear at the magnetron anode. The magnetron filament supply was on continously. The magnetron tube is rated to 6 kW continuous power output. Two adjustments allowed control of the power level of the emitted microwave radiation. The power output can be controlled by changing the potential at which the high voltage capacitors are charged and that appears on the magnetron anode during the pulse "on" time. Varying the value of the maximum positive grid voltage attained at the tetrode during the exposure period provided a second control of the power output of the magnetron by limiting the current through the tetrode. These two adjustments provided reproductible pulses in the millisecond range with power levels from 1 kW to almost 8 kW. (A more detailled description of the power source is given in Appendix A).

1.2. The Exposure Chamber

The exposure aparatus consisted of a piece of rectangular waveguide with the animal's head placed in a region of high magnetic field strength. The animal is immobilized in a modified 60 cc plastic syringe as shown in Figure 1. The device consisted of a 60 cc syringe with a teflon cone at the end. The animal was placed within the syringe, and the plunger was used to push the animal toward the end so its head fit tightly into the cone. The syringe containing the animal was inserted then in the exposure chamber.

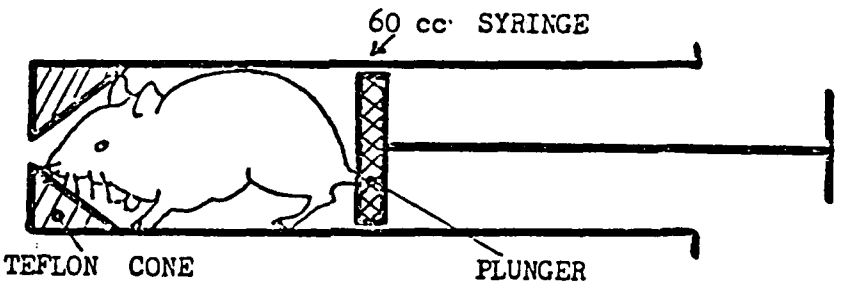

Figure 1 : Mouse holder for insertion in the exposure chamber.

Microwave power was coupled from the magnetron via a 1 5/8 inch solid coaxial conductor to an S-band waveguide (7.2 cm x 3.4 cm). Within the waveguide section was an exposure chamber which allowed the insertion, transverse to the direction of plane wave propagation, of the syringe containing the mouse. As shown in Figure 2, the exposure chamber had two

apertures for inserting the animal either in a region of high magnetic field and low electric field or in a region of high electric field and low magnetic field. Following the exposure chamber was a tunable short for optimizing power coupling into the animal. This exposure chamber was modeled after one developed at the University of Texas at San Antonio by W. Stavinoha.

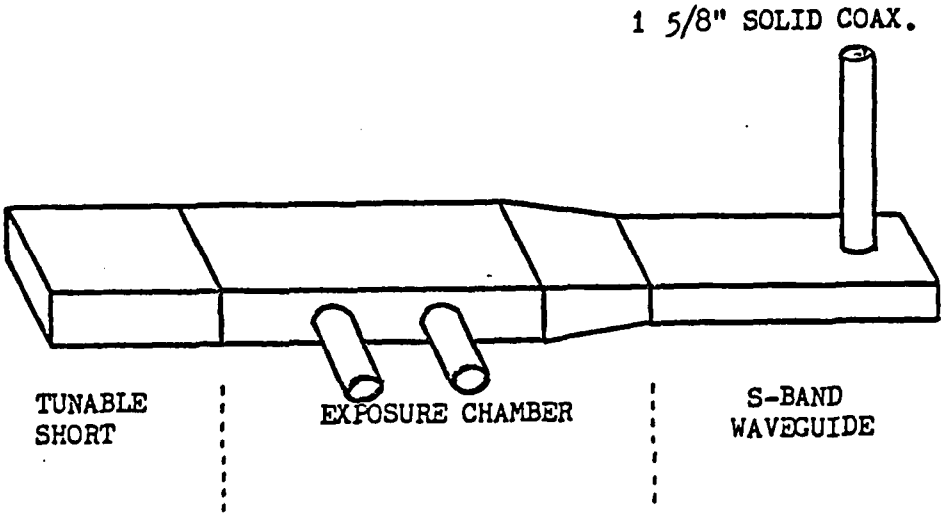

Figure 2 : Exposure chamber

Calculations show that at a frequency of 2450 MHz this size waveguide propagates the transverse electric mode (TE). It was discovered that at this frequency the mouse-syringe combination, when inserted into the exposure chamber at an electric field maximum, acted as a coaxial conductor coupling the electric field not only in the head region, but also axially through the body. This was an undesirable condition for our investigation. Most of the power should be deposited in the head region with relatively little in the body of the animal. This problem was solved by inserting the animal in a

region of maximum magnetic field and minimum electric field. Measurements indicated that over 90% of the incident power was absorbed by the animal. Measurements of temperature increases, in the transverse direction of the waveguide, showed that power absorption decreased sinusoidally from a maximum at the center of the waveguide to a minimum at the edge (Figure 3); as would be expected for the TE mode. Figures 4 and 5 show thermographic measurements made by Stavinoha et al [36] for this type of exposure system. These measurements show relatively consistent temperature rises throughout the cortex.

1.3. Dosimetry

Measurements of absorbed power were made by recording the temperature changes within the cortex accompanying exposure. An electrothermia monitor (Vitek model 101) was utilized. The probe was made of highly resistive carbon-loaded teflon, thus the interaction with the field during exposure was minimized. The thermistor probe was inserted about 3 mm into the cortex of an anesthetized animal, and the temperature changes were recorded during exposure. Figure 6 shows two typical time-temperature profiles recorded in this manner.

During the course of this investigation the proper operation of the microwave source and the energy content of individual pulse trains was checked in a similar manner using, instead of an anesthetized animal, 10 cc of water as a dummy load in the end of the syringe. Both procedures yielded consistent values lending a high degree of confidence (± 10 %) in the measured values of absorbed power.

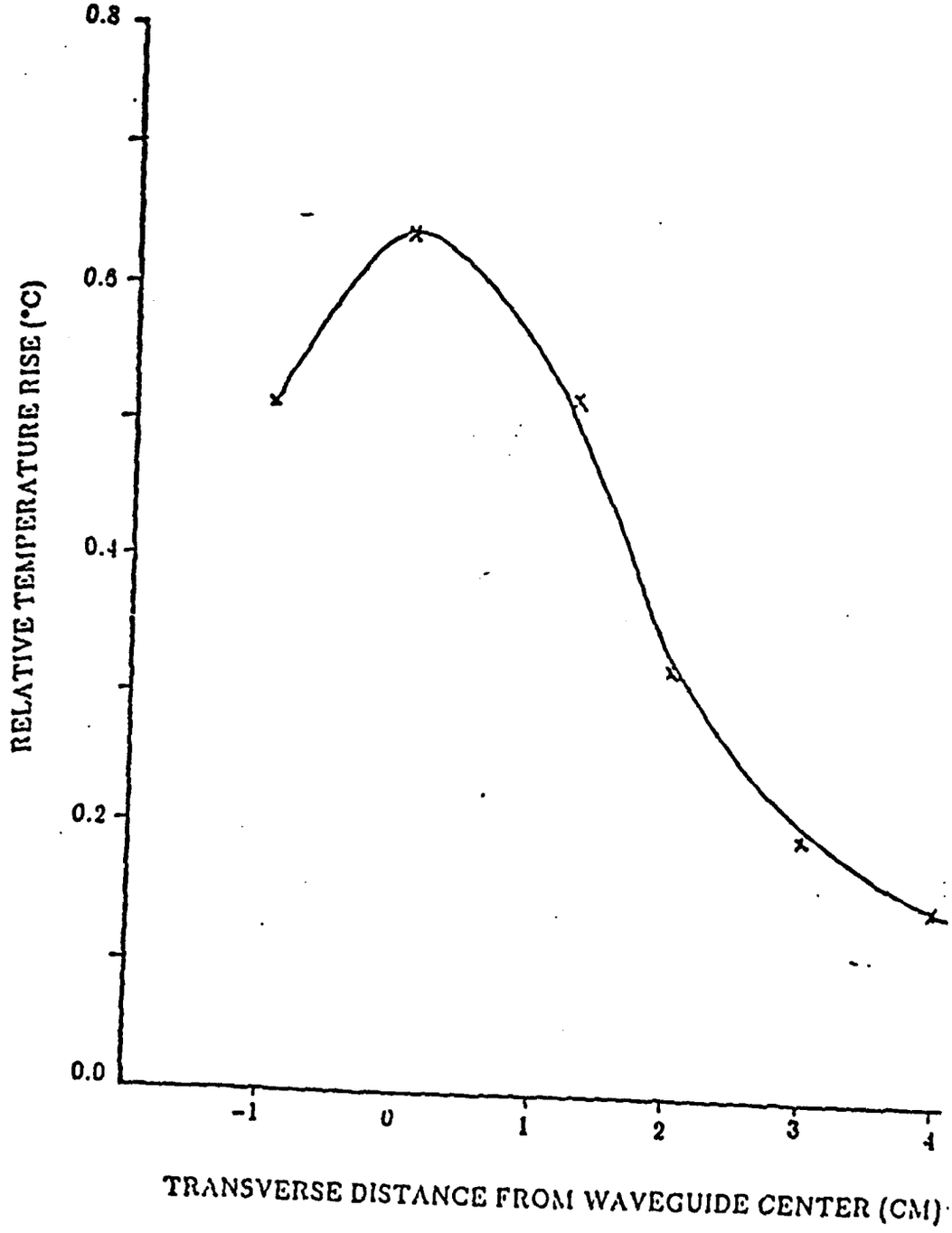

Figure 3 : Relative temperature distribution in agar dummy after microwave irradiation (from [29]).

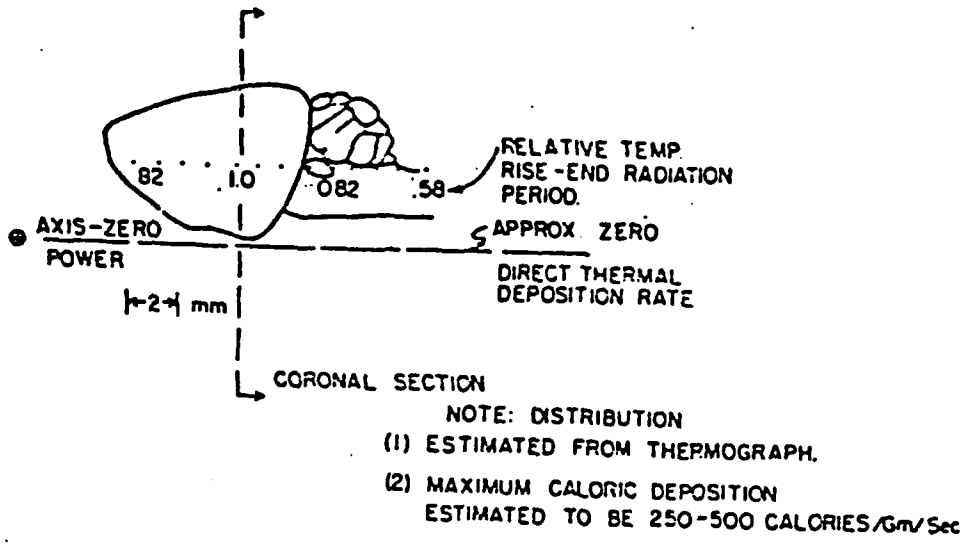

Figure 4 : Relative temperature rise in mouse brain 10s following a 2ms irradiation in situ by microwaves as reported by Stavinoha et al [36].

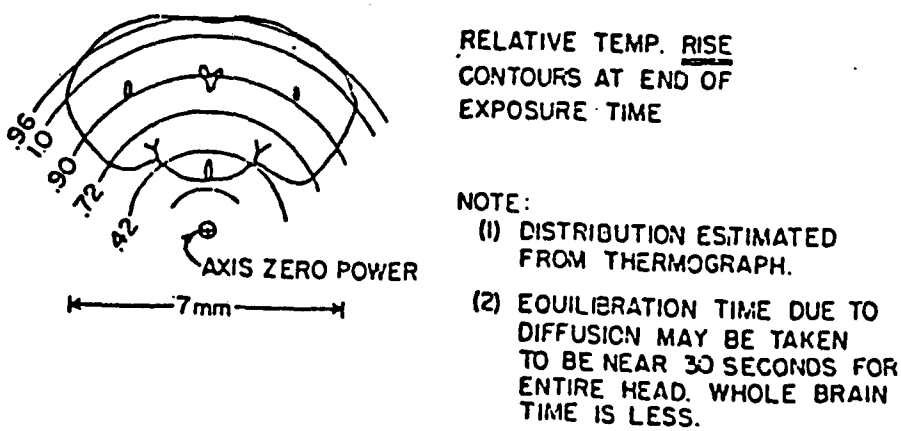

Figure 5 : Relative temperature rise in a coronal section of the mouse brain 10 s following a 2 ms irradiation in situ by microwaves as reported by Stavinoha et al [36].

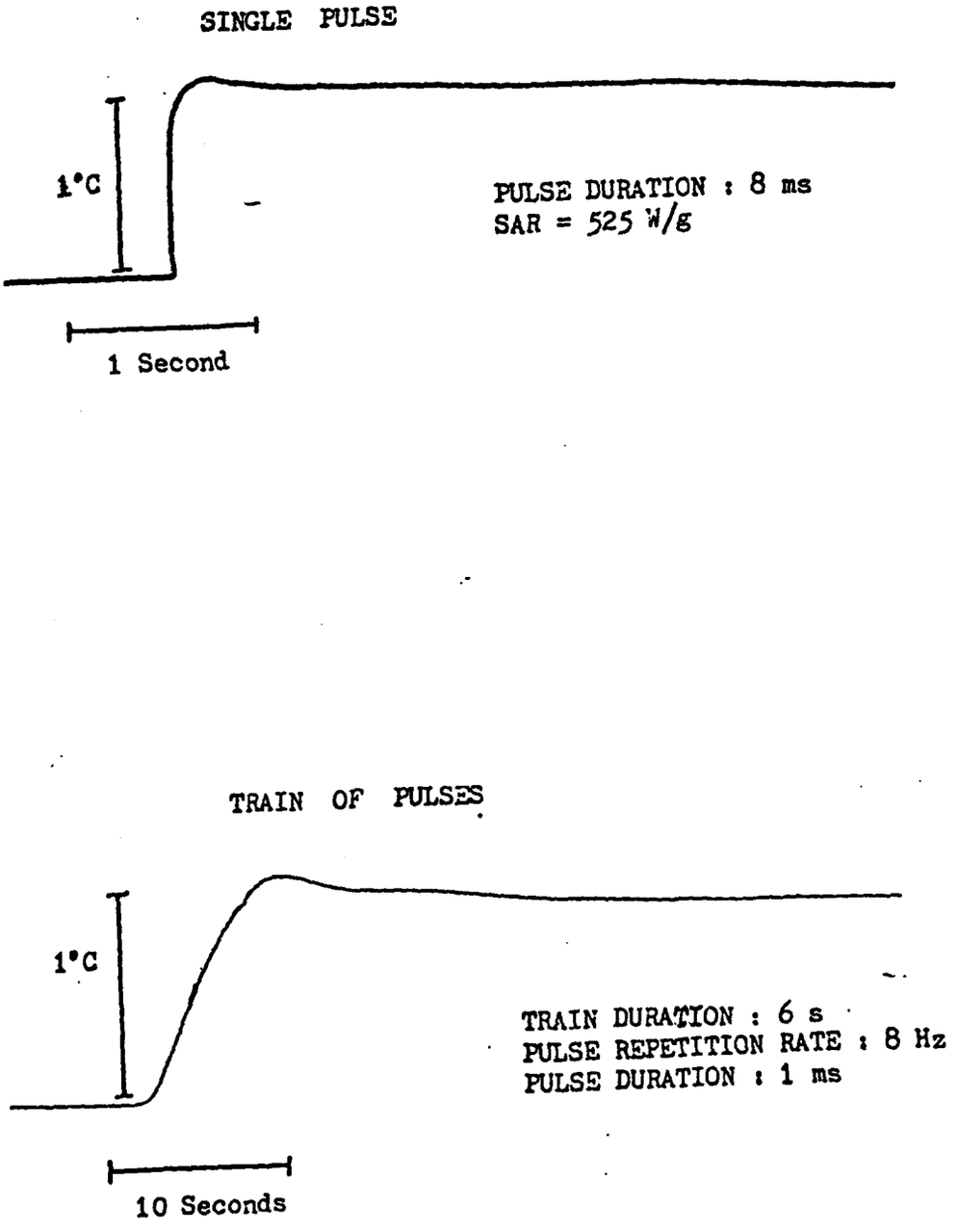

Figure 6 : Time-temperature profiles of in situ measure of cortical temperature rise during microwave exposure.

1.4. Electrodes

Carbon-loaded teflon electrodes were used. The material was supplied by the National Bureau of Standards, Boulder, CO., and is marketed under the trade name, Multaloy by Technical Fluocarbons Engineering, Inc., Rhode Island.

This carbon-loaded Teflon conductor has a resistivity of 125 ohm-cm, close to that of tissue. The low conductivity minimizes perturbation of the field and tissue damage due to induced currents from the incident fields. Carbon is also biologically inert. Therefore, this material is highly suitable for recording the EEG from animals exposed to electromagnetic radiation. Electrodes were constructed from a 0.25 mm thick sheet of carbon-loaded Teflon. They were 10 cm long and 1 mm in width yielding a resistance of about 500 kΩ. The high resistance causes the electrodes to be particularly susceptible to electrical noise. This was overcome through proper filtering of the EEG and the shielding provided by the metal waveguide.

C.K. Chou and A.W. Guy [37] showed that the EEG and its spectrum as recorded from the carbon-loaded Teflon electrodes are comparable to those recorded from conventional metal electrodes. The electrodes were implanted in rabbits and maintained for four to six months. Histological examination showed good tissue compatibility and exposure to microwave radiation showed no electromagnetic interference.

1.5. Amplification and Recording

The mice were restrained in the modified 60 cc syringe and then placed

in the exposure chamber. A flexible cable connected the carbon-loaded Teflon electrodes to a polygraph recording system (Grass model 78B). The EEGs were differentially amplified by a Grass model 7P511E amplifier. The frequency response of the amplifier was set at 0.3 Hz for the low frequency cutoff, and at 100 Hz for the high frequency cutoff. A 60 Hz notch Filter was used to eliminate power line noise. The EEGs were obtained directly from the 7P511E amplifier and were recorded digitally (128 samples/second) using an Apple IIe microcomputer and an eight bit analog to digital converter (Mountain Computer Inc.).

The microcomputer also provided precise timing and presentation of the trigger pulse for microwave exposure. Figure 7 shows the microwave exposure and EEG recording set up for the threshold experiments where the microcomputer presented the trigger pulse directly to the microwave source. In Figure 8, the set up for the repetitive pulses study is shown. The microcomputer in this case was used to trigger a Grass stimulator model S48, and the Grass stimulator provided the triggering signal to the microwave source and allowed control of the pulse repetition frequency and of the pulse duration.

2. Animals

The animals utilized were adult mice, HS strain. The mice (25 - 30 grams) were anesthetized with sodium pentobarbital (80 mg/kg intramuscularly). The head of the animal was secured and two holes 1 mm in diameter were drilled in the calvarium on either side of the midline suture, directly behind the coronal suture. The two holes were 1 to 2 mm apart. About 1

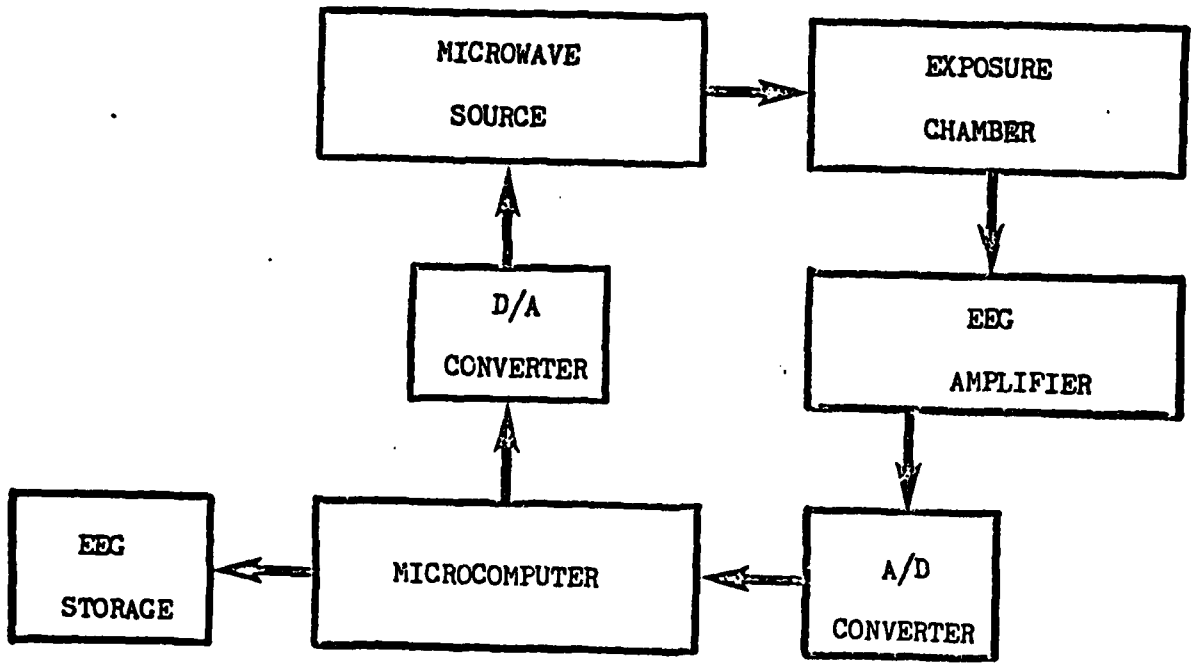

Figure 7 : Microwave exposure and EEG recording set up for the threshold study.

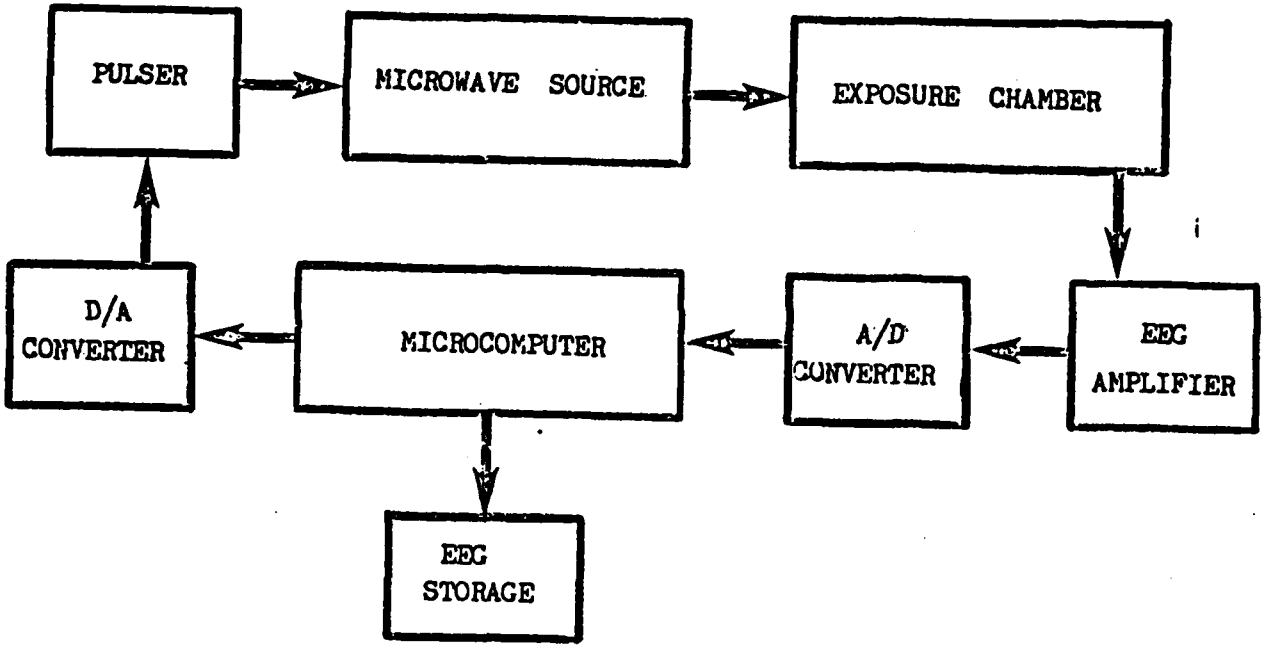

Figure 8 : Microwave exposure and EEG recording set up for the wide microwave pulse trains study.

mm of the end of each electrode was inserted through the hole, under the calvarium, onto the surface of the cortex. The electrodes were fixed to the calvarium with dental acrylic. Tissue damage was minimal. The animals were allowed 3 days for recovery.

Initial attempts at recording EEGs revealed behavioral problems. Due to the handling and constraint within the exposure chamber, the mice entered a torpor like state after about 30 minutes. In that condition the body temperature decreased 5 to 6° C and the EEG deviated from normal with low and mid-frequency bands increasing in power. To overcome this problem, mice were placed twice a day, during the three day recovery period, in 60 cc syringes similar to the one used in the exposure chamber. This accomodating process reduced body movements and delayed the onset of the torpor state. Also, the entire time the animals were left in the exposure chamber was limited to 10 minutes. In this manner, consistent EEG recordings were attained most of the time.

3. Experimental Protocol

Individual unanesthetized mice were placed in the modified syringe and the animal was secured in place by gently inserting the plunger behind him. The mouse was kept in a position that limited body movements and allowed respiration. The electrodes were insulated with small pieces of 1 mm in diameter polyethylene tubing. They were routed inside the syringe through openings in the plunger, to the outside. The leads from the electrodes were connected via aligator clips and a short section of shielded cable to the electrode selector panel of the polygraph recording system. The EEG

at the output of the differential amplifier was viewed with an oscilloscope and the gain was adjusted within the range of the analog to digital converter. Before recording was started, the animal was allowed a two-minute period to become calm and stop moving. Some animals refused to quiet. Occasionally, also, a respiration artifact due to abnormally high electrode resistance was dominant in the recording. Animals that did not quiet after the two-minute period or did not render clean EEGs were removed. Figure 9 shows an acceptable EEG recording.

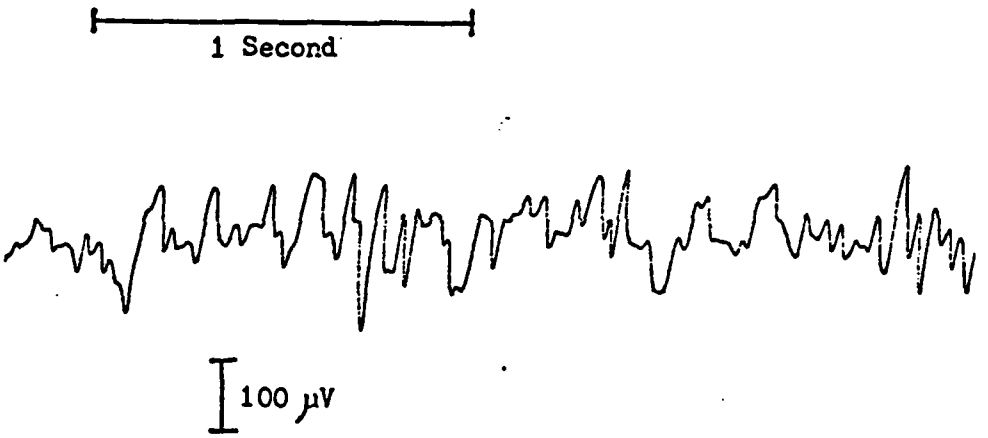

Figure 9 : Typical mouse EEG recording.

Once the EEG was acceptable, the trial commenced. The whole operation was controlled by the microcomputer. The EEG was sampled in six second epochs four times a minute and recorded on a magnetic disk. At the end of the first two minutes of sampling the microwave exposure was presented. The sampling was started again after two seconds; to allow amplifier saturation to subside. The sampling was continued after exposure for four minutes, resulting in a total record of six minutes (24 samples) for

each trial. Exposure groups consisted of six mice, each exposed in an identical fashion.

For the threshold study thirty-six mice with acceptable EEGs were used. Six of these were used as controls. Thirty were exposed to single microwave pulses. The exposure in these five groups differed in the energy content of the microwave pulse. The pulse widths were 32, 16, 8, 4, and 2 ms; yielding respectively a total cortical temperature rise of 1, 0.5, 0.25, 0.1, and 0.05° C.

Forty-two other mice (7 groups) were used during the repetitive pulses experiment. Twelve of these were used as controls. Thirty were exposed to six second trains of pulses. The exposure in these five groups was equicaloric in nature, and the pulses peak power was kept identical. The total cortical temperature rise was also identical (1° C). These exposures differed in the pulses repetition frequency, with repetition frequencies of 4, 6, 8, 10, and 12 Hz.

4. Data Transformation

The data transformation technique used in this study was initially developed by R. Jacobson [29]. Individual unanesthetized mice were placed in the exposure chamber, were kept in a position that limited body movements, and were allowed a two-minute period to become calm and stop moving. Once the EEG was acceptable, the trial commenced. EEG epochs were recorded every 15 seconds before and after microwave exposure. Occasionally some animals became active after the start of the experiment, producing EEG epochs contaminated with movement artifacts. The EEG

records were reviewed after each trial and contaminated epochs were deleted. The number of contaminated epochs was usually from 10% to 20% of the total. When more than 25% of all the epochs were contaminated the trial was not used. About 15% of all the trials were discarded for this reason. The frequency spectra associated with the remaining epochs was then calculated. The frequency spectra were computed as the discrete Fourier transform of the autocorrelation function of the individual epochs. A detailed description of the spectra computation is given in Appendix B. Power densities were calculated from 0 to 24 Hz every 4 Hz in the threshold study and every 2 Hz in the repetitive pulses study. Figure 10 shows an average spectral power distribution of a mouse EEG. The four spectra computed for each minute were averaged together. If in a given minute some contaminated epochs were removed, that minute was represented by an average containing only the spectra of the remaining samples. This produced spectral power bands ranging from 0 to 24 Hz averaged for each minute of each trial.

A single average was computed for all power densities over all the minutes for each individual mouse. Each trial was then scaled so that these overall averages were identical. This adjusted for differences in amplifier gain, electrode placement, and electrode resistance which resulted in magnitude differences between trials.

Since it is the relationship between spectra, increase or decrease, that is of importance to us rather than the absolute magnitudes which are measured, all computed spectra were normalized. The transformed value

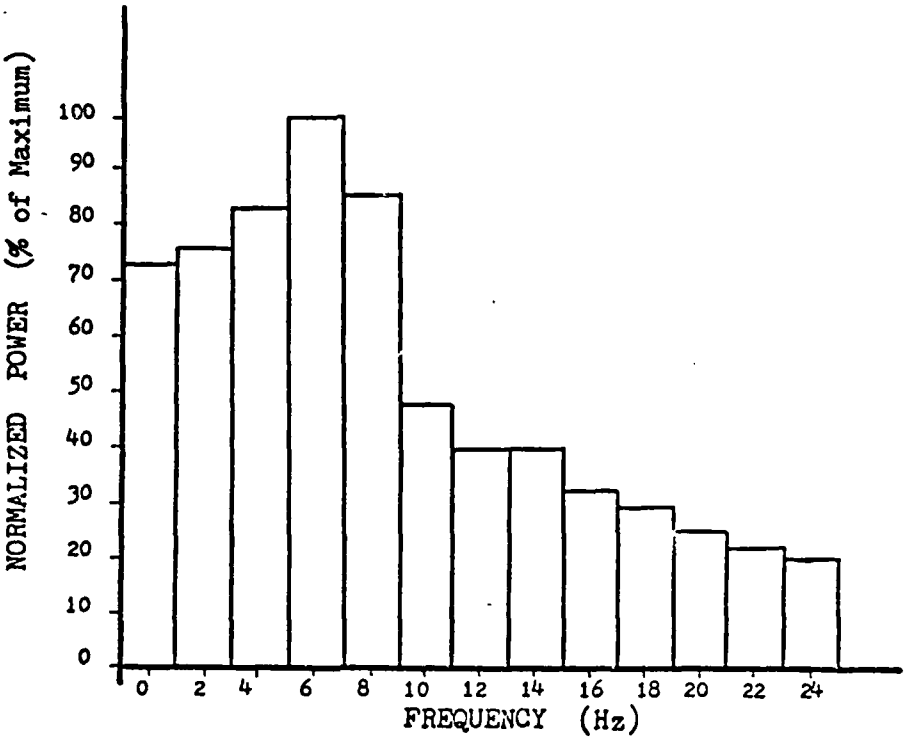

Figure 10 : Average spectral power distribution of a mouse EEG.

represents the deviation of the original value about the mean, expressed in units of the associated standard deviation. This is the commonly known z-score or difference score transformation. A negative z-score indicates a value below the average and a positive z-score indicates a value above the average.

These transformed spectral densities were then averaged by minute for all six subjects in each exposure group. This gave an average value for each one of the frequency bins for each minute of identical trials. Finally, the change in spectra by minute for each subject was obtained by subtracting

AD-A183 055 INTERRUPTION OF NEURAL FUNCTION(U) COLORADO UNIV AT BOULDER DEPT OF ELECTRICAL AND COMPUTER ENGINEERING H WACHTEL MAY 87 153-6823 N00014-81-K-0307 2/2

UNCLASSIFIED F/G 6/7 NL

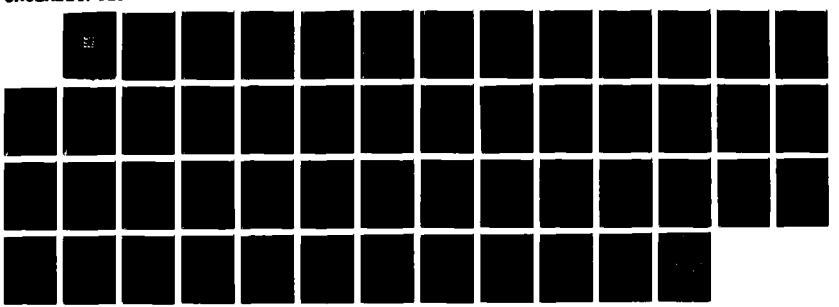

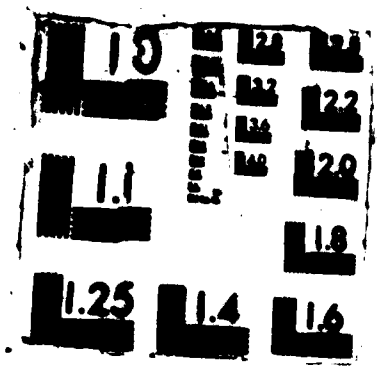
1.0
2.2
2.0
1.8
1.1
1.25
1.4
1.6

the previous value from each succeeding one. A negative value indicates that the EEG power present around that frequency decreased between minutes. A positive value represents an increase. These quantities were averaged for all six subjects in each exposure group. The data transformations are schematically shown in Figure 11.

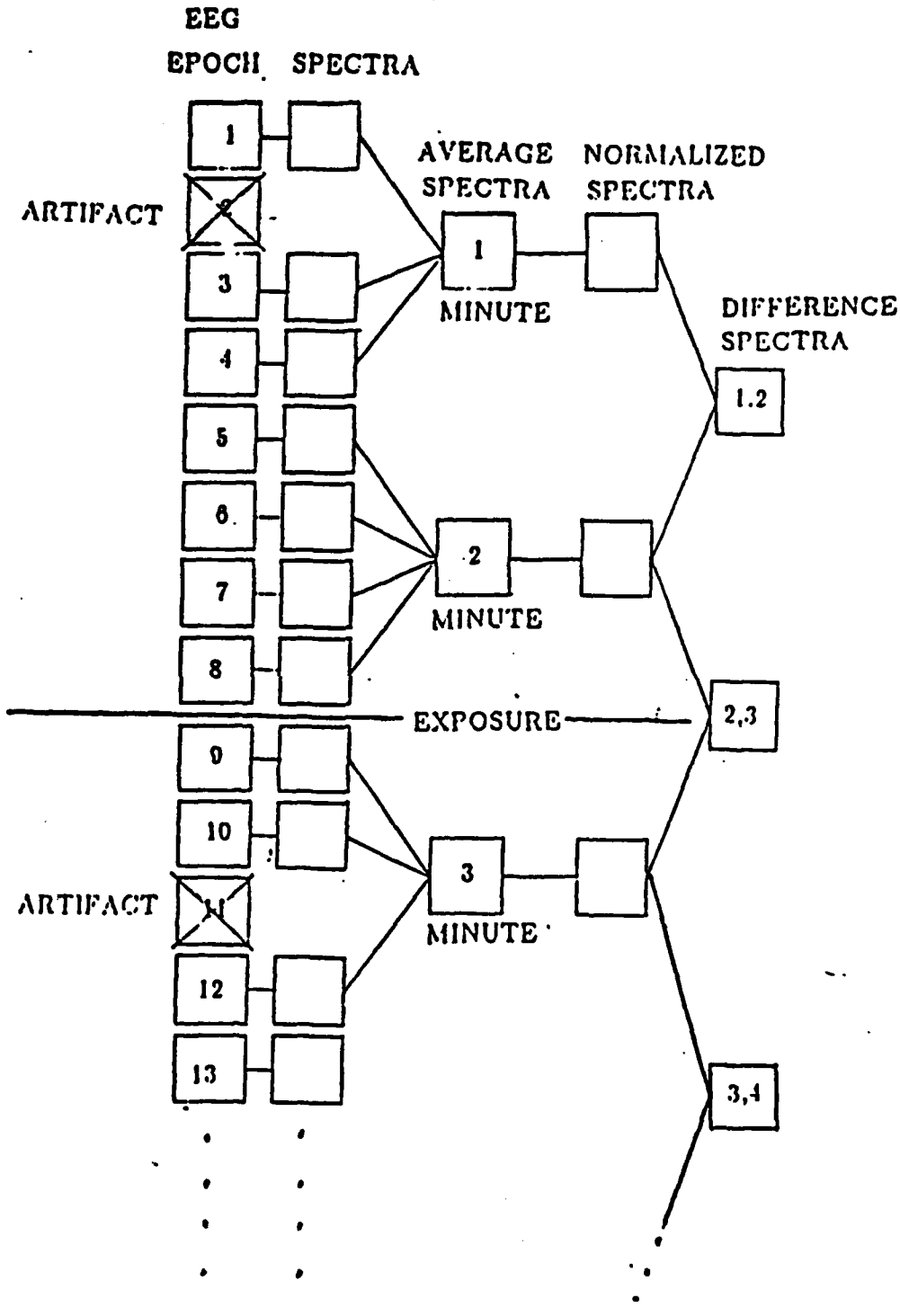

Figure 11 : EEG data transformations (from [29]).

CHAPTER 3

RESULTS

This section will consist of an outline of the results for both the threshold study experiments and the wide pulse trains experiments.

1. Threshold study

Thirty-six mice were used in this study (6 groups). Six of these were used as controls (1 group). Thirty (5 groups) were exposed to single microwave pulses. The exposure in these five groups differed in the energy content of the microwave pulse. The pulse widths were 32, 16, 8, 4, and 2 ms; yielding respectively a total cortical temperature rise of 1, 0.5, 0.25, 0.1, and 0.05°C. The peak power, and thus the rate of temperature rise, was kept constant.

A discriminant statistical analysis was performed to identify which frequencies were consistently altered by the exposure to a single wide microwave pulse [29]. Results of this analysis indicate that changes in the 8 Hz frequency band best separates the exposed groups from the control group. The power density in this frequency band was plotted for all groups, as a function of time, in Figure 12. Since the 8 Hz band was more affected by the exposure than any other frequency band, we focused our attention to the changes in power density for this band between the minutes before and

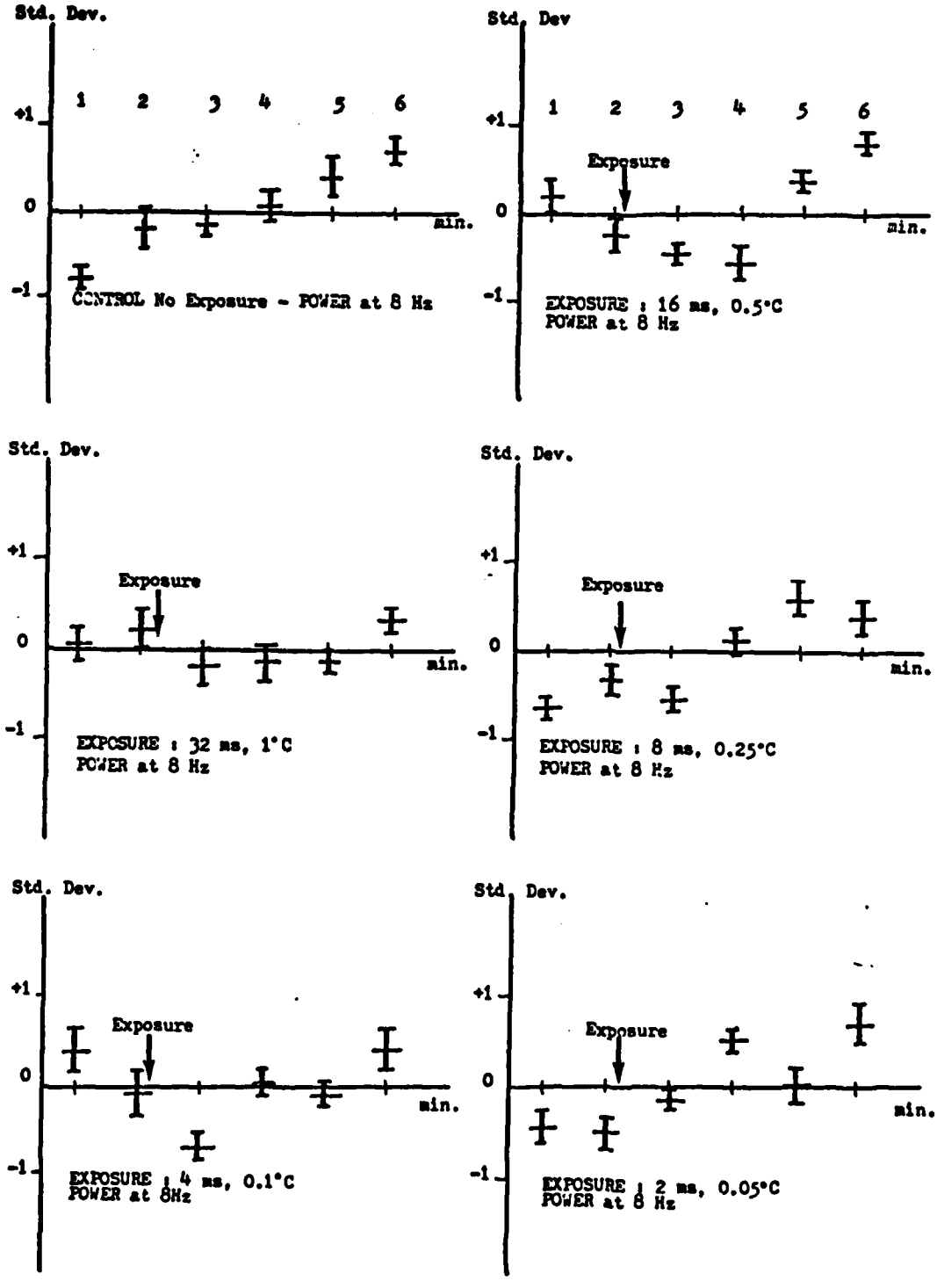

Figure 12 : Time course of the EEG power in the 8 Hz frequency bin for all groups in the threshold study.

after the exposure. These changes for groups are summarized in Figure 13.

2. Effects of Wide Microwave Pulse Trains

Forty-two mice (7 groups) were used in this study. Twelve of these (2 groups) were used as controls (i.e. no microwave exposure). The results from these two control groups were averaged together. The shifts in EEG power by minute averaged for all twelve mice are shown in Figure 14. The thirty other mice (5 groups) were exposed to wide microwave pulse (WMP) trains. The exposure in these five groups was equi-caloric in nature. The total cortical temperature rise was $1^{\circ}C$. The rate of temperature rise (T) was kept identical in all exposed groups. The exposures differed in the pulses repetition frequency. The repetition frequencies were 4, 6, 8, 10, and 12 Hz. The trains duration was 6 seconds and was identical for all exposed groups. These parameters are shown schematically in Figures 15 and 16. The changes in EEG power for all exposed groups for every one of the five repetition frequencies are shown in Figures 17 through 21. These figures show the changes in EEG power for every frequency band between successive minutes.

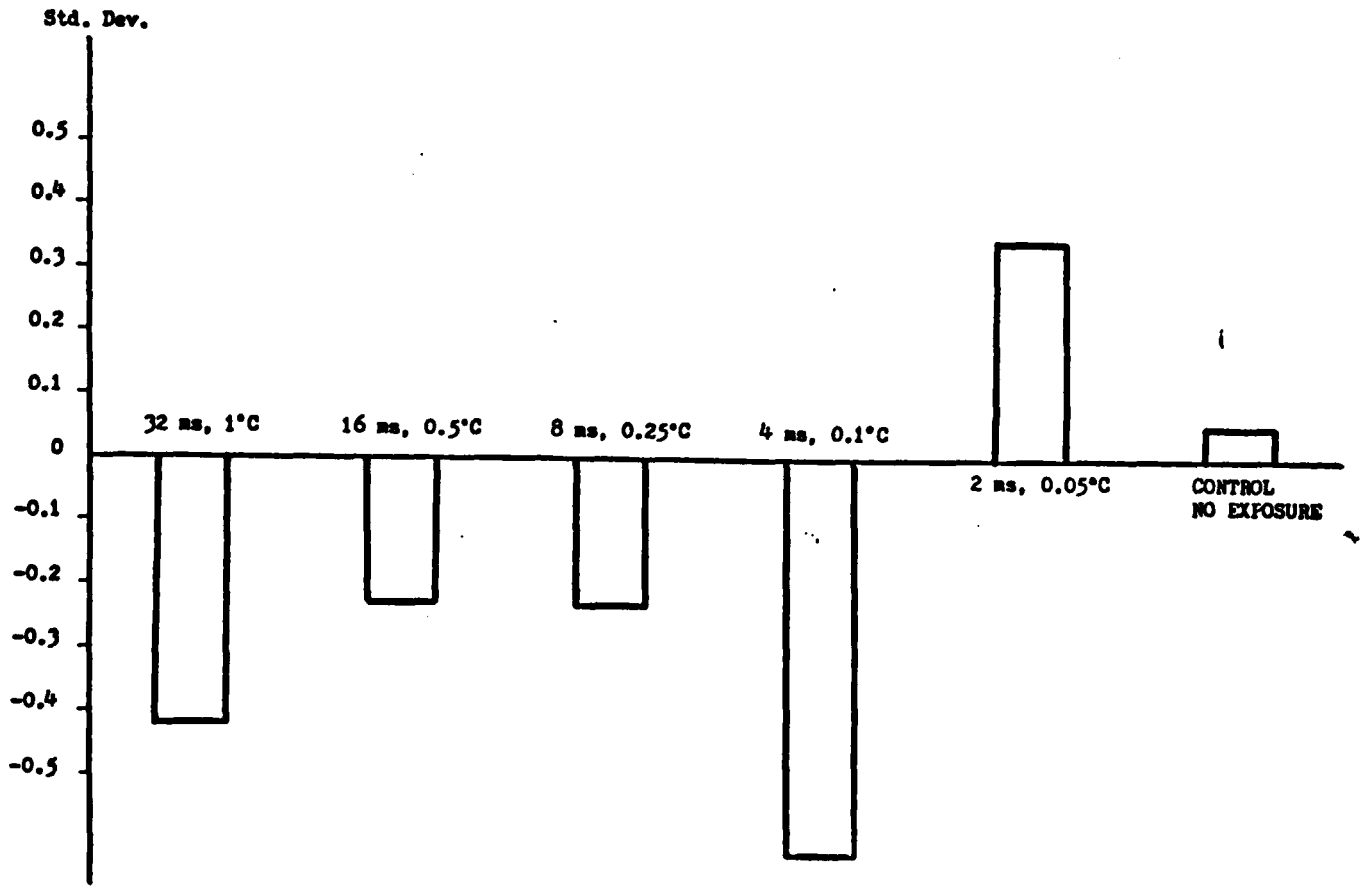

Figure 13 : Shifts in EEG power in the 8 Hz bin for all groups between minutes before and after mivrowave exposure.

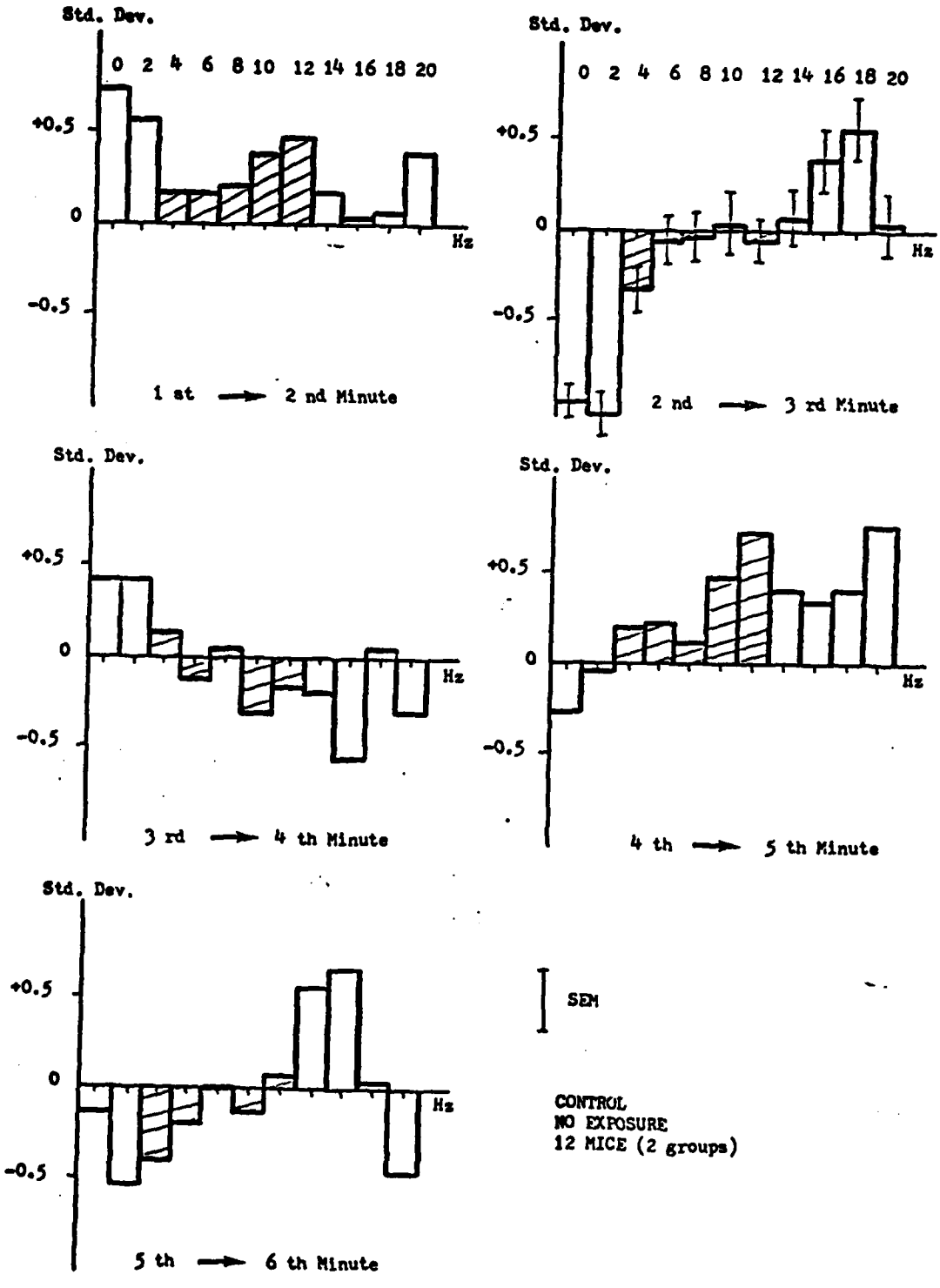

Figure 14 : Shifts in EEG power between minutes for control group.

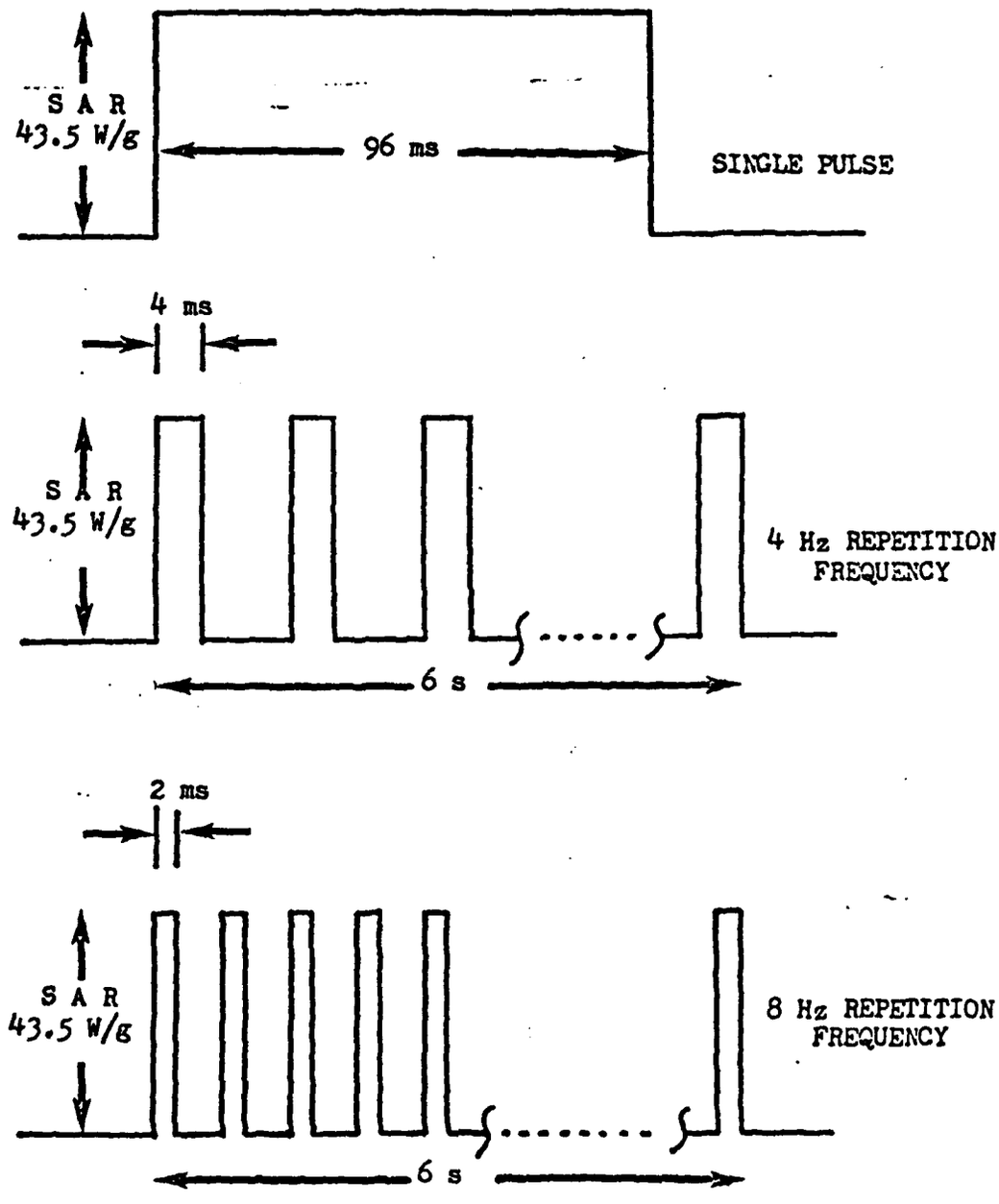

Figure 15 : Wide Microwave Pulse Trains
(Equi-caloric exposure leading 1° C temperature rise)

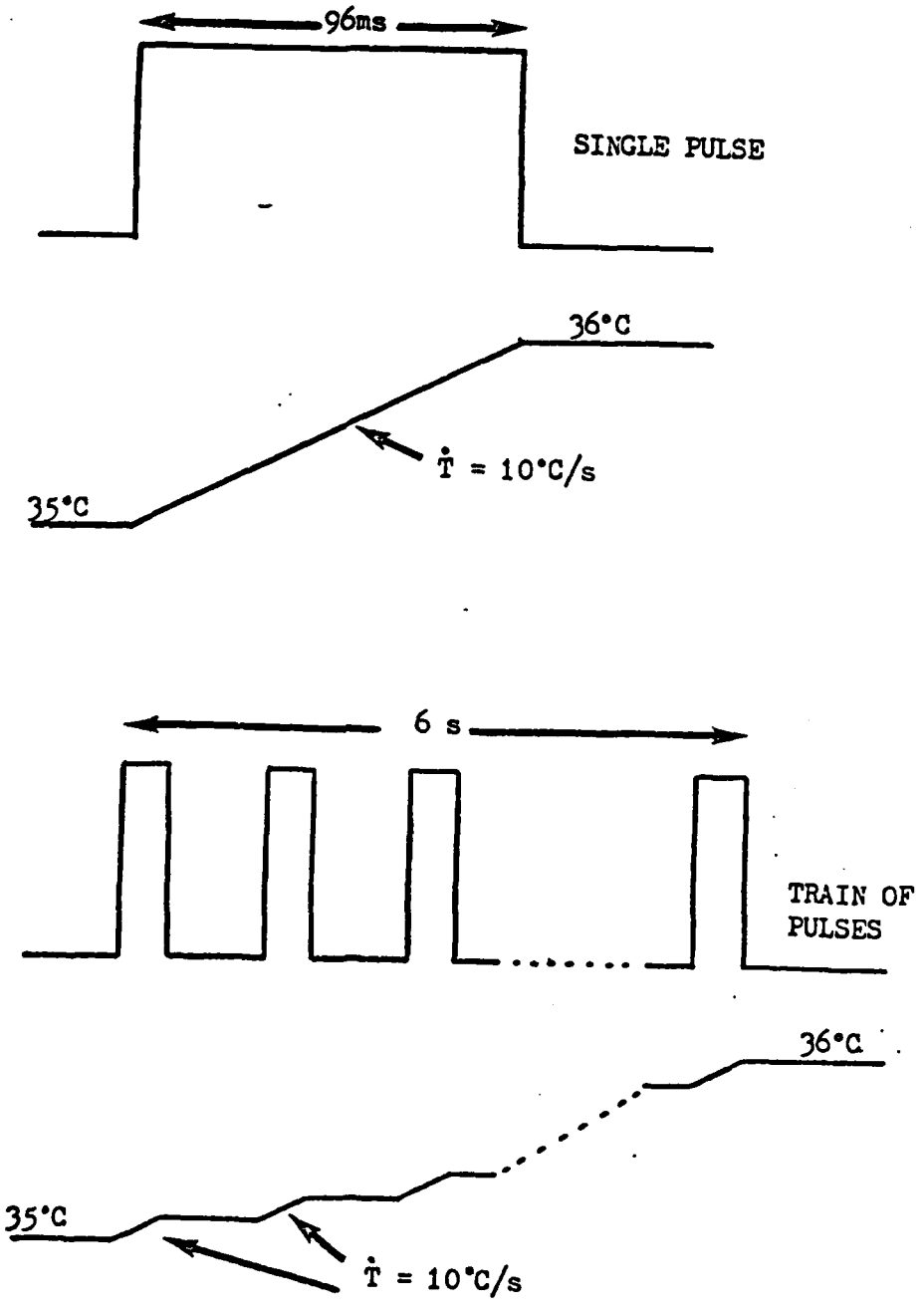

Figure 16 : Temperature profiles for WMP trains

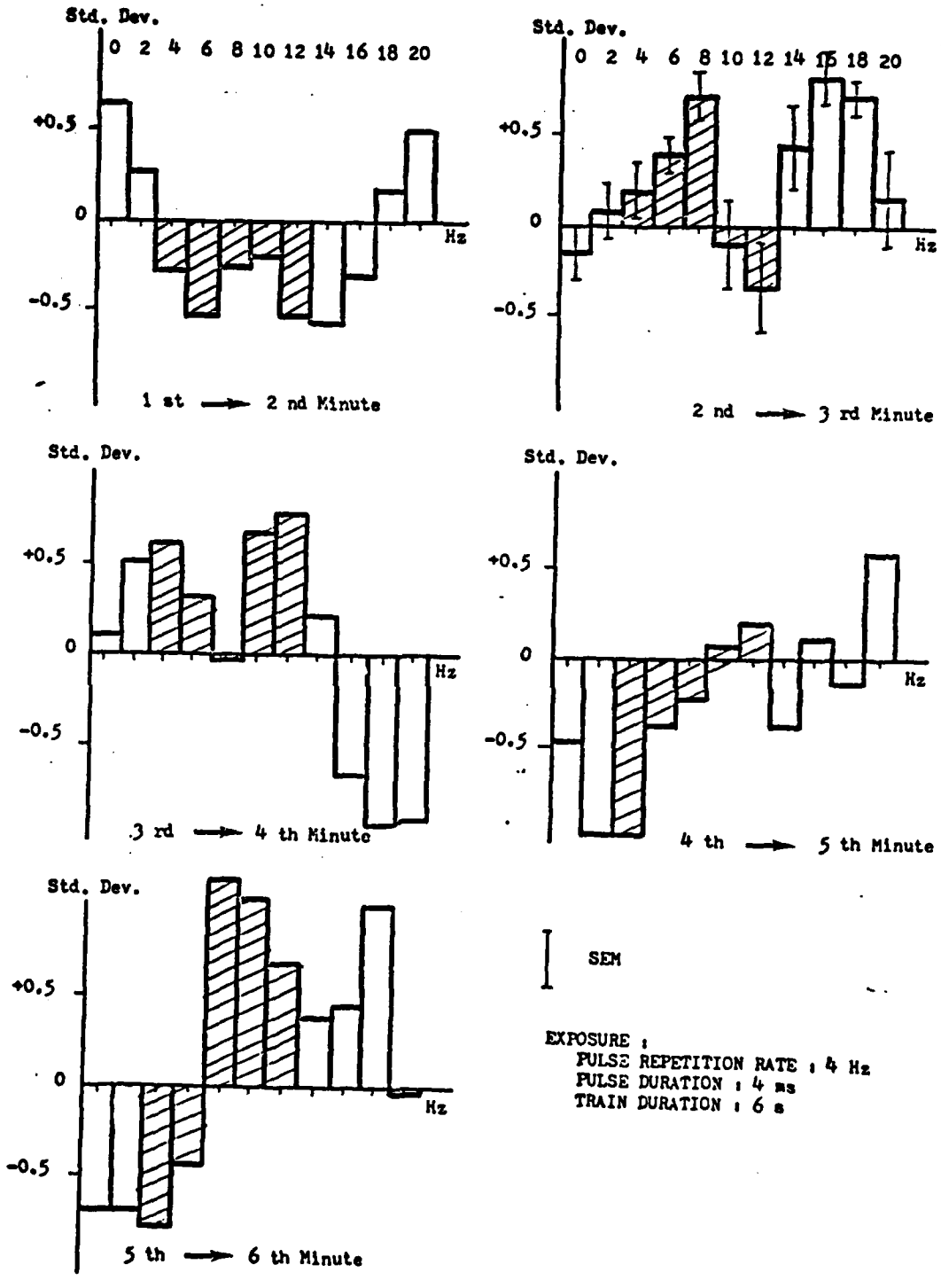

Figure 17 : Shifts in EEG power between minutes for the 4 Hz PRR group.

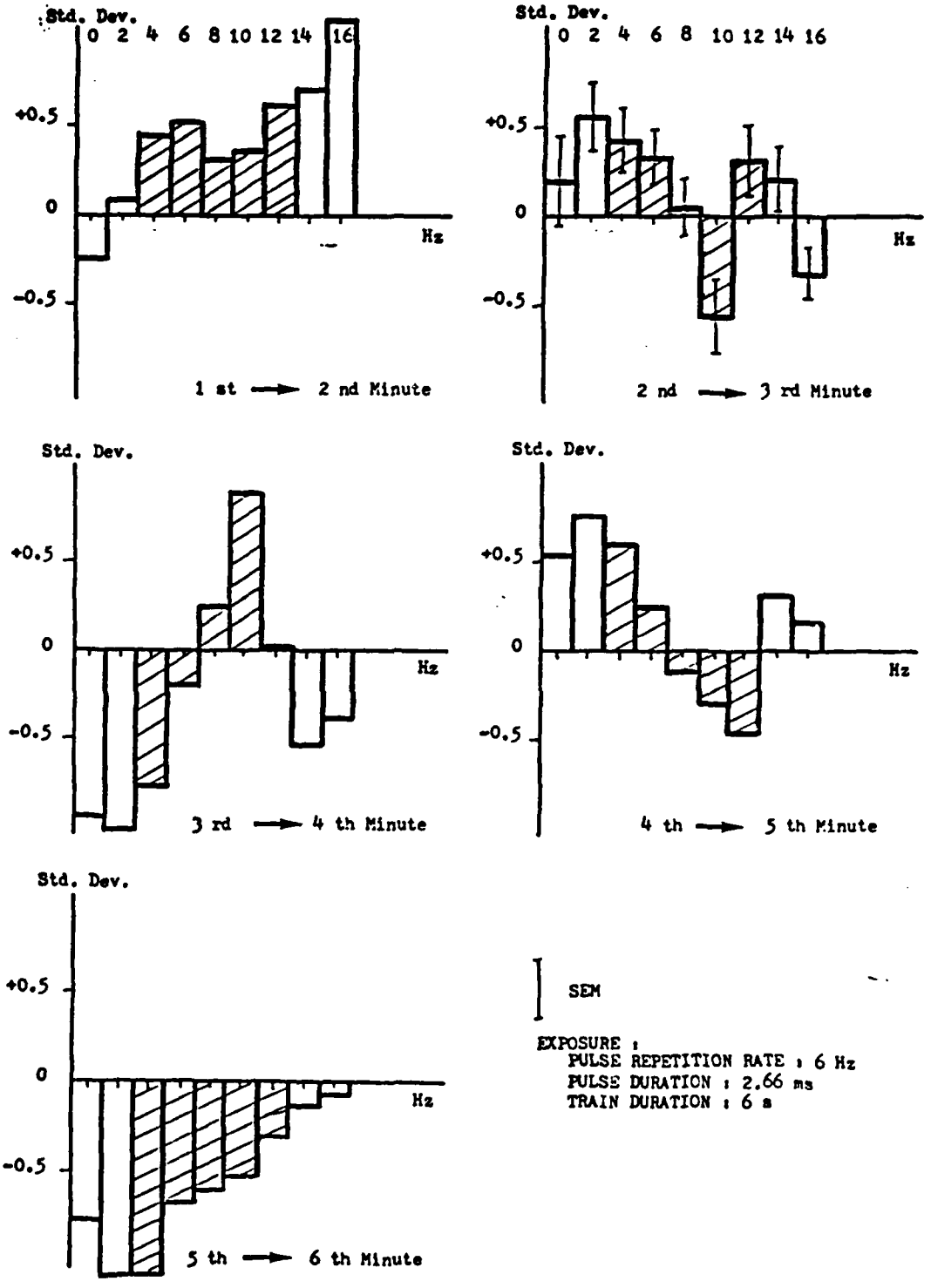

Figure 18 : Shifts in EEG power between minutes for the 6 Hz PRR group.

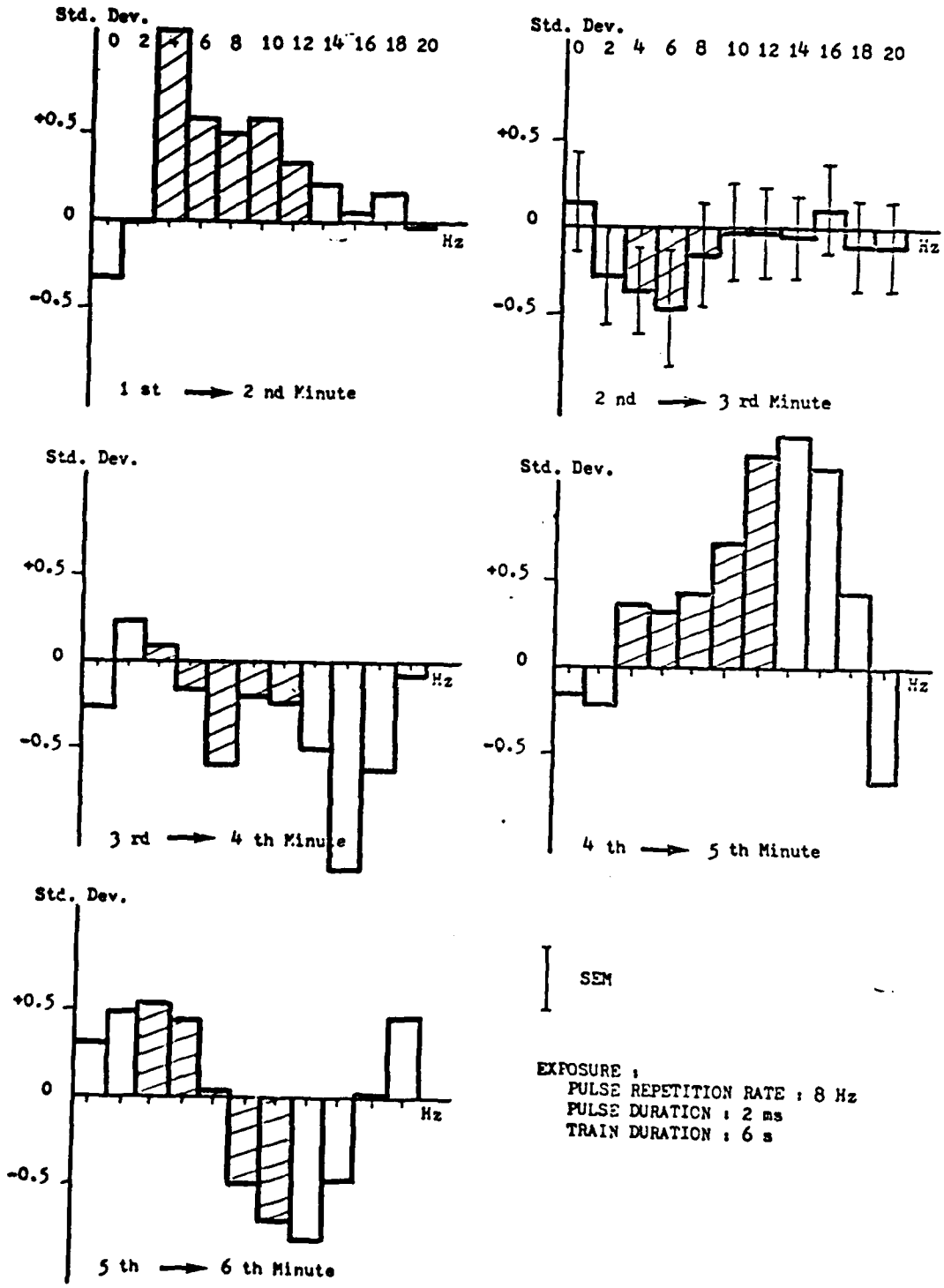

Figure 19 : Shifts in EEG power between minutes for the 8 Hz PRR group.

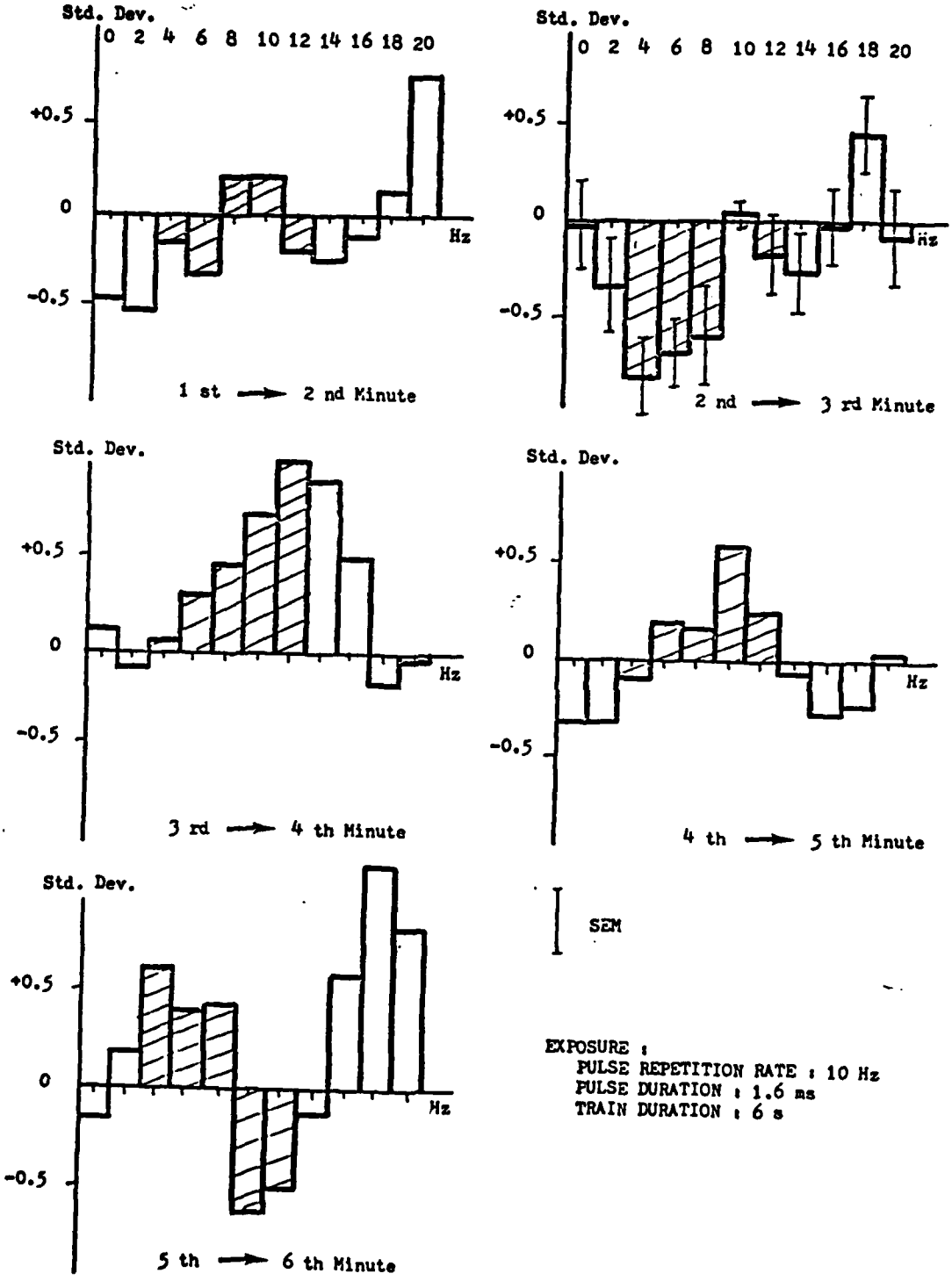

Figure 20 : Shifts in EEG power between minutes for the 10 Hz PRR group.

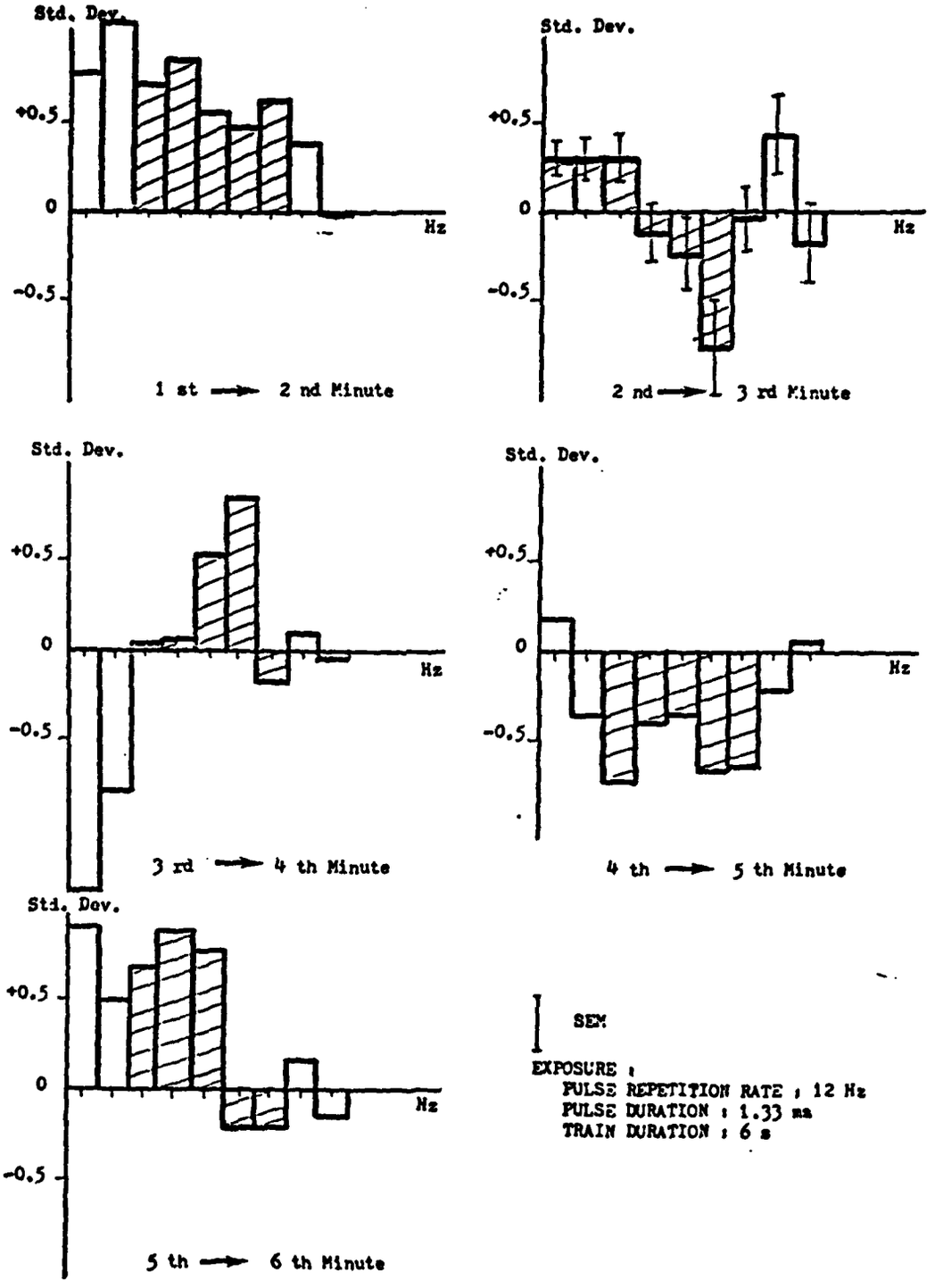

Figure 21 : Shifts in EEG power between minutes for the 12 Hz PRR group.

CHAPTER 4

DISCUSSION

In this section, before discussing the results, the basic neural mechanisms underlying the EEG will be outlined. Discussion of the results from both the threshold study and the repetitive study will follow. The section will be concluded by a presentation of some related studies that have taken place in our laboratory, and a summary of the results.

1. Basic Mechanisms Underlying the EEG

An electroencephalogram (EEG) is a record of fluctuations of electrical activity in the brain recorded from the surface of the cortex or the skull. The nature of the elementary EEG generators is disputed. The hypothesis that the EEG waves result from the summation of potential transients of excitable neuronal elements within or just below the cortex was formulated in 1935 by Adrian and Yamagiva [41]. Another hypothesis that EEG waves are due to the summation of postsynaptic potentials (PSPs) was suggested by several authors [41] (Appendix C). An analysis of the EEG essentially becomes a measure of synchrony existing between these generators. An observed change in the EEG may reflect a change in the state of arousal of the animal, the onset of some organic damage, or a temporary disruption of a basic neural process. The EEG may constitute a source of objective infor-

mation on the behavioral states of the animal. But on the other hand, there is no reliable information on electrical activity at the microscopic level. It is impossible to infer effects at the cellular level from measured EEG shifts. It is not possible to pinpoint the site of action of the microwave radiation.

Although the frequency characteristics of the EEG are extremely complex and the amplitude may vary considerably, a few dominant frequencies are typically observed. They are called alpha, beta, delta, and theta rythms (Appendix C). It is difficult to attach any functional significance to individual frequency bands defined in this study. Most of the power in a normal mouse EEG is present in the band from 1 Hz to 30 Hz. The lowest end of the spectrum (0 Hz and 2 Hz bands) tends to be contaminated by movement artifacts. At the high end (above 12 Hz) power levels fall off very quickly. Some of the midband activity represents the functioning of major anatomical systems within the cortex [42]. The arousal state of the animal is best reflected at these frequencies [43].

2. The Threshold Study

The power present in the EEG, at the 4 to 8 Hz frequencies, decreased immediately after exposure to a microwave pulse as reported by R. Jacobson [29]. Mice were exposed to a series of equicaloric microwave pulses leading to a 1° C cortical temperature rise. These experiments indicated that the exposure levels presented are a lot higher than those needed to elicit a response. In this study, by maintaining a single power level and decreasing the exposure period, effects were seen at temperature increases of 0.1° C. A summary of the results is shown in Figure 13. The exposure parameters

along with the changes in the 8 Hz frequency bin of the EEG are summarized in Table 1.

The magnitude of the E-field within the tissue can be calculated from the absorbed power (measured via the temperature change of the tissue). For a plane wave the relationship is given as [44] :

$$P = \frac{E^2}{\eta} \tag{1}$$

where P is the power density, E is the electric field, and η is given by :

$$\eta = \left[\frac{\mu_o}{\epsilon_o \epsilon_r}\right]^{1/2} \tag{2}$$

where the parameters for tissue are [29] :

$$\mu_o = 4\pi\left(10^{-7}\right)$$

$$\epsilon_o = 10^{-9}/36\pi$$

$$\epsilon_r = 47$$

The maximum E-field appearing across the cell membrane, for a single cell oriented parallel to the propagation vector, can be shown to be related to the ratio of the dielectric constants of the cell membrane and the intercellular fluid :

$$E_m = E_l \frac{\epsilon_l}{\epsilon_m} \tag{3}$$

where

Table 1

Threshold series :
Exposure characteristics and resulting
EEG changes in the 8 Hz frequency bin.

Pulse Width (ms)	Total Temp.Rise (°C)	SAR (W/g)	Rate of Temp.Rise (°C/s)	E-field (V/m)	Change in EEG (Std.Dev.)
32	1	130.6	31.25	1025	-0.449
16	0.5	130.6	31.25	1025	-0.215
8	0.25	130.6	31.25	1025	-0.2
4	0.1	130.6	25.0	1025	-0.615
2	0.05	130.6	25.0	1025	+0.357
Control	0	0	0	0	+0.05

E_m = field intensity at the membrane

E_l = field intensity at the liquid

ϵ_m = dielectric constant of the membrane

ϵ_l = dielectric constant of the liquid

These calculations yield large field strenghts, but they are still a small fraction of the naturally occuring fields due to the normal resting potential of the cell. Across a 200 Å membrane, the normal resting potential of the cell yields a field strength of 10^6 V/m.

The specific absorption rate (SAR) defines the rate of energy deposited per gram of material. For the 32 millisecond pulse, resulting in a 1° C temperature rise we have :

$$SAR = \frac{1^\circ C}{(1g)(32ms)} = \frac{4.18\ J}{(1g)(32\times 10^{-3}s)} = 130.63\ W/g \qquad (4)$$

The calculated rate of temperature rise for the same exposure is :

$$T = \frac{1^\circ C}{32\times 10^{-3}s} = 31.25^\circ C/s \qquad (5)$$

3. The Repetitive Pulse Trains Study

In this study seven groups (6 mice each) of mice were used. Two were used as controls, and the other five were exposed to pulse trains with different pulse repetition rates. The repetition frequencies were 4, 6, 8, 10, and 12 Hz. The train duration was kept the same (6 seconds). The pulse peak power was kept constant,thus the rate of temperature rise $\left(\dot{T}\right)$ was also the same. All trains had the same energy content leading to a 1° C

total cortical temperature rise. The exposure parameters along with the EEG changes in the frequency bin at the pulse repetition rate (PRR) are summarized in Table 2.

The controls showed no significant changes between minutes 2 and 3 for the EEG spectral frequencies in the 4 to 12 Hz range. The frequencies in this range reflect significantly any induced effect. The lower frequencies are contaminated by body movements and the power in frequencies above 12 Hz decreases very rapidly. The microwave pulse trains produced a variety of large, statistically significant, changes in the midband EEG frequencies, in the time interval following the exposure (minutes 2 to 3). Figure 22 shows the EEG changes between minutes 2 and 3 for all groups. The EEG changes produced by the pulse trains were different for all pulse repetition rates from the changes elicited by a single wide microwave pulse which has the same energy content (leads to the same temperature rise) and the same peak rate of temperature increase $\left(\dot{T}\right)$. These shifts in the EEG lasted for about two minutes and were followed by a rebound in the opposite direction. The changes in the EEG were highly dependent on the PRR. In general, The EEG shift was smallest in the frequency bin corresponding to the PRR. This phenomenon was opposite of our expectations of observing a resonance effect and could be reffered to as an "anti-resonance" effect. This is seen in Figure 23 where the shifts in the midband EEG frequencies (4 to 12 Hz) are plotted versus the PRR.

In general, the lower EEG frequency bins (2, 4, and 6 Hz) were shifted in one direction and the upper midband EEG frequencies (8, 10, and 12 Hz)

Table 2

Repetitive pulse trains series :
Exposure characteristics and EEG changes in
the frequency "bin" at the pulses repetition rate

Pulse Rep. Rate (Hz)	Train Duration (s)	Pulse Width (ms)	Total Temp. Rise (°C)	SAR (W/g)	Rate of Temp. Rise (°C/s)	Change in EEG (Std. Dev.)
4	6	4	1	43.5	10.41	+0.17
6	6	2.66	1	43.5	10.41	+0.33
8	6	2	1	43.5	10.41	-0.15
10	6	1.6	1	43.5	10.41	+0.04
12	6	1.33	1	43.5	10.41	-0.04

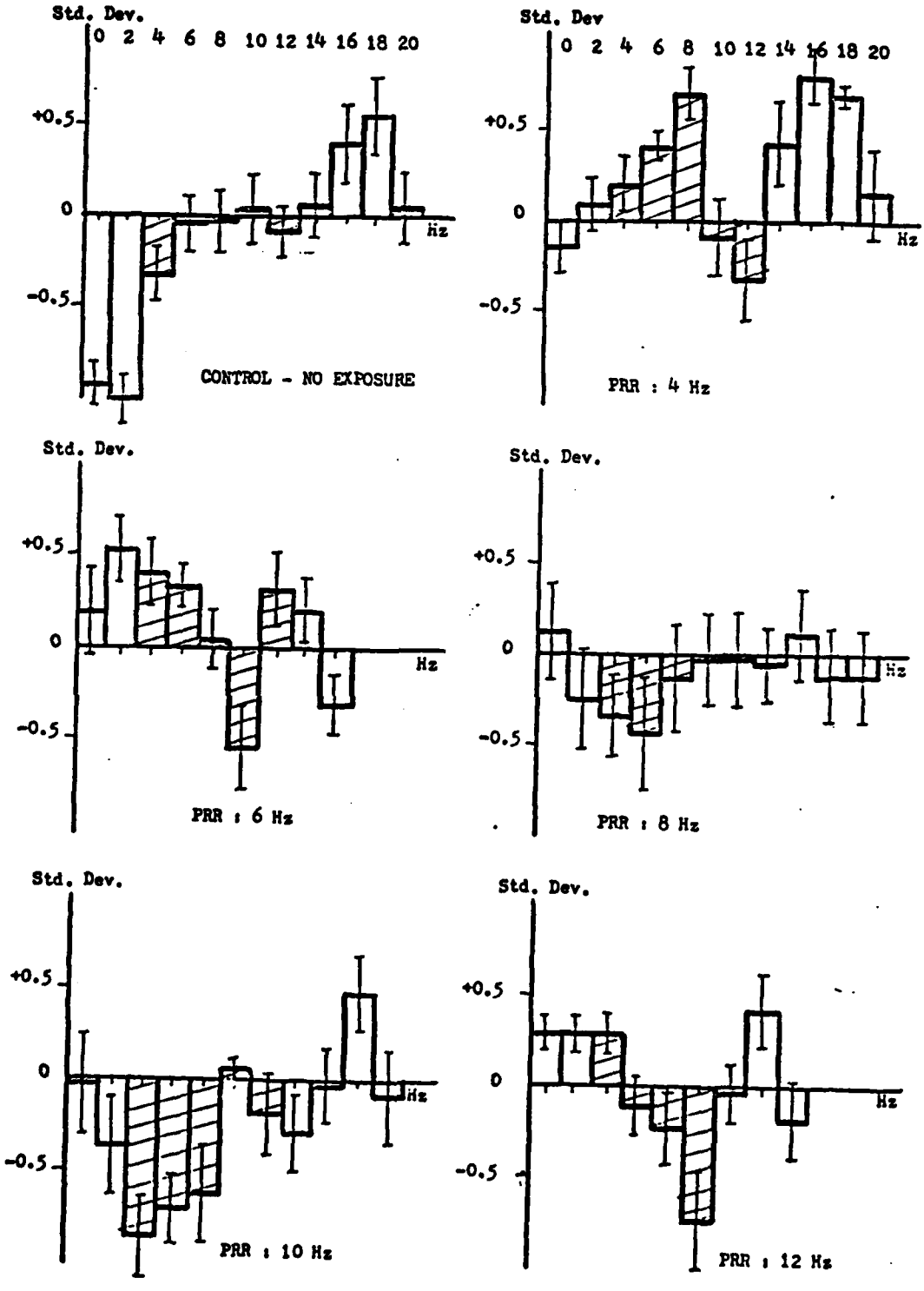

Figure 22 : Changes in EEG power between minutes 2,3 for all groups in the WMP trains study. (Vertical bars represent the SEM)

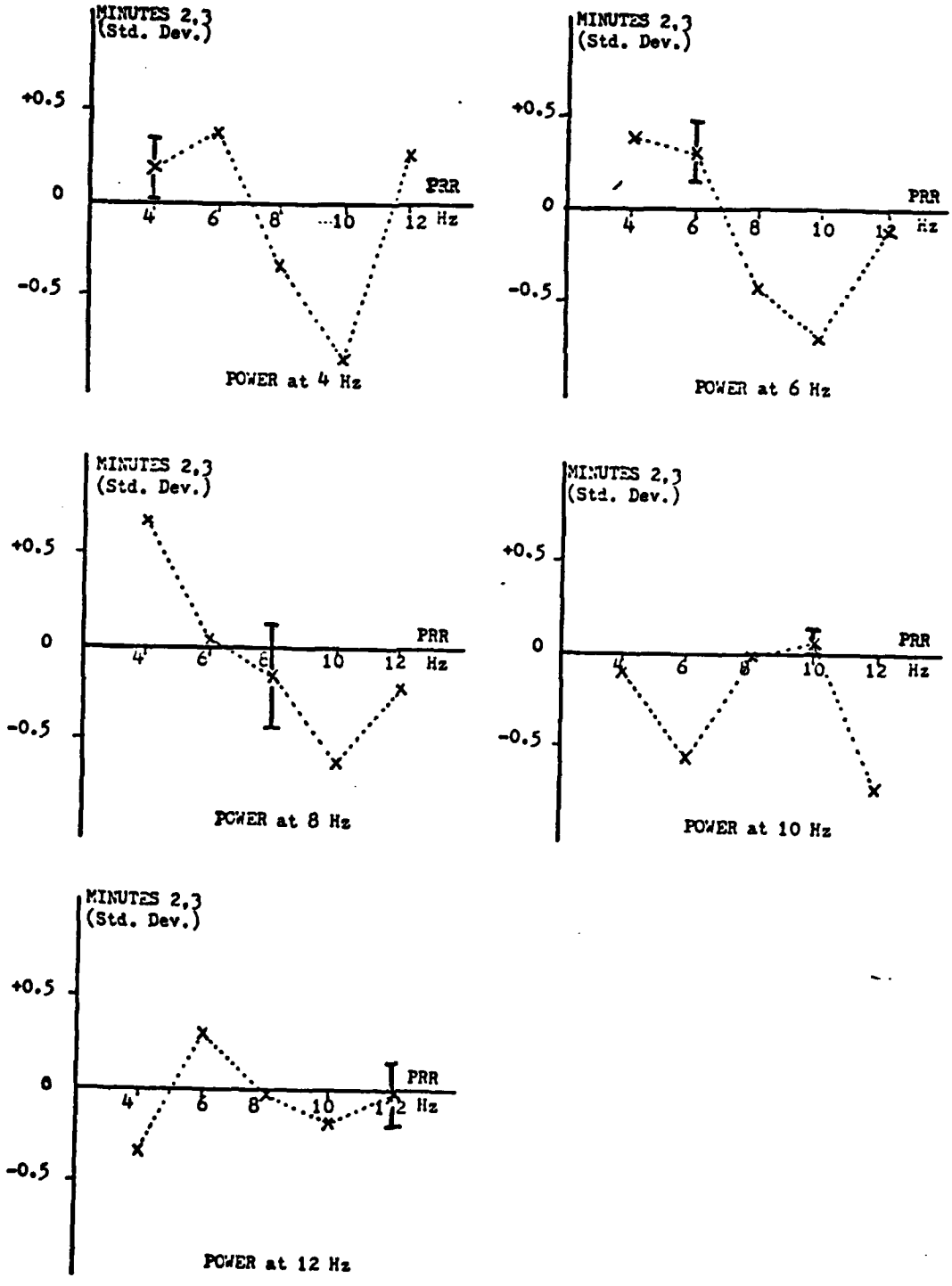

Figure 23 : Shifts in EEG power between minutes 2,3 for the midband EEG frequency bins.

were all shifted in one direction. A time course of the average power in the 2, 4, and 6 Hz spectral EEG bands for all groups is shown in Figure 24. A similar average for the 8, 10, and 12 Hz bins is plotted in Figure 25. The EEG changes for these averages were also different from the controls and different for every PRR.

Another observation was that the slope of the bars representing the EEG shifts between minutes 2 and 3 for the 4, 6, and 8 Hz frequency bins was different for every PRR. This slope was computed for all five PRRs and the results are shown in Figure 26.

The trains consisted of a series of identical pulses that yielded a total cortical temperature increase of 1° C. The energy content of a single pulse is below the threshold predicted by the threshold study. For example, the train at the 8 Hz PRR consisted of forty-eight microwave pulses. The temperature elevation induced by a single pulse was 0.02° C, which is well below 0.1° C, the threshold for the detection of a single pulse.

4. Related Studies

Several studies of the neurophysiological effects of wide microwave pulses have been carried out at the Bioengineering Laboratory of the University of Colorado at Boulder. These investigations have evolved from using single cells, through tissue slices, to the use of intact animals. Throughout all these experiments there has been a commonality of results underlying mechanisms similar to those of pharmalogical agents.

Experiments utilizing single pacemaker neurons of *Aplysia California*

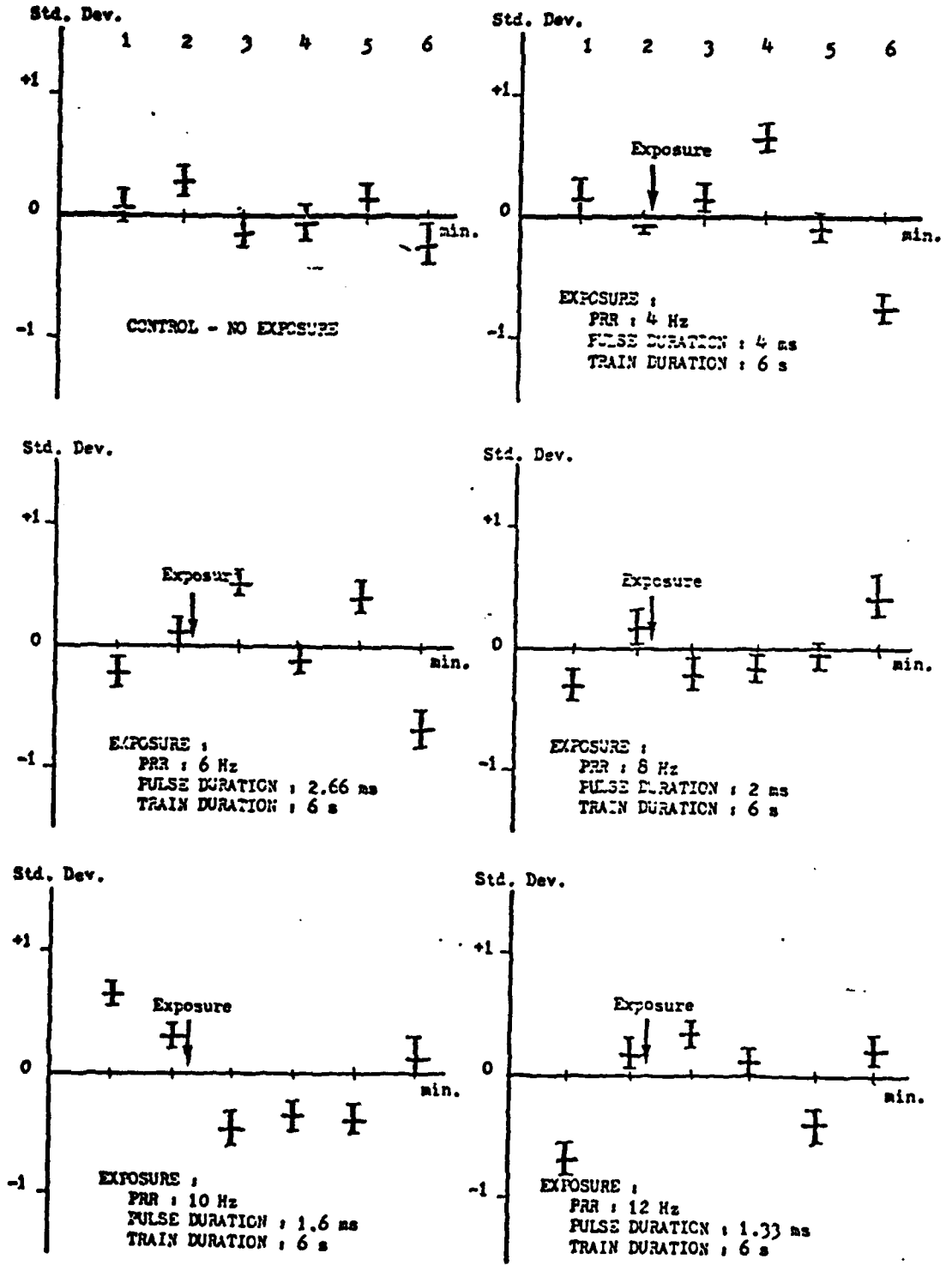

Figure 21 : Time course of the average power in the 2, 4, and 6 Hz frequency bins for all groups.

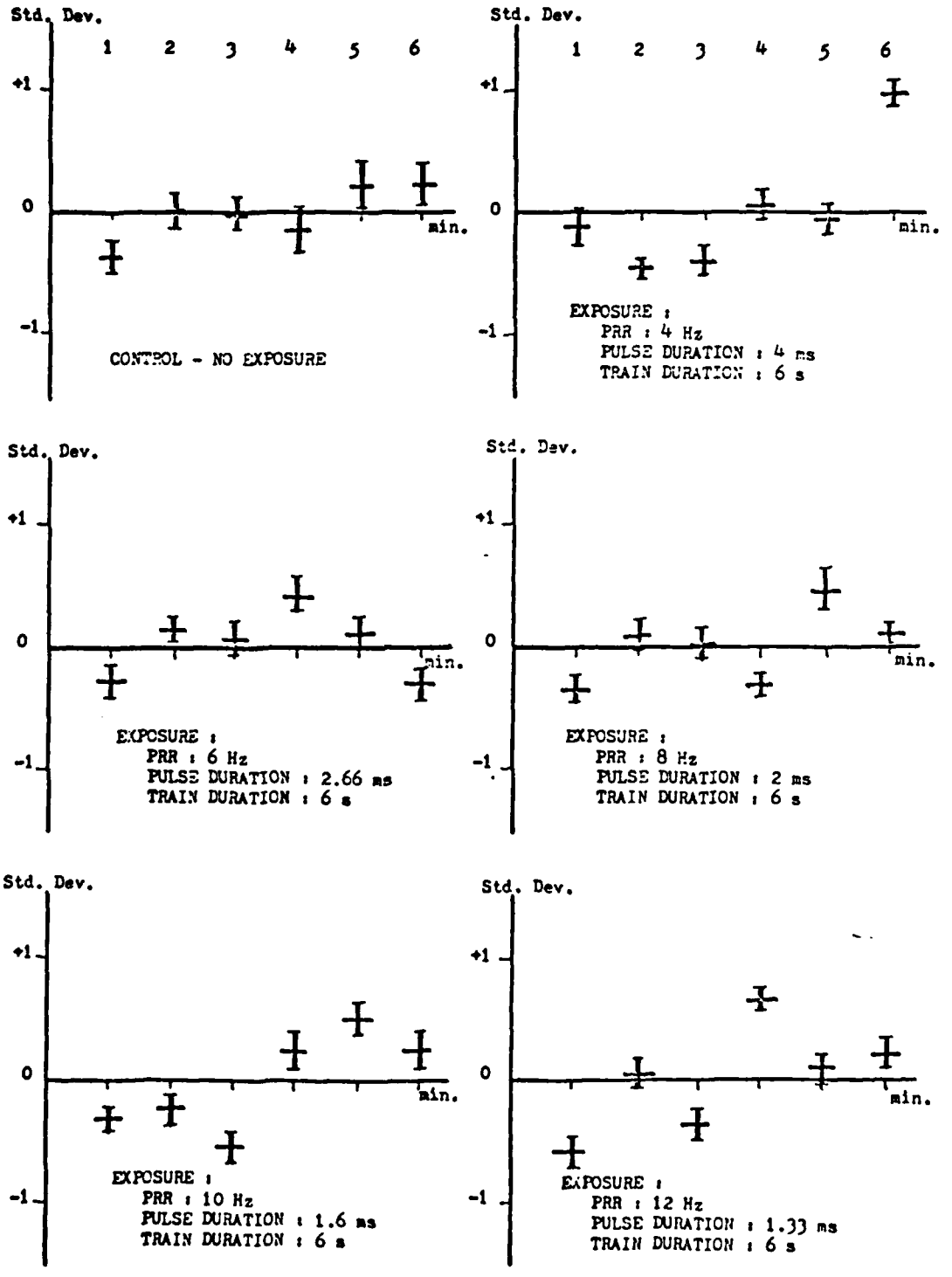

Figure 25 : Time course of the average power in the 8, 10, and 12 Hz frequency bins for all groups.

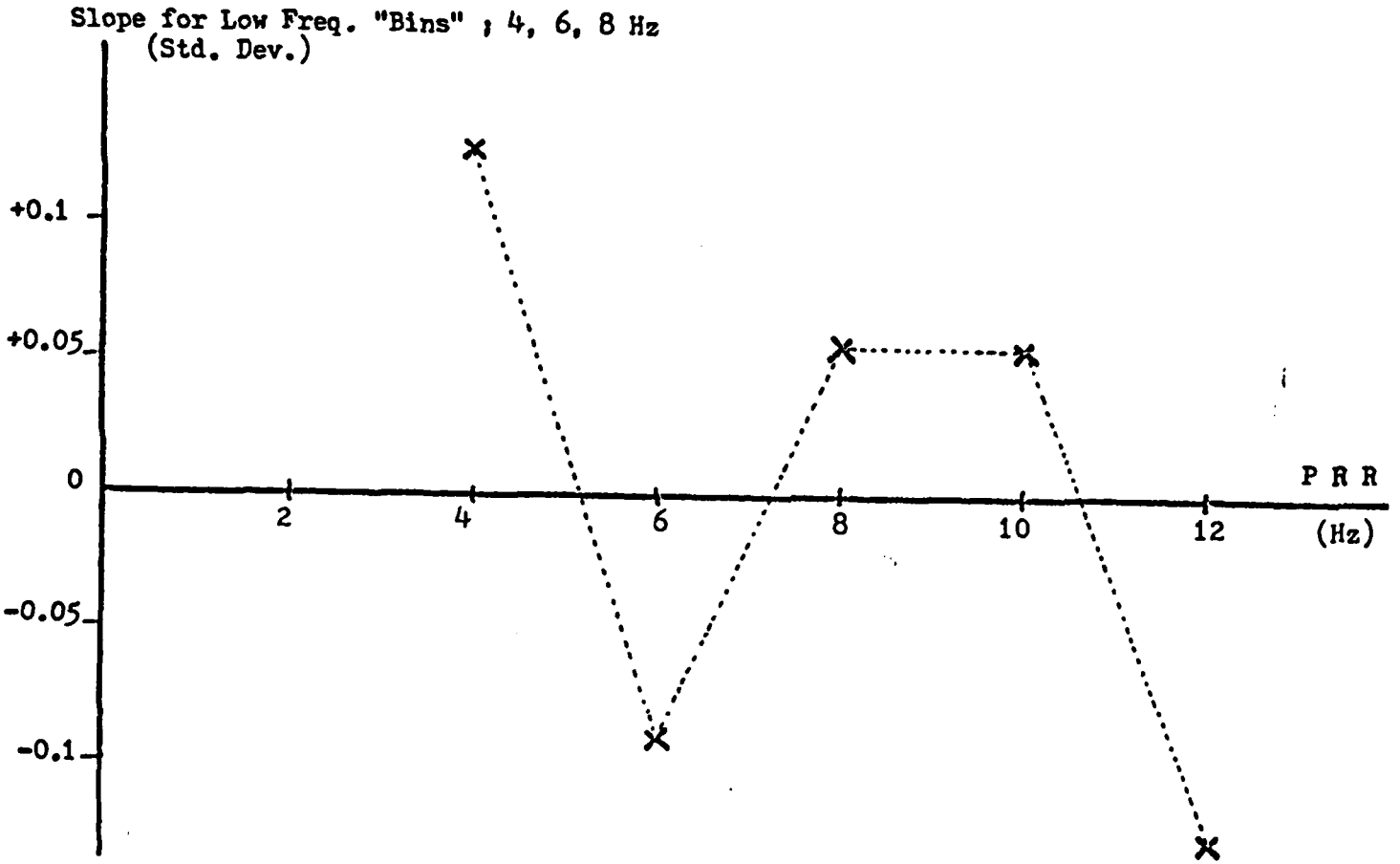

Figure 26 : Slope for the low frequency bins (4, 6, 8 Hz)

(abdominal ganglion cells $R_3 - R_{13}$) showed a slowing of the cell's firing rate after exposure to microwaves [32]. A single pulse of 2450 MHz microwaves lating 0.1 second with a peak SAR of about 40 W/g will cause a slowing of spontaneous firing that lasts for several seconds and is followed by a minute or more of excitatory rebound (increased firing rate) prior to a return to the preexposure firing rate. These changes in firing rate were reproducible by the direct application of heat via a hot water perfusion technique (Figures 27 and 28). This suggests a cellular effect based on thermal considerations, independent of any microwave effect. But the effect cannot be reproduced by heating alone unless the temperature rise rate is sufficiently high. Further experiments showed a dependency of the firing rate shift upon the temperature rise rate (Figure 29).

Analogous effects were noted when rodent hippocampal brain slices were exposed to comparable microwave pulses. Recordings of evoked population spikes show a dramatic decrease in amplitude following microwave exposure (Figure 30). This decrease also lasts 10 seconds or longer and is followed by rebound excitation which can last for many minutes. The microwave pulses needed in this case were much shorter than those in the *Aplysia* case and the SARs were comparable (about 25 to 50 W/g). Again these effects seem to be related to the rate of power deposition.

Another series of experiments using intact animals was carried out [29]. Effects of comparable microwave pulses on the EEG of intact mice were investigated. When a spectral analysis of the EEG was carried out, the EEG frequency range from 4 to 12 Hz showed a sizeable depression which

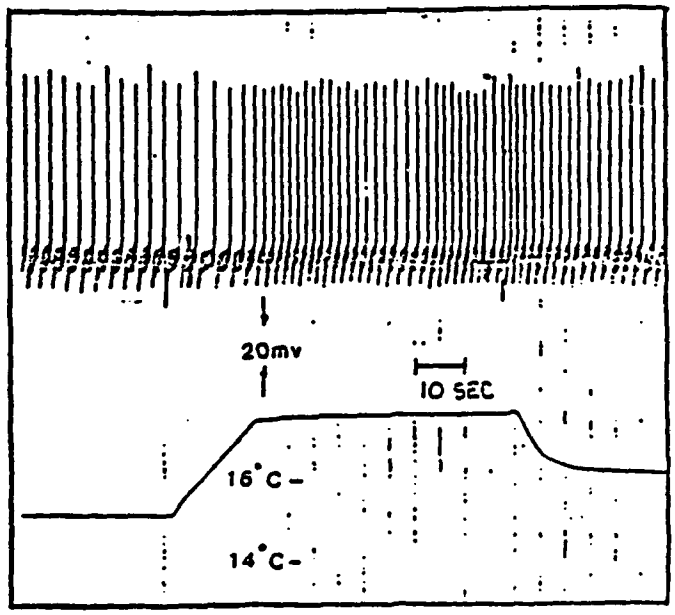

Figure 27 : A microwave induced temperature and firing rate profile of Aplysia pacemaker cell as reported by Chalker [32].

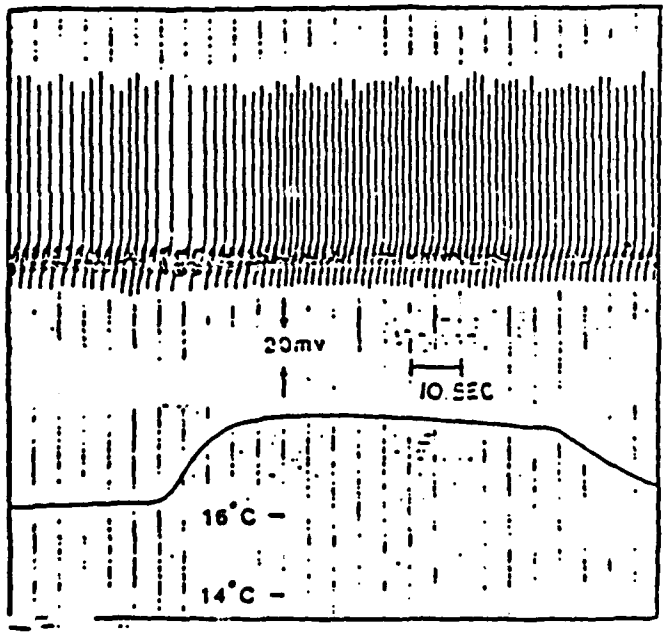

Figure 28 : A perfusion mimic of a microwave temperature profile with associated firing rate profile of Aplysia pacemaker cell as reported by Chalker [32].

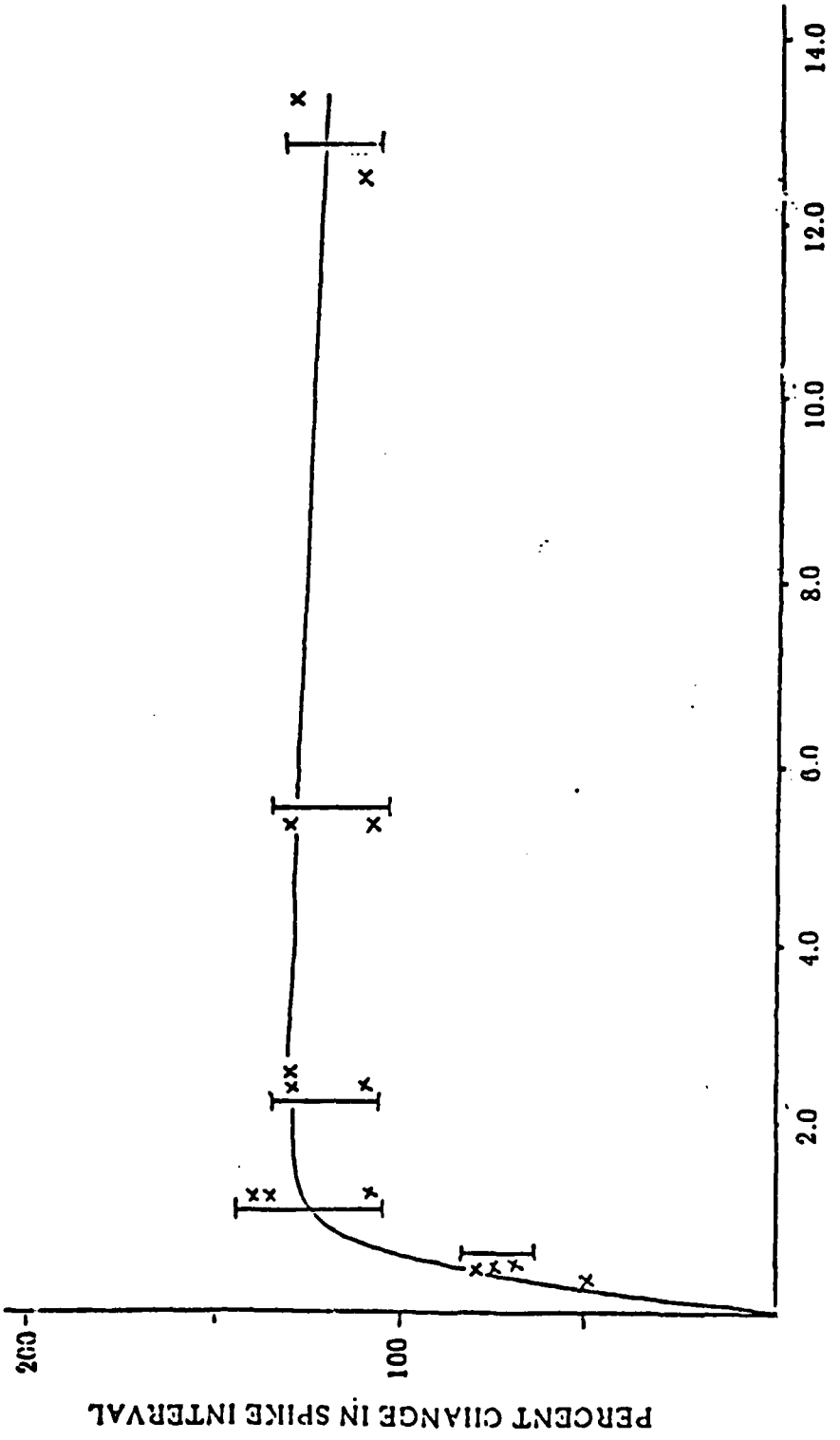

Figure 29 : Change in inter-spike interval vs. rate of temperature change at 15° C. (from [29])

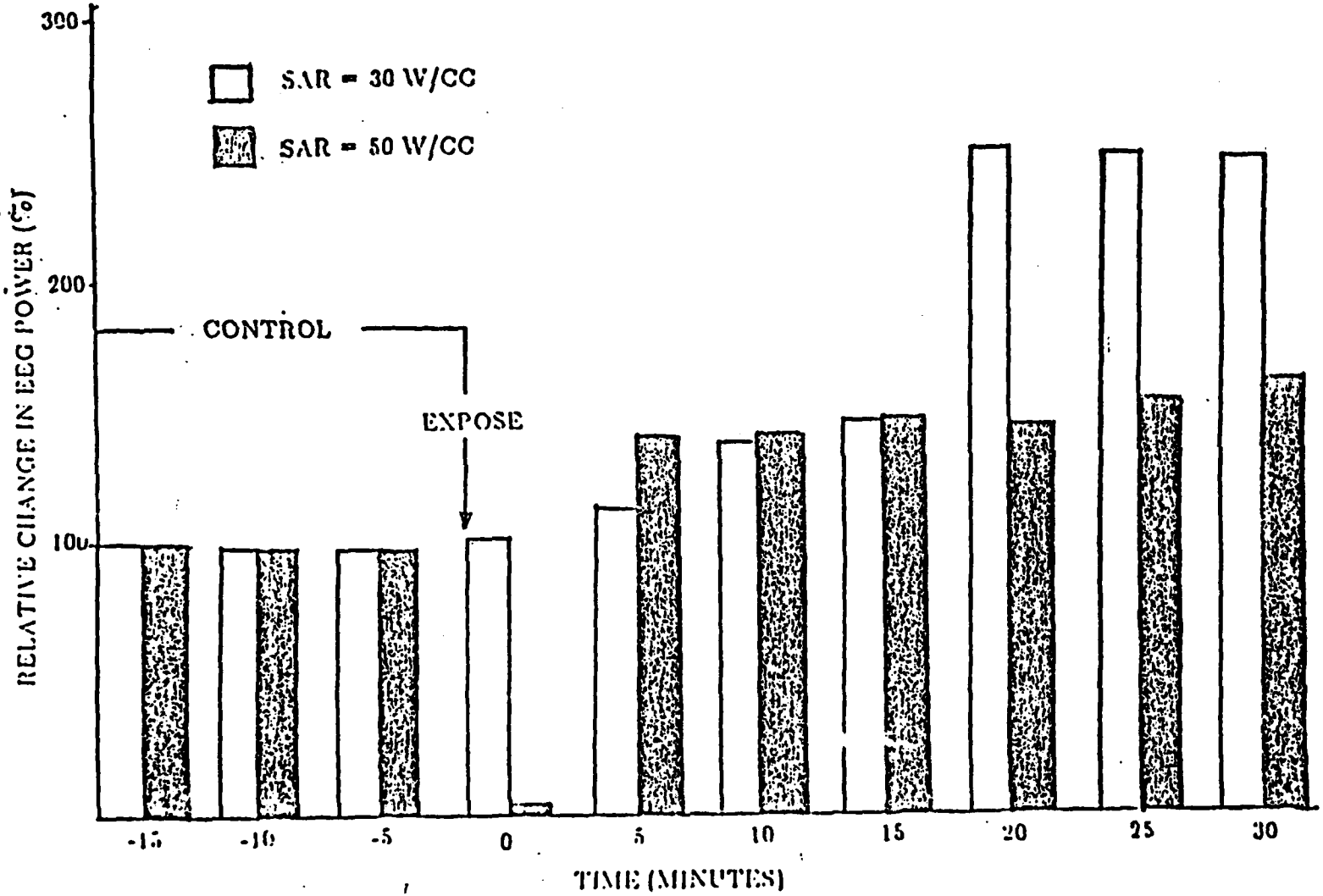

Figure 30 : Change in brain slice evoked potential during microwave irradiation for two power levels as reported by Adey [33].

lasted for about one minute, and was generally followed by a prolonged period of elevated activity. Figure 31 shows the changes in the EEG power in the 4 and 8 Hz spectral bins before and after a 16 ms microwave pulse.

All three of these phenomena fit the same pattern. A fairly long inhibition of neuroelectric activity followed by an even longer excitatory rebound phase. The total time course of these effects far exceeds that which might be expected from a direct electrical effect of the microwave field (rectification). Instead, their action and time course are similar to those that would be expected from pharmacological responses.

5. Conclusion

Experiments involving the exposure of intact animals to microwave radiation must differ in practical terms from those involving single cells and the results of these two kinds of experiments must be viewed differently. Single cell experiments allow accurate dosimetry. Accurate orientation of the cell and control of the amount of power deposited within the cell are also possible. The induced changes following exposure to microwaves are easily determined via intracellular recordings of the membrane potential. With intact, conscious animals, it is more complex to estimate the effects of microwave exposure. Accurate dosimetry is also difficult due to the more complex geometries involved and the inhomogeneity of the tissues.

The rates of energy deposition in this study are relatively high compared to environmental levels or to studies using long exposure periods. In this study the exposure periods are in the millisecond range, consequently the total thermal energy deposited resulted in only a cortical temperature

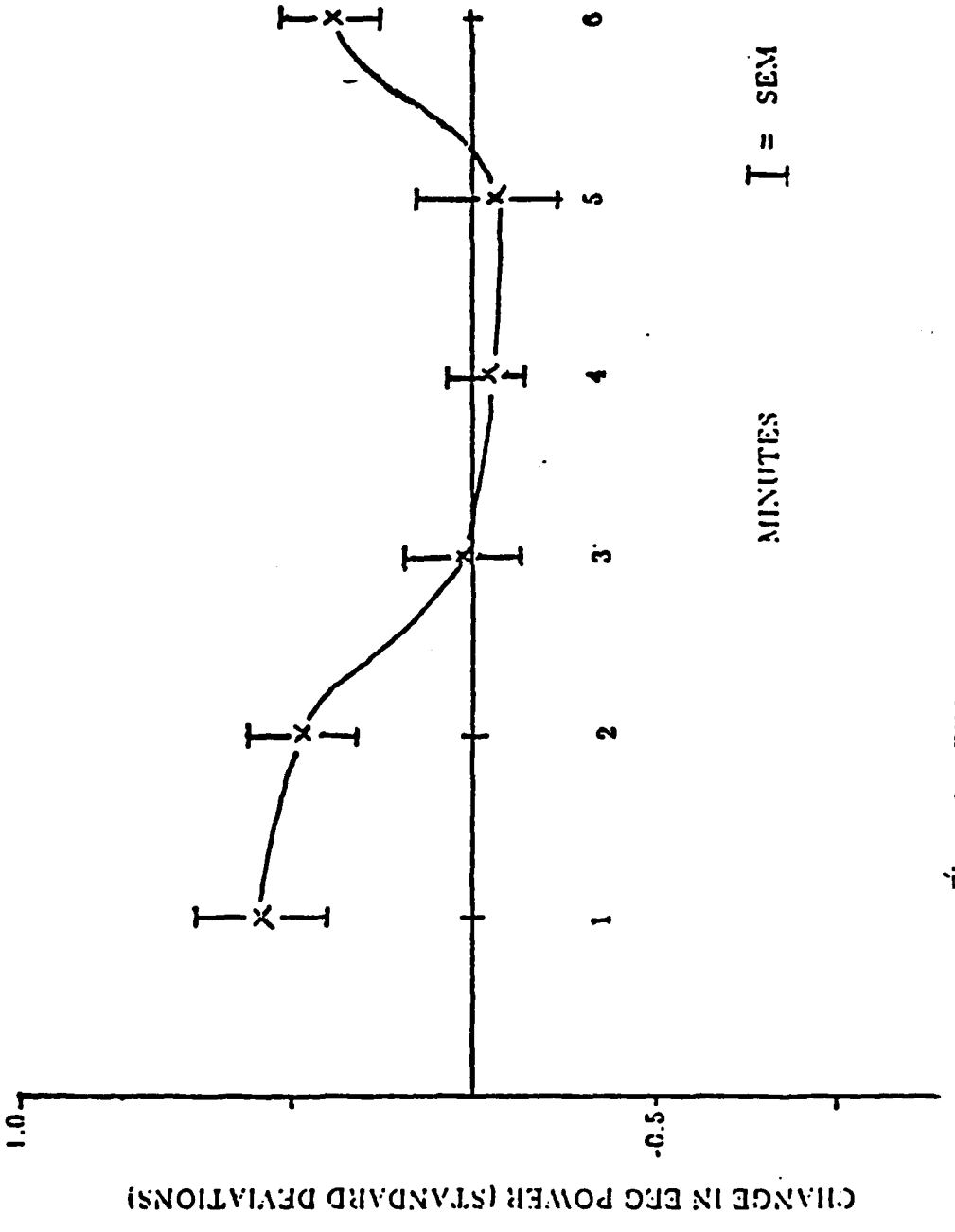

Figure 31 : EEG power (8 - 12 Hz) before and after a single microwave pulse (16 ms) as reported by Jacobson [29].

increase of 1° C despite the high powers involved.

Although the temperature increase induced by a single pulse within the train was below 0.1° C, the threshold for the detection of a single pulse, the trains of pulses ellicited significant effects.

The results obtained suggest some obvious directions in which to proceed with this experimentation. What would happen with trains of longer duration (30 seconds or more)? Will the changes observed converge towards those elicited by a single pulse when the trains duration is shortened? Would the same effects be observed with single cells or brain slices? The use of simpler biological systems such as single cells or brain slices would give cleaner results than those from intact conscious animals, would reduce the large variance inherent to this sort of EEG measure, and thus would reduce the number of trials needed for statistical significance.

The conclusions of this study are summarized as follows :

1) Spectral analysis of the EEG taken immediately before and after microwave exposure provides a valid measure of the effects of microwaves on the central nervous system.

2) Components of the EEG in the 4 to 12 Hz range are reversibly depressed by single microwave pulses of high intensity.

3) The threshold for the effect of a single pulse is low. Effects were elicited by pulses whose energy content yielded a cortical temperature increase of 0.1° C.

4) Microwave pulse trains produced a variety of large, statistically

significant, changes in EEG spectral frequencies in the 4 to 12 Hz range.

5) These EEG changes produced by a 6 second pulse train leading to a 1° C cortical temperature rise were quite different for all pulse repetition rates than that elicited by a single wide microwave pulse which yields the same temperature rise and the same peak rate of temperature rise $\left(\dot{T}\right)$.

6) The change in the EEG was highly dependent on the pulse repetition rate (PRR).

7) In general, the EEG shift was smallest in the spectral frequency bin corresponding to the pulse repetition rate : "Anti-Resonance" effect.

8) Wide microwave pulse trains could be used to send "signals" into the brain without causing dangerous temperature increases.

REFERENCES

[1] Silverman, C., "Nervous and behavioral effects of microwave radiation in humans", *Journal of Epidemiology,* Vol. 97, pp. 219-224, April 1973.

[2] Marha, K. M., J. Musil, and H. Tuha, *"Electromagnetic fields and the life environment",* San Francisco Press, 1971, p. 77.

[3] *"Health effects of ionizing and non-ionizing radiation"* Report of a working group, The Hague, November 15-17, 1971, Regional Office for Europe, WHO, 1972, p18.

[4] Barnes, F.S. "Effects of DC Electric Fields on Biological Systems", Unpublished.

[5] Polk, C., "Sources, propagation, amplitude, and temporal variations of extremely low frequency (1-100 Hz) electromagnetic fields", in : " *Biologic and Clinical Effects of low frequency Magnetic and Electric fields",* Llaurado, V., ed., Thomas Springfield, Illinois.

[6] Adey, W.R., "Some fundamental aspects of Biological Effects of extremely low frequency (ELF)", in : *"Biological Effects and Dosimetry of nonionizing radiation",* Grandolfo, M., Ed. Plenium, New York, 1983.

[7] Guy, A.W., "Quantization of Electromagnetic Fields in Biological systems" in : *"Bilogical Effects of EM Radiation",* Osepchuk, J. M., IEEE Press, 1983.

[8] Ghandi, O. P., "Medical Applications of EM Fields" in : *"Biological Effects of EM Radiation",* Osepchuk, J. M., IEEE Press, 1983.

[9] Bassett, A., R. Pawluk, and A. Pilla, "Acceleration of fracture repair by EM fields : A surgically noninvasive method", *Annals of N.Y. Academy of Sciences,* Vol. 238, 1974, pp. 242-282.

[10] Bawin, S. M., L. K. Kaczmarek, and W. R. Adey, "Effects of modulated VHF fields on the central nervous system", *Ann. N.Y. Acad. Sci.,* Vol. 247, pp. 74-81, 1975.

[23] Taylor, L. S., "The mechanisms of athermal microwave biological effects", *Bioelectromagnetics*, Vol. 2. 1981, pp. 259-267.

[24] Wu, T. M., and S. Austin, "Biological Bose condensation and the time threshold for biological effects", *Phys. Lett.*, Vol. 73A, pp. 266-268, 1979.

[25] Scott, A. C., et al, "The soliton : A new concept in applied science", *Proc. IEEE*, Vol. 61, 1973, pp. 1443-1483.

[26] Singer, S. J. and G. L. Nicholson, "The fluid mosaic model of the structure of cell membranes", *Science*, Vol. 175, 1972. pp. 729-730.

[27] Schwarz, G., "Electric-field effects on macromolecules and the mechanisms of voltage-dependent processes in biological membranes", in : *"The Neurosciences"*, F. O. Schmitt, F. G. Worden Eds., Cambridge, Mass., MIT Press, Ch. 36.

[28] Adey, W. R., "Frequency and power windowing in tissue interaction with weak electromagnetic fields", *Proc. IEEE*, Vol. 60, 1980, pp. 119-125.

[29] Jacobson, M. R., *"The effects of pulsed microwave exposure on the central nervous system of mice"*, M.S. Thesis, Department of Electrical Engineering, University of Colorado, Boulder, 1984.

[29a] Montaigne, K., and W. F. Picard, "Offset of the Vascular Potential of Characean Cells in Response to Electromagnetic Radiation over the Range 250 Hz-250 kHz", *Bioelectromagnetics*, Vol. 5, pp. 31-38, 1984.

[30] Adey, W. R., "Molecular aspects of cell membranes as substrates for interaction with weak electromagnetic fields", in : *"Synergetics of the Brain"*, H. Haken and A. Mandell, eds., Springer, Berlin, 1983.

[31] Durney, C. H., *"Radiofrequency Radiation Dosimetry Handbook"*, Departments of Electrical Engineering and Bioengineering, The University of Utah, 1978.

[32] Chalker, R., *"The effects of microwave absorption and associated temperature dynamics on nerve cell activity in Aplysia"*, M.S. Thesis, Department of Electrical Engineering, University of Colorado, Boulder, 1982.

[33] Adey, G., M.S. Thesis, University of Colorado, Boulder, Unpublished.

[34] Wachtel, H., F. S. Barnes, Modak, and Dean, "Microwave induced hypokenesis; Effects of varying pulse intensity and width", *Third Annual Bioelectromagnetics Society Meeting*, August 1981.

[11] Bawin, S. M., A. Sheppard, and W. R. Adey, "Possible mechanisms of weak electromagnetic field coupling in brain tissue", *Biochem. & Bioenergetics,* Vol. 5, pp. 67-76, 1978.

[12] Pickard, W., and F. Rosenbaum, "Biological effects of microwaves at the membrane level : Two possible athermal electrophysiological mechanisms and a proposed experimental test", *Mathematical Bio-Sciences,* Vol. 29, pp. 235-253, 1978.

[13] Kuffler, S. W., J. G. Nicholls, and A. R. Martin, *"From Neuron to Brain",* Sinauer Associates Inc., 2nd Ed., 1984.

[14] Kandel, E. R., *"Cellular basis of behavior",* Freeman and Company, 1976.

[15] Wachtel, H., R. Seaman, and W. Joines, "Effects of low intensity microwaves on isolated neurons", *Annals of N.Y. Academy of Sciences,* Vol. 247, pp. 46-62, 1975.

[16] Guy, A. W., and C. K. Chou, "Effects of high intensity microwave pulse exposure of rat brain", *Radio Science,* Vol. 17, 1982, pp. 169-177.

[17] Adey, W., and S. M. Bawin, "Non equilibrium processes in binding and release of brain calcium by low-level electromagnetic fields", *Bioelectrochemistry.*

[18] Gorman, A. L. F., and M. F. Marmor, "Temperature dependence of the Sodium- Potassium permeability ratio of a Molluscan neurone", *J. Physiol.,* Vol. 210, 1970, pp. 919-931.

[18a] Barnes, F. S., "Cell Membrane Temperature Rate Sensitivity Predicted from the Nernst Equation", *Bioelectromagnetics,* Vol. 5, pp. 113-115, 1984.

[19] Carpenter, D. O., and B. Alving, "A contribution of an electrogenic Na^+ pump to membrane potential in *Aplysia* neurons", *J. Gen. Physiol.,* Vol. 50, 1968, pp. 1-21.

[20] Fröhlich, H., "Long range coherence and energy storage in biological systems", *Int. J. Quant. Chem.,* Vol. II, pp. 643-649, 1968.

[21] Fröhlich, H., "Possibilities of long and short-range electric interactions of biological systems", *Neurosci. Res. Prog. Bull.,* Vol. 15, pp. 67-72, 1977.

[22] Fröhlich, H., "Coherent electric vibrations in biological systems and the cancer problem", *IEEE Trans. Microwave Theory Tech.,* Vol. 26, pp. 613-617, 1978.

[35] Guy, A. W. and C. K. Chou, "Effects of high-intensity microwave pulse exposure of rat brain", *Radio Science,* Vol. 17, 1982, pp. 169-178.

[36] Stavinoha, W. B., J. Frazer, and A. T. Modak, "Microwave fixation for the study of acetylcholine metabolism", in : *"Cholinergic Mechanisms and Psychopharmacology",* D. Jenden, ed., NY, Plenum, 1978, pp. 169-179.

[37] Chou, C. K. and A. W. Guy, "Carbon-loaded Teflon electrodes for chronic EEG recordings in microwave research", *J. of Microwave Power,* Vol. 14, 1979, pp. 399-404.

[38] Stearns, S., *"Digital Signal Analysis",* Hayden Book Co., Rochelle, NJ., 1975.

[39] Blackman. R. B. and J. W. Tukey, *"The measurement of power spectra",* Dover Publications, New York, 1958.

[40] Walter, D. O., "Spectral analysis for electroencephalograms : Mathematical determination of neurophysiological relationships from records of limited duration", *Experimental Neurology,* Vol. 8, 1963, pp. 155-181.

[41] Creutzfeldt, O. D., "Neuronal Mechanisms Underlying the EEG", in : *"Basic Mechanisms of the Epilepsies",* H. H. Jasper, A. A. Ward, and A. Pope, Ed., Little Brow and Co., Boston, 1969, pp. 397-410.

[42] Shepherd, G. M., *"The Synaptic Organization of the Brain",* Oxford Press, NY., 1979.

[43] Vanderwolf, C. H. and T. E. Robinson, "Reticulo-cortical activity and behavior : A critique of the arousal theory and a new synthesis", *The Behavioral and Brain Sciences,* Vol. 4, pp. 459-514.

[44] Barnes, F. S. and C. J. Hu, "Model for some nonthermal effects of radio and microwave fields on biological membranes", *IEEE Trans. on Microwave The. and Tech.* , Vol. MTT-25, 1977, pp. 742-746.

[45] Kandel, E. R. and J. H. Schwartz, *"Principles of Neural Science",* Elsevier North Holland, New York, 1981.

APPENDIX A

MICROWAVE SOURCE

The microwave source used in our investigation was designed and built by the Instrument Development Laboratory within the Department of Electrical Engineering at the University of Colorado at Boulder. Figure A1 shows a diagram of the source. It consisted of a pulsed CW 2450 MHz magnetron tube (Amperex Corp. 4J119A). A tetrode vaccum tube (Eimac 4PR1000A) is used to pulse the magnetron on and off. The magnetron high voltage supply was derived from a capacitive storage system connected to the magnetron via the tetrode. A high voltage transformer converts the 208 V ac wall supply to high voltage ac which is then rectified with a diode bridge. The high voltage dc then appears across a capacitance. Thus, when the magnetron is fired, the capacitors act as a dc power source. Pulsed operation was attained by pulsing the grid voltage of the tetrode, allowing the high voltage to appear at the magnetron anode. The magnetron filament supply was on continuously.

The magnetron tube is rated to 6 kW continuous power output. Two adjustments allowed control of the power level of the emitted microwave radiation. The power output is controlled by changing the potential to which the high voltage capacitors are charged and that appears on the magnetron anode during the pulse "on" time. This high voltage potential is set

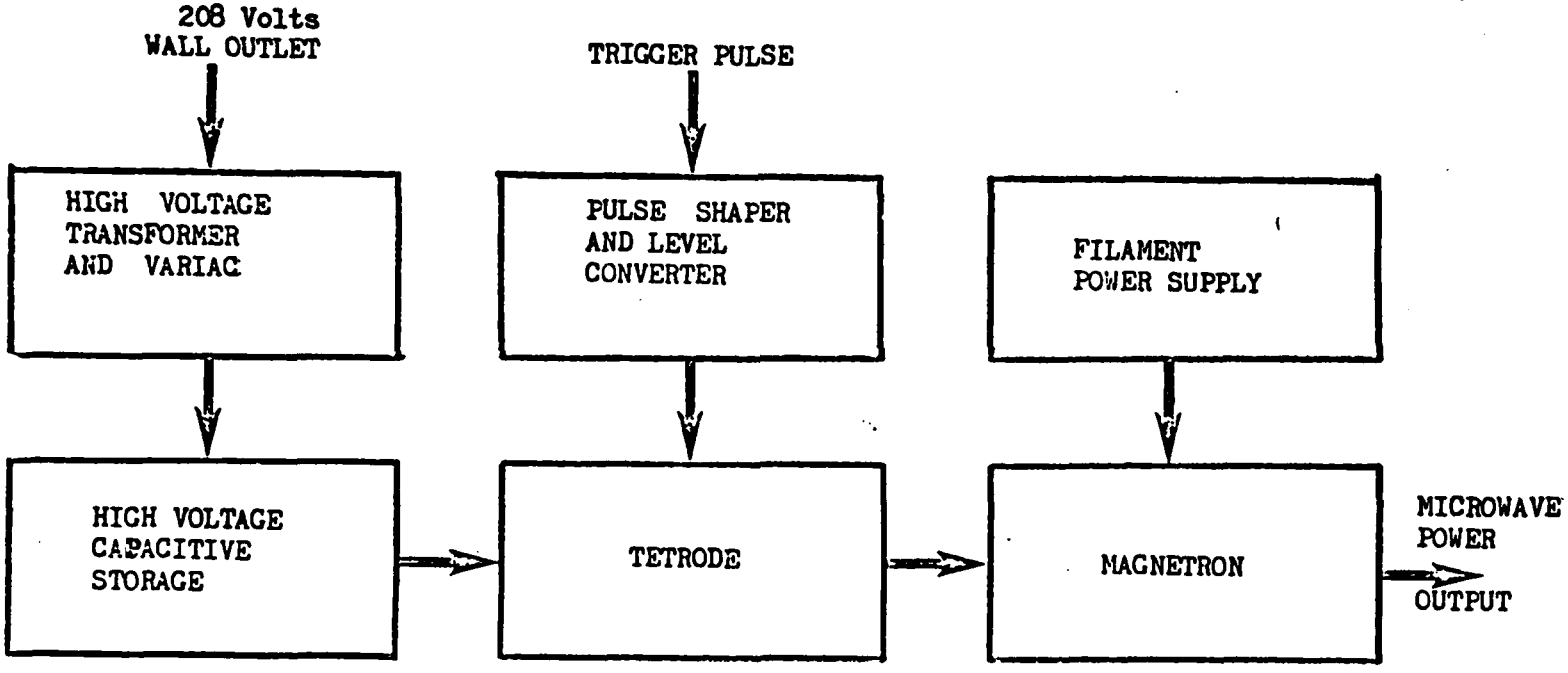

Figure A1 : Microwave source

by a variac between 0 and 9 kV. Varying the value of the maximum positive grid voltage attained at the tetrode during the exposure period provided a second control of the power output of the magnetron. The tetrode tube is switched on and off by changing the grid voltage. In the off state the grid is at about -400 V. To turn the tube on, the grid must be pulsed to about 0 V, or slightly positive. Varying the value of the positive grid voltage controls the power output of the magnetron by limiting the current through the tube. These two adjustments provided reproductible high power microwave pulses in the millisecond range with power levels from 1 kW to almost 8 kW.

APPENDIX B

DIGITAL SAMPLING OF THE EEG AND COMPUTATION OF THE POWER DENSITY FUNCTION

The calculations in this study were oriented toward digital computation, which of course requires conversion of the data to digital form. Conversion of the EEG into digital form involves defining the digital sampling rate, the quantization error, and the sampled epoch length. The power density function or spectra was computed as the discrete Fourier transform of the autocorrelation function.

1. Sampling Rate

The choice of the sampling rate is important. The sampling rate is determined by the highest frequency present in the signal. The effort of processing numerous samples lead to minimization of the sampling rate, but a lower limit is set by the undesirable aliasing process. Basic digital signal analysis specifies that the sampling rate must be at least twice that of the highest frequency present in the data [38]. If the sampling rate is chosen too low aliasing occurs, higher frequency activity is confounded with lower frequency. Avoidance of this problem requires some a priori knowledge of the frequency content of the signal in addition to proper filtering.

It is well known that the EEG signal is rapidly attenuated at frequen-

cies above 30 Hz. In our study, a 3 dB/octave low pass filter with a one half power at a frequency of a 100 Hz was employed in the EEG amplifier. A sampling rate of 128 samples per second, with an aliasing frequency of 64 Hz, was sufficient with the exception of the noise present in the 64 to 100 Hz range. The lack of appreciable signal in the 64 to 100 Hz range was determined by a pilot spectral analysis taken at 256 samples per second done by R. Jacobson [29]. At this rate noise up to 128 Hz, point at which the low pass filter activity begins, could be identified. This estimation indicated no noise that could be aliased at the lower rate of 128 samples per second.

2. Quantization

Quantization contributes a small amount of noise to the original signal. The effect is to place a lower bound on the intensity that can be detected.

The analog to digital converters used in this study had an eight bit digital range with an accuracy of ± 1 least significant bit. This produced a resolution of ± 40 mV out of the 10 V (± 5 V) input range. This level of accuracy was more than sufficient for our purposes.

3. Epoch Length

The epoch length is mainly a function of the desired level of statistical confidence required in the computed spectra. It is also necessary, when defining a sample size, to consider the microcomputer's data handling and storage rates.

The epoch duration, frequency resolution, and confidence level are related by [39,40] :

$$D = \frac{\left[\frac{1}{2} + \frac{200}{C^2} + \frac{1}{3}\right]}{R} \qquad (1)$$

where :

D = epoch duration in seconds

C = 90% confidence range in dB

R = resolution of power estimates in Hz.

In the threshold experiments the spectra were computed at 4 Hz intervals. For 90% of the computed spectra to be accurate within ±1.5 dB, the required epoch length is 5.76 seconds. The speed at which the microcomputer can handle and store data on a disk limited the amount of data that can be processed to less than 28 seconds of data each minute. This led to the selection of six second epochs taken every 15 seconds. For the repetitive pulse trains experiments the spectra were computed at 2 Hz intervals. The six second epochs allowed a 90% confidence level within ±2.1 dB. The averaging of four spectra over a minute yields an accuracy surpassing the 90% confidence level. This allowed for the removal of the contaminated samples within each minute.

4. Computation of the Power Density Function

The power density function or spectra was computed as the discrete Fourier transform of the autocorrelation function. The autocorrelation

function is a multiplication of the sampled set by a displaced copy of itself. The autocorrelation function emphasizes the regular activity in each sample at the expense of the irregular activity. The autocorrelation function is defined by [40] :

$$AC(L) = \frac{1}{N-L} \sum_{i=1}^{N-L} X(i)\, X(i+L) \qquad (2)$$

where :

N = total number of samples

L = lagged product number

X(i) = i th sampled value.

The discrete Fourier transform of the autocorrelation function yields the power density function or autospectrogram and is defined as [40] :

$$AS(f_i) = \frac{1}{m}\left[AC(0) + \sum_{q=1}^{q=m-1} 2AC(q)\cos q\pi f_i/f' + AC(m)\cos m\pi f_i/f'\right] \qquad (3)$$

where :

$AS(f_i)$ = autospectrogram at frequency f_i

m = maximum lag used

f' = folding frequency (Nyquist frequency).

This digital process is similar to conversion of functions of time into functions of frequency using a set of analog filters. Each filter has a maximum output in one frequency band. The response of these digital filters is not ideal in giving unit response within their band and zero outside it. The filtering action decays about the center frequency and does not have well

defined shoulders. Also side lobes do exist and can cause negative filter responses. This is an inevitable consequence of having a sample of finite length. To reduce these problems the autospectrogram is subjected to a Hanning technique which consists of smoothing the spectra over frequency. This widens the response of the individual filters and reduces the effects of side lobes. It also adds some covariance to adjacent spectra estimates. The Hanning window applied to the power density results is given by :

$$HAS\left(f_i\right) = 0.25AS\left(f_{i-1}\right) + 0.5AS\left(f_i\right) + 0.25AS\left(f_{i+1}\right) \qquad (4)$$

where :

$HAS(f_i)$ = Hanned autospectrogram at frequency f_i

$AS(f_{i+-1})$ = autospectrogram adjacent to $AS(f_i)$.

Small DC offsets in the sampled data or changes in the absolute calibration from day to day can result in misleading computations of power density around zero frequency. To avoid this problem, the data is standardized after digitization. The mean of the entire sampled set is subtracted from each value, resulting in a new set of data with a mean of zero. A spectral analysis of signals of known frequency content, done by the technique described above, is shown in Figure A2.

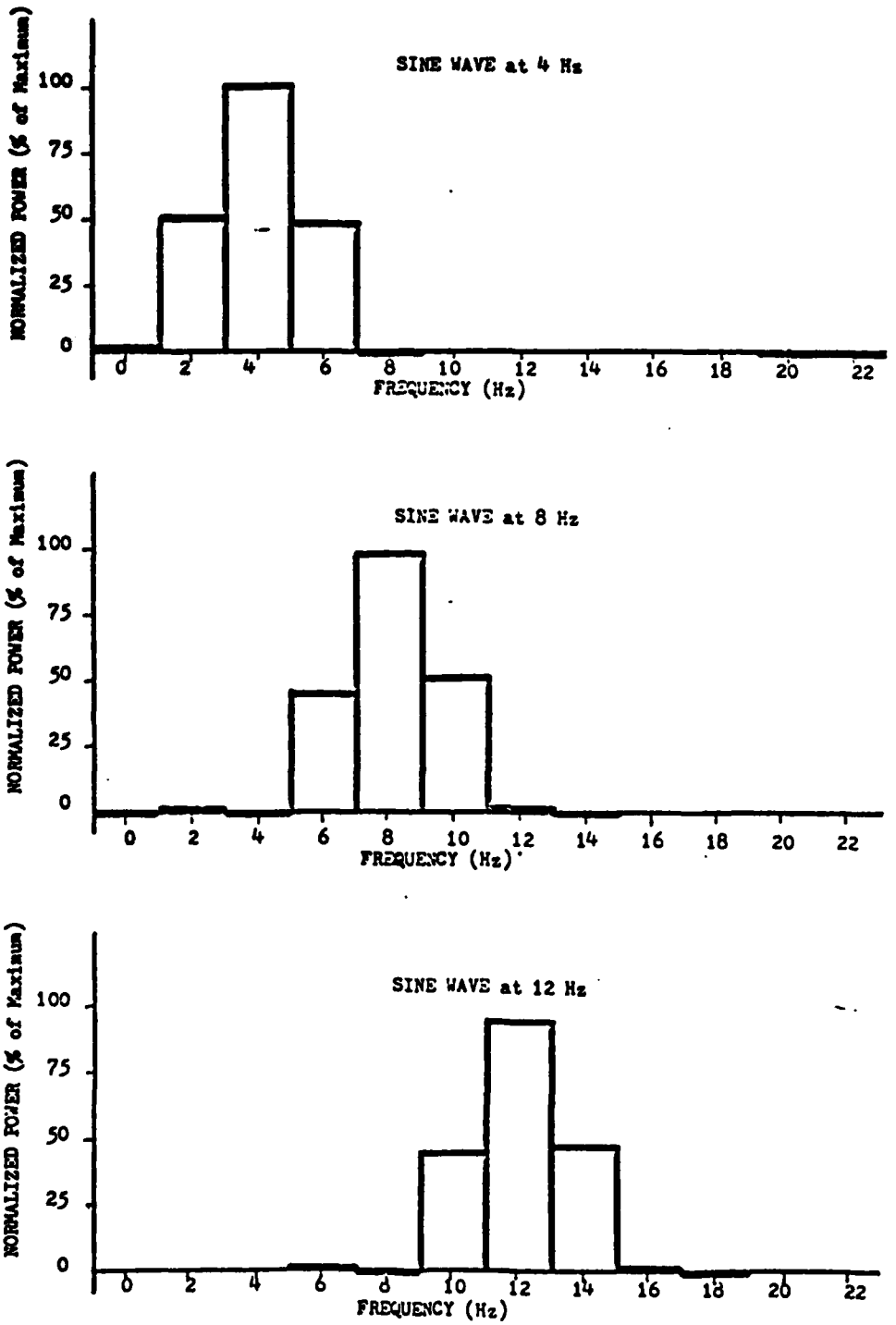

Figure A2 : Spectral analysis of known sinusoidal signals

APPENDIX C

BASIC MECHANISMS UNDERLYING THE EEG

An electroencephalogram (EEG) is a record of fluctuations of electrical activity in the brain recorded from the surface of the cortex or the skull. Although the nature of the elementary EEG generators is disputed, it is generally agreed that they exist as individual neurons or small groups of neurons. The hypothesis that the EEG waves result from the summation of potential tramsients of excitable neuronal elements within or just below the cortex was formulated in 1935 by Adrian and Yamagiva [41]. Another hypothesis that EEG waves are due to the summation of postsynaptic potentials (PSPs) is suggested by several authors [41], who also provided extensive experimental support.

The resting membrane potential is considered static in time and does not contribute to the EEG. While it might seem that the most obvious source for these extracellular potentials is the action potential (the largest signal generated by neurons); action potentials contribute little to the EEG because of their quick time courses and their spatially varying nature. The high frequency components of action potentials are severely attenuated by the capacitance of the surrounding tissue. They contribute only if there is highly synchronized activity within a large group of neurons. The major contributors to the EEG are the summated postsynaptic potentials in

synchronously activated vertically oriented pyramidal cells. Pyramidal cells are oriented parallel to one another and perpendicular to the surface of the cortex. Therefore, they encounter little attenuation due to geometrical factors. The contribution of the glial cells to the EEG is probably less important than that of the pyramidal cells because they are not oriented in any particular fashion relative to one another or to the pyramidal cells.

Nerve cell activity is accompanied by a current flow across the cell membrane between the extracellular and the intracellular fluid. This flow of charges along the intercellular space induces an ionic flow away from the cell membrane in the extracellular fluid due to the membrane capacitance. The induced current flows back along the cell towards areas of lesser charge density, producing continuous loops of current spreading along the cell membrane. These loops of current produce an electrical dipole. The electric field associated with the dipole is projected along the dipole vector. The signal suffers attenuation as it travels through the cortex. These signals add together to produce the EEG at the surface of the cortex.

Although the frequency characteristics of the EEG are extremely complex a few dominant frequencies and amplitudes are typically observed. They are called alpha, beta, delta, and theta rythms. For a man, the frequencies corresponding to these patterns of activity are : alpha 8-13 Hz, beta 13-30 Hz, delta 0.5-4 Hz, and theta 4-7 Hz [15]. The normal EEG is surprisingly synchronous. Any outside influence which alters this synchrony is reflected in the EEG. Different states of arousal; sleep, wakefulness, attentiveness, are discernible from the EEG. Behavioral states are detect-

able through changes in the alpha activity [43]. Alterations in neural transduction, in the thermodynamics of the ionic equilibrium, or in the neurohormonal activity will also affect the EEG. But on the other hand there is no reliable information on electrical activity at the microscopic level in the EEG potential.

END

9-87

DTIC